The Hong Kong Polytechnic University

Department of Health Technology and Informatics

FABRICATION OF RGD PEPTIDE GRADIENT POLY(ETHYLENE GLYCOL) (PEG) HYDROGEL IN MICROFLUIDIC GRADIENT GENERATORS TO CONTROL MESENCHYMAL STEM CELL BEHAVIOUR

By

LIU ZONGBIN

A thesis submitted in partial fulfillment of the requirements of the degree of Doctor of Philosophy

February 2010

Certification of Originality

I hereby declare that this thesis is my own work and that, to the best of my knowledge and belief, I reproduce no material previously published or written, nor material that has been accepted for the award of any other degree or diploma, except where due acknowledgement has been made in the text.

_____

LIU ZONGBIN

Abstract

Mesenchymal stem cells (MSCs) have the ability to differentiate into a wide range of specialized cell types, such as adipocytes, chondrocytes, and osteoblasts. MSCs have the potential use for tissue regeneration in three-dimensional (3D) scaffold through the control and guidance of MSCs differentiation. However, as there is little understanding of mechanisms for MSCs differentiation in biomaterials, it is still difficult for the regeneration of viable complex three-dimensional (3D) tissues from constructs of stem cells and biomaterials. The biomolecules and their concentrations in biomaterials have important impacts on MSCs behaviour. Therefore, it is of particular interest to fabricate a supportive three-dimensional (3D) biofunctional biomaterial with spatial control of biomolecules and their concentration as a platform to more effectively study MSCs adhesion, proliferation and differentiation with biomaterials.

In this study, a microfluidic gradient generator was developed as a platform to fabricate poly(ethylene glycol) (PEG) hydrogel with gradient distribution of arginine-glycine-aspartic (RGD) peptide. The effect of RGD and its concentration on MSCs differentiation was studied. The gradient PEG hydrogel can achieve identity and concentration control of biomolecules. RGD peptide is a biomolecule and often used for enhancing cell adhesion. Moreover, it was also found to have impacts on stem cells differentiation. Therefore, the effect of RGD peptide on MSCs differentiation was studied.

In order to fabricate RGD gradient PEG hydrogel, a PDMS microfluidic gradient generator was designed and fabricated using photolithography and soft lithography technique. Simulations were done to find the optimal parameters to achieve stable and continuous bio-molecule gradient. After fabrication of the PDMS microfluidic gradient generator, flow characterization was explored to find the optimal flow parameters for the generation of colour gradient of dye solution.

RGD peptide was incorporated to PEG molecule to form acrylate-PEG-RGD (ACRL-PEG-RGD) by the reaction of $–NH_2$ group of RGD with –NHS group of ACRL-PEG-NHS. Fourier-transform infrared spectrometer (FTIR) was used to characterize the conjugation reaction. The RGD gradient PEG solution was then formed using the PDMS microfluidic gradient generator by injecting the PEG-DA solution with/ without ACRL-PEG-RGD into the two inlets. The RGD gradient PEG hydrogel was then solidified after UV polymerization.

MSCs were then cultured on two dimensional (2D) RGD gradient PEG hydrogel. With the increase of RGD concentration on the gradient PEG hydrogel, the adherent cell density and single cell spreading area increased. The impact of different RGD gradients on MSCs adhesion was also studied. It was found that there was a critical concentration, below which fewer cells can attach on the hydrogel surface. The effect of RGD gradient on MSCs orientation or alignment was also explored.

MSCs were encapsulated into PEG hydrogel with different RGD concentrations for three dimensional (3D) cell culture. The cells viability was tested by live/dead assay. MSCs were induced to osteogenic differentiation. Vonkossa staining of mineralization was used to characterize the osteogenisis. The results showed that the cells viability increased with the increase of RGD concentration. RGD peptide can promote the osteogenisis of MSCs in osteogenic medium. MSCs were also encapsulated into PEG hydrogel with RGD concentration gradient with UV polymerization. The stem cells encapsulated in the RGD gradient PEG hydrogel were induced to osteogenic differentiation. The effect of RGD gradient on cells viability and osteogenisis was studied.

Acknowledgement

I would like to express my sincere gratitude to my supervisor Prof. Arthur Fuk-Tat MAK for his guidance, encouragement and support in this project. In the past three years, Prof. Mak always gave me some valuable advice in writing proposal, doing conformation and writing dissertation.

I would like to express my sincere gratitude to my co-supervisor Dr Mo YANG, who provided me with all the necessary support, guidance, patience, encouragement and constructive advice, which are indispensable to the success of my postgraduate studies. Dr Mo Yang is the person who possesses the distinguished scientific talent and knowledge.

I sincerely thank my co-supervisor Dr Parco Ming-Fai SIU for his support and training in immunoassaying.

I am thankful to Dr Baojian XU for his help in theoretical simulation of my project. I am grateful to Mr Jinjiang YU for the data analysis. I thank Mr Yu Fung POW for his help in cell culture. I thank Ms Xueshan QIN for her support and help in fabricating 2D PEG hydrogel and cell culture. I thank Mr Kenneth LI for his help in the characterization of microfluidic device.

I would also like to thank Mr Fei TAN, Dr Qingjun LIU, Ms Lidan XIAO, Dr Yu ZHANG, Ms Xuan LIU for their suggestions and support.

I would like to thank all the research staff and students in the Department of Health Technology and Informatics for giving me a supporting and collaborating environment throughout my studies.

Lastly, I would like to dedicate this thesis to my wife Zhiying YAO, my parents and my brother for their support and caring throughout the past three years.

Content

List of Figures

Acronyms

MSCs	Mesenchymal stem cells
PEG	Poly(ethylene glycol)
RGD	Arginine-glycine-aspartic acid
PDMS	Poly(dimethylsiloxane)
PEGDA	Polyethylene glycol diacrylate
FEM	Finite element modelling
TPM	3-(Trimethoxysilyl) propyl methacrylate
ACRL-PEG-NHS	Acrylate-poly(ethylene) glycol-NHS
PBS	Phosphate buffered saline
XPS	X-ray photoelectron spectroscopy
UV	Ultraviolet
DMEM	Dulbecco’s modified eagle medium
DAPI	4,6-diamidino-2-phenylindole, dihydrochloride
FDA	Fluorescein diacetate
PI	Propidium iodide

Chapter 1 Introduction

1.1 Motivation and Objective

Mesenchymal stem cells (MSCs) are a kind of cells that remain the ability of cell division and can also differentiate into specialized cell types such as adipocyte, chondrocyte, and osteoblast. Recent studies in tissue engineering have shown that MSCs can be potentially used for tissue regeneration in three-dimensional (3D) scaffold through control and guidance of MSCs proliferation and differentiation.

However, as there is little understanding of mechanisms for MSCs differentiation in biomaterials, it is still difficult for the regeneration of viable complex three-dimensional (3D) tissues from constructs of stem cells and biomaterials. The stem cells differentiation can be induced by soluble biochemical stimuli, such as retinoic acid, cytokines, insulin and T3 towards preferential specific lineages. Some peptides or biomolecules such as RGD and heparin can have different influence on the efficiency of stem cells differentiation. Besides the identity of biomolecules, their concentrations within biomaterial scaffold also have important effects on MSCs behaviour. Although many efforts have been spent to study the effect of these factors on MSCs behaviour, precise controlling of these factors for guiding MSCs proliferation and differentiation into high order tissues is not yet well established. Therefore, it is of particular interest to fabricate a supportive three-dimensional (3D) biofunctional biomaterial scaffold with spatial control of biomolecules

concentrations as a platform to conveniently explore the effects of specific biomolecules on MSCs adhesion, proliferation and differentiation.

Poly(ethylene glycol) (PEG) is a biocompatible material that has been applied widely in tissue engineering. The hydrophilic and uncharged properties of PEG can make highly hydrated polymer coils on biomaterial surfaces, which can avoid further proteins adhesion effectively. Due to the thermodynamic mechanism, hydrated PEG coil on the biomaterials surface makes the process of protein adsorption extremely unfavourable. This mechanism can be used to create inert polymer surfaces with further modification with appropriate biomolecules such as peptides or proteins to achieve the cell specific interactions. Therefore, PEG was chosen as the biomaterial for MSCs study in the project. PEG offers a good control of matrix structure and chemical composition, but has low biological activities. One approach creating biofunctional biomaterial is to incorporate the bioactive elements, such as protein, glycosminoglycan and peptides from the extracellular matrix to synthetic biomaterial for increasing cell adhesion and proliferation. In the project, peptide RGD was incorporated to PEG chains to study their effects on MSCs proliferation and differentiation. The incorporation was based on the reaction of –NHS group of Acryl-PEG-NHS with $–NH_2$ group of RGD peptide.

The purpose of this project is to fabricate the poly (ethylene glycol) (PEG) hydrogel with gradient presentation of cell adhesion peptide Arginine-Glycine-Aspartic (RGD) and to study the concentration effects on mesenchymal stem cells (MSCs) adhesion,

proliferation and differentiation. The gradient PEG hydrogel can integrate the identity and concentration control of biomolecules. The PEG hydrogel was fabricated by a microfluidic/photopolymerization technique. The RGD peptide could be incorporated into the PEG hydrogel to form a gradient distribution. MSCs were seeded onto the surface of 2D gradient PEG hydrogel to study the cell adhesion. The MSCs were also seeded into the 3D PEG hydrogel in situ. The effect of the gradients on MSCs viability and differentiation was also studied.

1.2 Scope and Outline of Thesis

This research project consists of the following two main parts

1) Design, simulation, fabrication and characterization of microfluidic gradient generator to establish stable biomolecule gradient

2) Fabrication the poly (ethylene glycol) (PEG) hydrogel with gradient presentation of cell adhesion peptide Arginine-Glycine-Aspartic (RGD) and to study the concentration effects on mesenchymal stem cells (MSCs) adhesion, proliferation and differentiation in 2D and 3D environment.

The thesis is divided into 10 chapters. Chapter 1 consists of an overview of this thesis. Chapter 2 provides the background of this project. Chapter 3 describes the computational fluid dynamics simulations of the microfluidic gradient and derive the optimal parameters for the fast generation of stable biomolecule gradient. Chapter 4 reports the fabrication of the microfluidic gradient device using photolithography and soft lithography techniques. The characterization of fabricated microfluidic gradient

generator is reported in Chapter 5. After fabrication of the microfluidic device, characterization was done to test the generation of gradient of dye solution. Blue dye solution was injected into the device to form the dye gradient. The dye gradient profile can be influenced by the injection velocity. Optimal parameters were selected to generate the gradient. Fluorescence labelled polymer micro-beads were also used to characterize the performance of this gradient generator device.

The MSCs culture on 2D PEG hydrogel is discussed in Chapter 6. Before MSCs culture on RGD gradient PEG hydrogel, MSCs were first cultured on two dimensional (2D) PEG hydrogel without RGD gradient. Optical microscope was used to observe cells growth. Actin and nucleus staining of MSCs were also done. The results showed that the cell adhesion number and cell adhesion area increased with the increase of RGD concentration. Therefore, RGD can promote MSCs adhesion on PEG hydrogel. There was a jump of RGD concentration range, in which adherent cell number increased dramatically. Chapter 7 describes MSCs culture on 2D RGD gradient PEG hydrogel. With the increase of RGD concentration on the gradient PEG hydrogel, the cells adhesion number and density increased. The impact of different RGD gradients on MSCs adhesion was studied. There was a jump concentration, below which fewer cells can attach on the hydrogel surface. Chapter 8 describes 3D MSCs encapsulation and culture in PEG hdyrogel with different RGD concentrations. The cells viability was tested by live/dead assay. MSCs were induced to osteogenic differentiation. Vonkossa staining of mineralization was used to characterize the osteogenisis. Chapter 9 describes MSCs encapsulation in PEG

hydrogel with RGD concentration gradient. The encapsulation was in the microfluidic gradient generator under UV light. The cells were also induced to osteogenic differentiation in osteogenisis. The effect of RGD gradient on cells viability and osteogenisis was studied. Chapter 10 is the conclusion of the thesis. The limitations of the present research and future work are also discussed.

Chapter 2: Background

2.1 Mesenchymal stem cells

Adult bone marrow can typically generate mesenchymal stem cells (MSCs). In fresh bone marrow, only 0.01-0.0001% marrow cells are mesenchymal stem cells (MSCs) (Dazzi F et al., 2006; Sakaguchi Y et al., 2005). Recently, MSCs can be also isolated from other tissues. In the tissue of adult peripheral blood, adipose tissue, skin tissue, trabecular bone, as well as fetal blood, liver, and lung, MSCs have been also successfully identified (Jackson L et al., 2007).

MSCs are typically grown as a monolayer in culture medium. Compared with many other adult stem cells, MSCs are traditionally regarded to only differentiate into cell types of their own original cells. However, many research works have shown that MSCs have the ability to differentiate into osteoblasts, chondrocytes, adipocytes, muscle, tendon/ligment and other connective tissues both *in vitro* and *in vivo* (Figure 2.1) (Caplan AI, 1989; Caplan AI, 1991; Caplan AI, 2005; Jackson L et al., 2007).

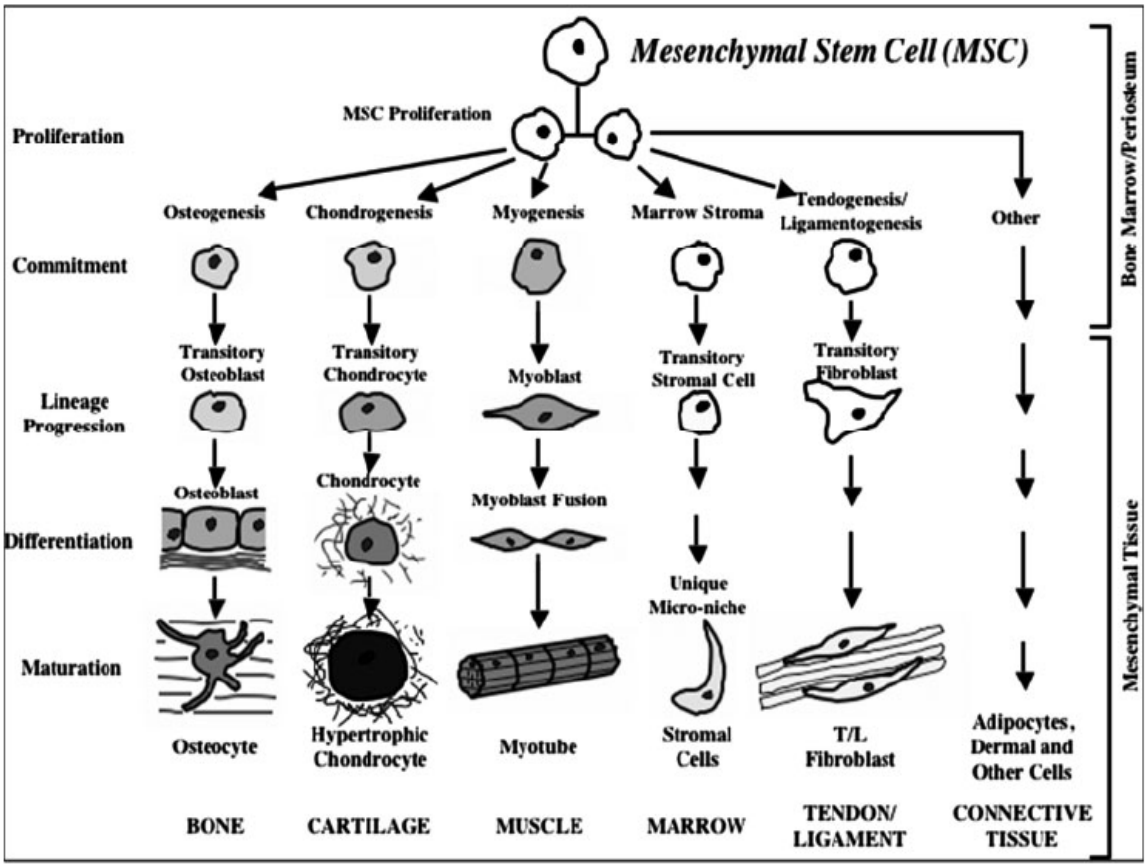

Figure 2.1 Differentiation of Mesenchymal stem cells (MSCs) (Caplan AI, 1989)

A monolayer culture with a pro-osteogenic cocktail is often used to induce osteogenic differentiation of MSCs. Standard differentiation medium for osteogenic differentiation consists of dexamethasone, ascorbic acid-2-phosphate and beta-glycerophosphate (Jackson L et al., 2007). Mineralized deposits can appear after a week. Additional calcium is also used to increase *in vitro* mineralization. Aggregation of 200,000 to 300,000 MSC in chondrogenic medium can traditionally induce chondrogenic differentiation. The chondrogenic medium includes ascorbic acid phosphate, dexamethasone, L-glutamine and TGF-betal et al. MSCs treated with cell culture medium supplemented with dexamethasone, isobutylmethylxanthine,

insulin and a PPAR-gamma agonist can induce the formation of mature adipocytes. MSCs have been also shown to differentiate into other cells, such as cardiomyocytes and neural cells (Hwang NS et al., 2009; Hoemann CD et al., 2009). However, the mechanism underlying MSCs differentiation into these cells is not clearly studied.

On the basis that MSCs can differentiate into osteocytes, chondrocytes and adipocytes, a lot of work has been done to use expanded MSCs for tissue engineering. MSCs from bone marrow were seeded on the hydroxyapatite and then implanted *in vivo* into mice, and subsequently bone formation was observed (Krampera M et al., 2006). Natural or synthetic biomaterials have also been used as carriers for MSCs delivery. Hydroxyapatite/tricalcium phosphate ceramics was loaded with MSCs *in vitro* and then implanted *in vivo*, which can lead to healing of critical segmental bone defects (Bruder SP et al., 1998). In 1994, local injection of chondrocyte suspension was first used to cure human joint cartilage defects, which has led to the development of MSCs based tissue engineering to induce in situ MSCs differentiation into cartilage (Brittberg M et al., 1994). Goat MSCs have been injected with a hyaluronan carrier into goat knees after medial meniscectomy and resection of the anterior crucial ligament. Most goats treated with MSCs in hyaluronan can induce meniscus compared with controls treated with only carrier without MSCs (Murphy JM et al., 2000). Other carriers, such as PEG hydrogel, have also been used to load with MSCs for cartilage regeneration.

MSCs can also differentiate into skeletal, smooth and cardiac muscle cells. Some

research groups treated myocardial infarction in animal models with MSCs, which showed MSCs differentiation and improved cardiac function. The results indicated that this approach could be useful for regenerating cardiomyocytes and reducing the complications of cardiac disease in humans (Min JY et al., 2000; Pittenger MF et al., 2004).

At present, MSCs have been applied in tissue engineering *in vitro*. However, *in vitro* differentiation of MSCs relies on biological factors such as growth factors and cytokines. If MSCs differentiation can be achieved without adding biological biomolecules but with the biomaterial itself, it would be more useful in the application of tissue engineering (Curran JM et al., 2006). However, it is still unknown about how material factors such as material composition and ratio can control stem cell behaviour such as adhesion, proliferation and differentiation. Therefore, it is of particular interest to study MSCs proliferation and differentiation with biomaterials.

2.2 PEG hydrogel

Tissue engineering is a new interdisciplinary field in biomedical engineering and the objective of tissue engineering is to regenerate new tissue to replace the diseased ones using cells (Patrick CW et al., 1998). In the past twenty years, tissue engineering has developed rapidly in regenerating functional tissues and organs. It is urgent to develop tissue engineering due to the increasing need of organs and tissues for transplantation.

Tissue engineering utilizes living cells as engineering materials which are cultured on scaffild platforms. These scaffolds act as synthetic extracelllular matrix (ECM), which can organize the cells in a three-dimensional structure for regenerating potential tissue (Jeanie LD et al., 2003). The requirements for the properties of biomaterials could be quite different, which are determined by the interests of tissues and the related specific applications.

Common materials used for tissue engineering are biodegradable materials such as poly(lactide-co-glycolide) (PLG) (Jain RA, 2000; Nair LS et al., 2007). PLG is a kind of FDA approved degradable polymer. However, the hydrophobic property and the severe processing conditions of PLG make it a challenge for encapsulating viable cells in 3D scaffold environment.

Instead of these hydrophobic materials, hydrated polymer materials such as hydrogels are explored as a better alternative. Hydrogels are insoluble polymer networks with swollen water. The high water content and tissue-like elasticity lead to properties which are similar to many tissues (Peppas NA et al., 2000). There are two categories of hydrogels: synthetic hydrogel and naturally derived hydrogel. Synthetic hydrogels can be reproducibly produced with specific molecular weights, block structure and crosslinking degrees. The chemistry and properties of synthetic hydrogel can be controllable and reproducible. Synthetic PEG and poly(vinyl alcohol) hydrogels are often used for tissue engineering (Nguyen KT et al., 2002; Schmedlen

RH et al., 2002). Naturally derived hydrogels are widely used in tissue engineering as they have components similar to natural ECM. Naturally derived hydrogels such as hyaluronic acid (HA), alginate and chitosan have also been used for tissue engineering (Cascone MG et al., 2001; Miralles G et al., 2001; Oerther S et al., 1999). Hydrogels are often used as synthetic extracellular matrix for 3D culture of cells.

Hydrogels can be synthesized from pure synthetic components that create an environment to limit cellular interactions. And this niche can be modified by cell secreted extracellular molecules. In contrast, adhesion peptides or proteins can be chemically bonded to hydrogels as a new method to study the interactions between cells and matrix in a controlled manner. Up to now, a lot of efforts have been spent to use hydrogels as the scaffold materials in the culture of many kinds of cells including chondrocytes, osteoblasts, valvular interstitial cells, smooth muscle cells, fibroblasts and mesenchymal stem cells (Nuttelman CR et al., 2005).

Poly(ethylene glycol) (PEG) is a biocompatible material that has been applied widely in tissue engineering, especially for fabrication of hydrogel biomaterials. PEG is a kind of highly hydrophilic polymer, which is currently approved by FDA for several medical applications. The molecular structure of PEG is shown in Figure 2.2. PEG molecule has carbon-oxygen ether bond and hydroxyl end groups, which make PEG molecule uncharged and hydrophilic.

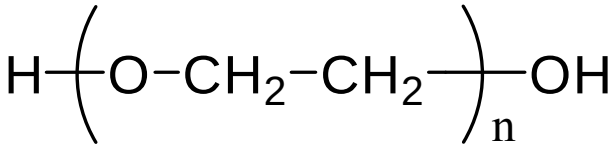

Figure 2.2 Molecular structure of PEG

As a biomaterial, PEG has several advantageous properties which result from its unique chemical structures. The hydrophilic and uncharged properties of PEG can make highly hydrated polymer coils on biomaterial surfaces, which can avoid further proteins adhesion effectively. Due to the thermodynamic mechanism, hydrated PEG coil on the biomaterials surface makes the process of protein adsorption extremely unfavourable. This mechanism can be used to create inert polymer surfaces with further modification with appropriate biomolecules such as peptides or proteins to achieve the cell specific interactions (Tessmar JK et al., 2007). Different terminal functional groups of PEG can be used for copolymerization. Figure 2.3 shows the chemical structure of PEGDA and ARCL-PEG-NHS, which are derivatives from PEG. The vinyl group in Figure 2.3 can be used for polymerization in the existence of radicals while the –NHS group can incorporate some biological peptides or proteins to make PEG bioactive.

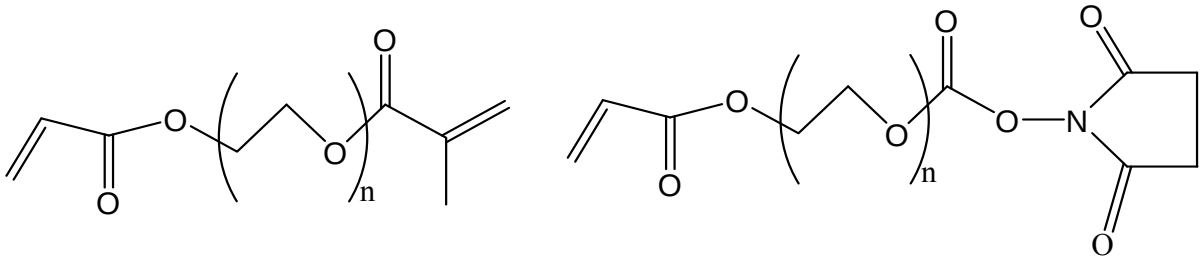

PEGDA ACRL-PEG-NHS

Figure 2.3 Molecular structures of PEGDA and ACRL-PEG-NHS

PEGDA and ACRL-PEG-NHS, as well as their derivatives, can be used to for hydrogel polymerization. PEG hydrogel has been widely used in tissue engineering, especially in culture of Mesenchymal stem cells (MSC) (Tessmar JK et al., 2007). The main focus of these research works is to incorporate some specific biomolecules to the PEG chain to make the PEG hydrogel more suitable for MSCs proliferation and differentiation. The RGD (arginine-glycine-aspartic acid) sequence is a highly conserved sequence that is found in many adhesion proteins. RGD sequences could be tethered to the photopolymerizable acrylate PEG molecule (PEGDA) to promote MSCs attachment. RGD-modified PEGDA hydrogels can dramatically improve MSCs attachment and spreading (Nuttelman CR et al., 2005; Yang F et al., 2005). Ethylene glycol methacrylate phosphate (EGMP) which is a molecule for promoting osteogenic differention has been grafted to the PEG chain in the research of KS Anseth group. EGMP can sequester the important cell adhesion protein osteopontin, and promote human MSCs adhesion, spreading and osteogenic differentiation (Nuttelman CR et al., 2006). In the same research group, heparin was modified with methacrylate groups and copolymerized with PEGDA to form functional PEG

hydrogel. It was found that heparin could promote human MSCs adhesion, proliferation, and osteogenic differentiation (Benoit DSW et al., 2005). Elisseeff J has done the research of chondroitin sulphate (CS) based PEG hydrogel niches for chondrogenic differentiation of MSCs. The results showed the PEG hydrogel with CS had an enhancement of both chonrogenic gene expressions and cartilage specific matrix production compared with the control groups for PEG hydrogels without CS (Varqhese S et al., 2008). The above research works indicate that PEG hydrogel provides a good inert platform to study MSCs proliferation and differentiation with specific biomolecules. Therefore, PEG hydrogel is chosen to study MSCs behaviour by incorporating specific biomolecules in our project.

2.3 Arginine-Glycine-Aspartic (RGD)

Arginine-Glycine-Aspartic (RGD) is a tripeptide. The molecular structure of RGD is shown in Figure 2.4. RGD peptide is first identified by Ruoslahti and his collaborators as amino acid sequence for promoting cell adhesion about 20 years ago (Pierschbacher, MD et al., 1984). The RGD sequence as an adhesion promoting motif can be found in many materials such as collagen, fibronectin, laminin and other ECM proteins (Cutler SM et al., 2003; Pierschbacher, MD et al., 1984). RGD peptide is widely distributed in organisms, and it is also the most effective peptide sequence for promoting cell adhesion. RGD has been widely used in biomaterial scaffold fabrication. The RGD sequence has important biological impact on cell anchoring, spreading and survival.

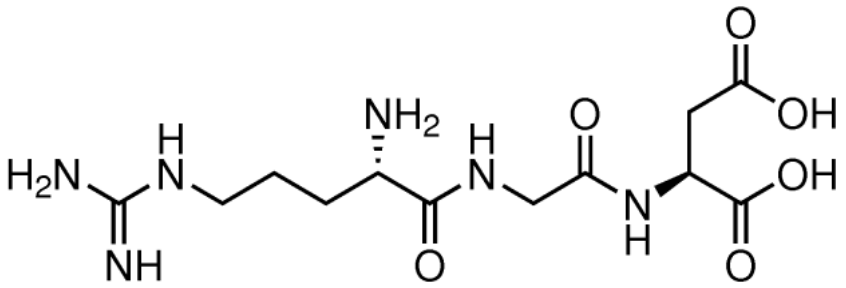

Figure 2.4 The molecular structure of RGD peptide

The RGD sequence is the ligand for integrin-mediated cell adhesion. The cell adhesion includes four reactions including cell attachment, cell spreading, actin-skeleton formation and focal adhesion formation (Chen CS et al., 2003). In organisms, the contacts between cells and surrounding ECM are mediated by cell adhesion receptors. The integrin family of cell adhesion receptors and their ligands play important roles in regulating cell behaviors, such as cell adhesion, migration, proliferation and differentiation. Integrins contain two distinct transmembrane subunits, called α (alpha) and β (beta) subunits. To date, 18α and 8β have been characterized. The combination of α and β forms 24 different unique integrins (Hynes R, 2002; Van Der Flier A et al., 2001). For integrins, there are two main functions including attachment of the cell to the ECM and signal transduction from ECM to the cell. For RGD sequence, it is a very important ligand for the integrins. About half of the 24 integrins have the ability to bind with the RGD sequence. These integrins are α3β1, α5β1, α8β1, αIIbβ3, αvβ1, αvβ3, αvβ5, αvβ6, αvβ8, and to some extent α2β1 and α4β1 (Pfaff M, 1997; Takagi J, 2004).

As mentioned above, the integrin-mediated cell adhesion includes four reactions-cell

attachment, cell spreading, actin-skeleton formation and focal adhesion formation. For the cell attachment, the cells contact the surface of substrate and some ligands bind to cells. Next, the cell body becomes flat and the plasma membrane of cells begins to spread on the surface. After that, cell spreading results in the actin-skeleton formation. Finally, focal adhesion occurs between ECM and the actin cytoskeleton (Hersel U et al., 2003). The cell adhesion is a complicated process between integrins and ligands.

Biofunctional materials are required to provide cells structure support as well as improve cellular response such as cell adhesion, proliferation and differentiation. A lot of research has been done to study the effect of RGD on different cell behaviors in biomaterials. Mann et al. studied the interaction of RGD peptide with smooth muscle cells, endothelial cells and fibroblast cells (Mann BK et al., 1999) and the results indicated that RGD can increase cells interaction with biomaterials. Myoblasts are cultured on a RGD-coated alginate hydrogel surface in the research of Rowley et al. (Rowley JA et al., 2002) and it is found that RGD can promote cell adhesion, spreading and proliferation. The effect of RGD on rat calvarial osteoblasts was studied by Burdick et al. (Burdick JA et al., 2002), results of which showed that the osteoblast attachment and spreading could be improved in a dose-dependent manner.

The effect of RGD peptide on stem cells differentiation has also been studied. A lot of research has shown that biomaterials modified with RGD containing peptide can

promote osteogenic differentiation in osteogenesis medium (Shin H et al., 2005; Yang F et al., 2005; Zreiqat H et al., 2002). RGD can also promote chondrogenic differentiation of stem cells in chondrogenesis medium (Chang JC et al., 2009; Hwang NS et al., 2006; Salinas CN et al., 2008). The RGD peptide can play an important role in promoting stem cells differentiation as well as maintaining stem cells viability. Therefore, RGD peptide is chosen to be incorporated to PEG hydrogel to study the specific interaction with MSCs.

2.4 Cell interaction with biomaterials

In native tissues, cells are incubated in a 3-dimensional (3D) microenvironment which includes soluble molecules such as cytokines and growth factors and non-soluble factors which are mainly ECM. The microenvironment can provide structural support and also control a lot of biological processes such as directing cell adhesion, proliferation, and differentiation (Gaarcia AJ, 2005; Shin H, 2007). For biomaterials, it provides a synthetic environment, which replaces the function of natural ECM of cells. Functional biomaterials can mimic the native environment of cells. The basic requirement for biomaterials is the biocompatibility, which is the ability of a material without toxicity or injurious effect on cells or tissues. The biocompatibility is influenced by the properties of biomaterials such as mechanical property and hydrophilicity. The properties of biomaterials can be regulated based on their physical and chemical properties as shown in Figure 2.5 (Yliperttula M et al., 2008). Physical properties of biomaterials include the mechanical and macroscopic features of the biomaterials et al. while the chemical properties include the

hydrophilicity, pH and functional end groups on biomaterials surface et al. Both physical and chemical properties of biomaterials have important impact on cells behavior (Allen LT et al., 2003). In addition, bioactive molecules such as ECM molecules can be also used to modify biomaterials and affect cells microenvironment (DeMali KA et al., 2003; Shin H, 2007).

In microenvironment, the interactions between cells, ECM and soluble factors can regulate cell behavior (Gaarcia AJ, 2005; Goodman SL et al., 1996). The interaction manner between biomaterials and cells partially depends on the source of biomaterials. For natural biomaterials, they can interact with cells directly. As to the interaction between ECM and cells, ECM can affect cell behaviors in two ways. One is that the cell-ECM interaction can directly control cell behaviors by receptor-mediated signaling. The other way is that cell-ECM reaction can control the mobilization of growth factors, thus modulating cell behaviors. For the interaction between growth factors and cells, the ECM plays an important role in the immobilization of growth factors. For growth factors-ECM interaction, it can control cell behaviors in many ways. For example, the direct binding of growth factors to the ECM can affect the local concentration and the biological activity of growth factors (Rosso F et al., 2004).

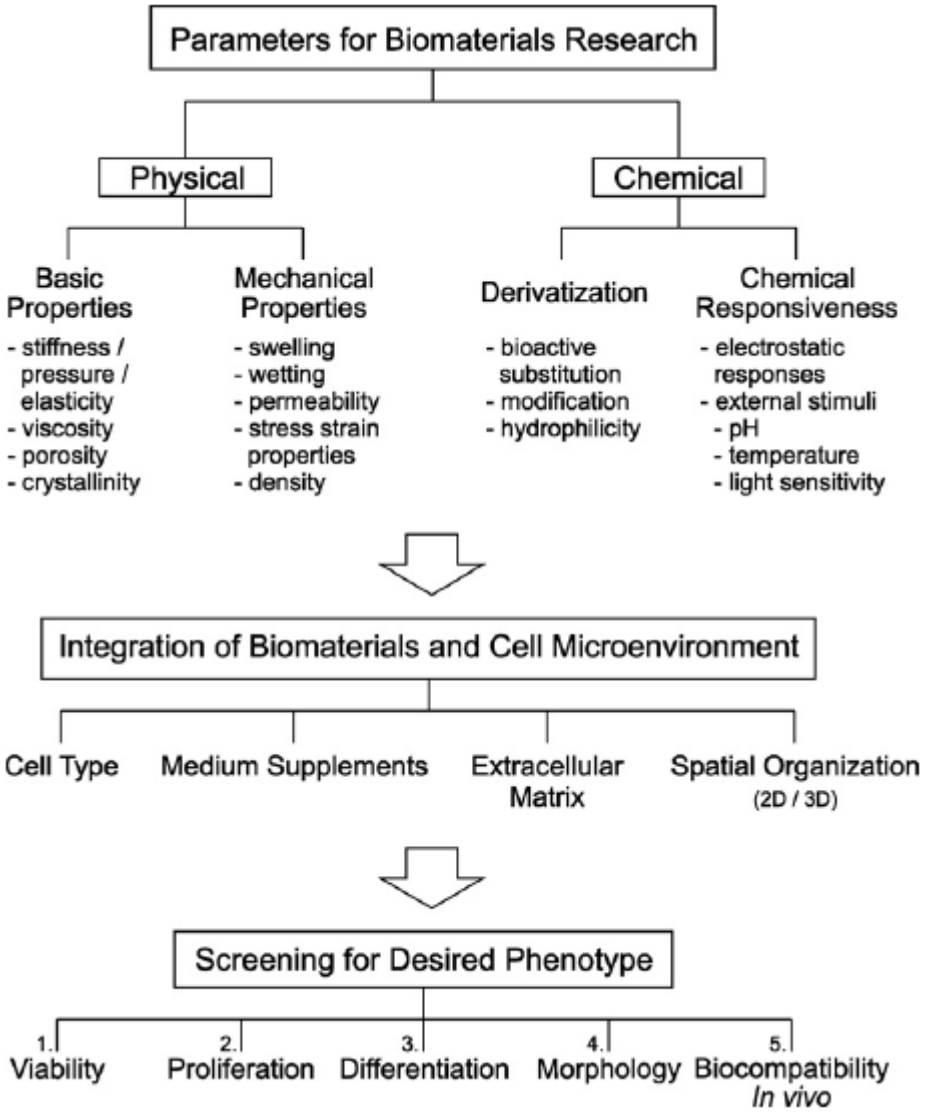

Figure 2.5 The design of biomaterials that can significantly affect cellular behavior and microenvironment (Yliperttula M et al., 2008)

The response of cells to biomaterials is often initially controlled by cell contact and adhesion to the biomaterial surface. The cell adhesion to biomaterials is often regulated by proteins that are either part of the biomaterials or adsorbed onto the surface of the biomaterials from the culture media or secreted by cells (Fittkau MH et al., 2005; Yamada Y et al., 1992). The proteins such as fibronectin, laminin and collagen can interact with specific receptors on the surface of the cells (DeMali, KA et al., 2003). After adhesion, cells can divide and the activation of the intercellular adhesive complexes can be initiated by integrin binding of the ECM proteins (Fittkau MH et al., 2005; Massia SP et al., 2001).

Biomaterials play an important role in providing a synthetic environment to regulate cells behaviours. The biomolecular recognition of materials by cells is important. There are generally two strategies to enhance the interaction of cells and biomaterials. One strategy is to make biomaterials bioactive by immobilizing soluble bioactive molecules such as growth factors into the biomaterials carriers. In this case the biomolecules can be released from the biomaterials later (Babensee JE et al., 2000; Whitaker MJ et al., 2001). Another approach is to do the physical, chemical and biological modifications to biomaterials. Chemical modifications to biomaterials can change surface properties and microenvironment structure of biomaterials, which can further regulate cell behaviours by manipulating the signal pathways in cells. A lot of biomaterials modification methods have been used to improve the interaction between cells and biomaterials, such as surface modification with uniform chemical grafting of biomolecules or selectively patterning, and bulk modification of

biomaterials.

The surface chemistry and topography of biomaterials are important parameters that influence protein adsorption and cell interaction. A lot of studies have shown that the surface modification of biomaterials with bioactive molecules is an effect way to make bioactive materials. Some proteins such as fibronectin (FN), vitronectin (VN) and laminin have been coated or chemically incorporated to biomaterials to promote cell adhesion and proliferation (Li X et al., 2008; Steele JG et al., 1995). Some short peptide fragments which are from signalling domains of proteins are found to promote cell adhesion (Humphries MJ et al., 1986). These adhesion peptides have been also used for surface modification of biomaterials. The most commonly used peptide for surface modification is RGD peptide, which is from fibronectin (FN) and laminin (LN). As mentioned in 2.2, PEG hydrogel is often used in tissue engineering. However, PEG is an inactive biomaterial without protein adsorption. RGD peptide can be then incorporated into the PEG hydrogel to improve cell adhesion (Yang F et al., 2005). Other peptides such as Arg-Glu-Asp-Val (REDV) have been also used for surface modification (Hubbell JA et al., 1991; Mcmillan R et al., 2001).

Growth factor is a kind of powerful regulator of cellular behaviours including cell proliferation, migration and differentiation. There are many kinds of growth factors such as fibroblast growth factor (FGF), transforming growth factor (TGF) and Insulin-like growth factor (IGF) et al. These growth factors can be used for surface modification of biomaterials to improve the interaction with cells (Kokubu E et al.,

2009; Mann BK et al., 2001).

The patterning of biomaterials can be used to change the topography to increase the bioactivity of biomaterials. Recent developments in micro and nanofabrication techniques have provided possibilities in studying and controlling the cells behavior. These techniques allow for the controlled design of highly reproducible features on a cellular level as well as creating spatially and temporally patterned biomaterials structures. Figure 2.6 shows a cell patterning method with selective molecular assembly patterning (SMAP) (Lussi JW et al., 2004). Proteins adsorbed on the SiO_2/TiO_2 surface forming patterned proteins. Cells were then cultured on the patterning surface. Selected areas with adsorbed proteins had increased interaction with cells.

Surface modification with biomolecules controls cell behaviour on the surface of biomaterials. However, surface modification has some limitations. As surface modification can not modify the bulk properties of biomaterials, the modified biomaterials may not be directly used as tissue engineering scaffolds. With the bulk modification of biomaterials, the cell signalling biomolecules are incorporated into the biomaterials and the signalling sites are not only present on the surface but also in the bulk of the biomaterials. The cell adhesion peptides such as fibronectin and RGD have been introduced into three dimensional networks through chemical bonding. For example, a lot of research used RGD peptide to incorporate into PEG hydrogel to increase the cell adhesion between cells and PEG hydrogels (Yang F et al., 2005;

Burdick JA et al., 2002). In our present research, bulk modification of PEG hydrogel with RGD peptide was done to increase the interaction of PEG hydrogel with biomaterials.

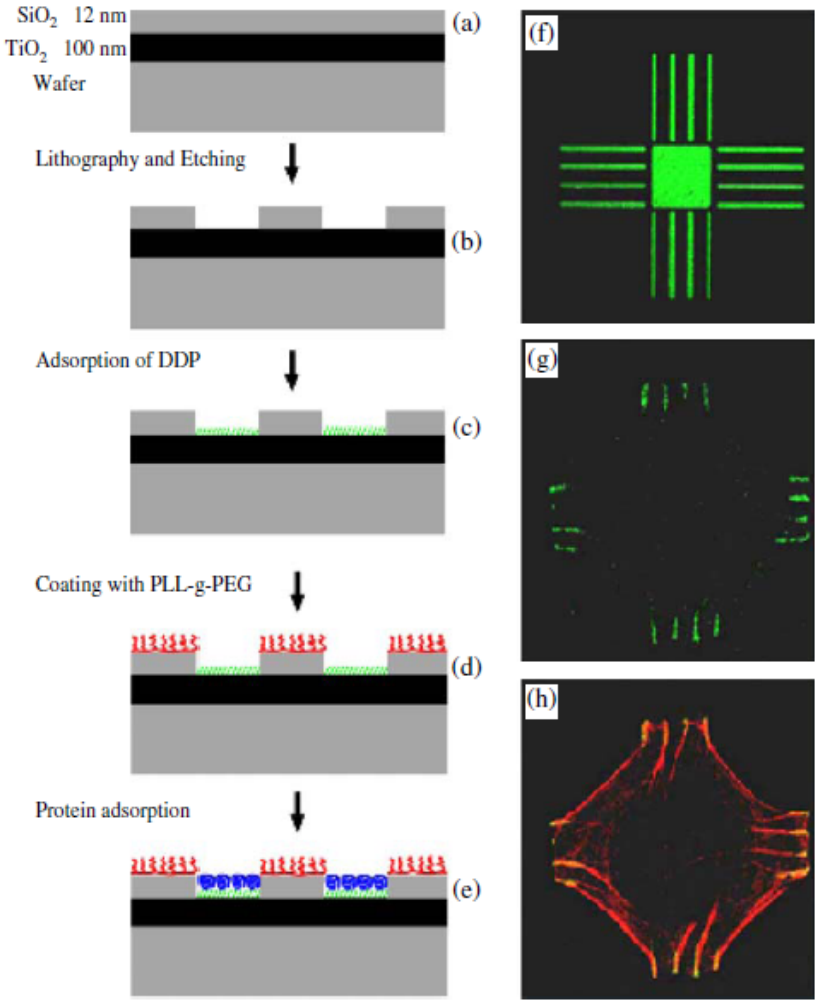

Figure 2.6 The SMAP process converts an inorganic pattern contrast (produced by sputter coating, photolighography and etching) into a chemical pattern (schematics a and b). The TiO2/SiO2 patterned surface is dipped into an aqueous solution of methyl-terminated dodecyl phosphate (DDP). The DDP molecules form an oriented self-assembled monolayer on TiO2, rendering it hydrophobic (c). There is no interaction between DDP and the SiO2 surface, which is left completely bare. After rinsing with water, PLL-g-PEG adsorbs from a buffered solution to the bare SiO2 and making the background resistant to the adsorption of proteins (d). The chemical contrast between hydrophobic and protein-resistant areas can then be converted into an adhesive/biofunctional contrast by simply exposing the surface to proteins (e). The fibronectin contrast was visualized by immunofluorescence (f). Single cells were shown to form focal adhesions (vinculin stain) co-localized with f-actin fibers (rhodaminephalloidin stain) (g and h) (Lussi JW et al., 2004)

2.5 Gradient technology

It is very important to generate chemical agent or biological molecule gradient in many biological and chemical processes. It is a challenge to generate well-defined gradients to study chemotaxis on scales of a few microns to a few hundred microns. Chemotactic cells can sensitize concentration differences as low as 2% between the front and back of the cell, which makes particular challenges. Gradients with resolutions 10-100 μm in the order of a single cell are needed (Jeon NL et al., 2000).

In biology, gradients are an important signalling mechanism for guiding the growth, migration, and differentiation of cells within the dynamic, three-dimensional environment of living tissue. Gradients play an important role in many phenomena including development, inflammation, wound healing, and cancer therapy. Interest in these phenomena has led to the development of numerous *in vitro* methods for exposing cells to chemical gradients, which have revealed that gradient signalling could be an intricate, highly regulated process. The ultimate cellular response is determined by the concentration profiles and spatial distribution characteristics of the gradients, which have great effects to the cells exposed (Keenan TM et al., 2008).

The traditional methods for generating gradients in solution are to use a pipette tip or a reservoir in a gel (Jeon NL et al., 2000). These methods are not ideal for gradient research, as they can not produce precise, user-defined gradients with tailored spatial and temporal profiles. The chemical gradients generated by traditional methods often evolve unpredictably or uncontrollably over space and time, and can be difficult to

characterize quantitatively. The gradients form and dissipate within a few hours, greatly limiting the cell types and questions that can be studied.

Molecules diffuse unrestricted in free solution. The formation of gradients requires constant supply and removal of molecules at certain spatial locations (Jeon NL et al., 2000). Microfluidic technology can be used to control the fluids precisely with significant levels of automation in the micrometer dimensions to create gradients in the microscale for cellular study. Recently, a lot of microfluidic devices have been designed and developed for the generation of predictable and reproducible gradient. Many devices offer significant controlling over the shape and temporal characteristics of the gradient.

Whitesides group has generated solution and surface gradients using microfluidic systems (Jeon NL et al., 2000). The microfluidic system was fabricated with PDMS and substrate through the photolithography and soft lithography techniques. In the fabricated device, there are two or three inlets and one outlet. There are also many microchannels, which repeatedly split and recombined to form gradients. The picture of the device is shown in Figure 2.7.

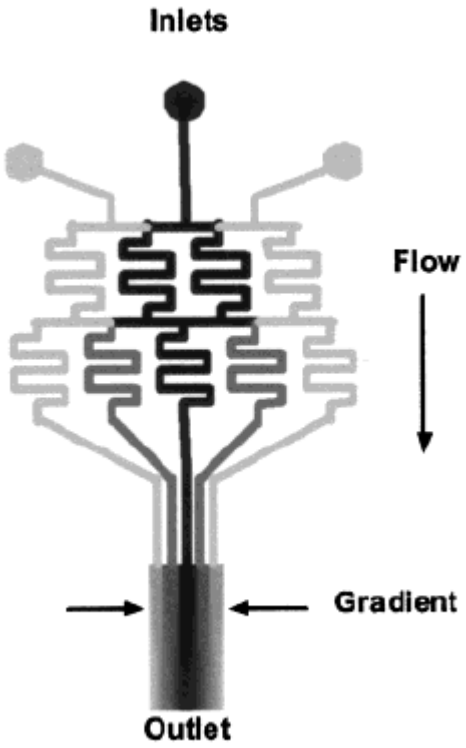

Figure 2.7 Microfluidic device for generating gradient solution (Jeon NL et al., 2000)

This kind of device has been used to generate biomolecule gradients to study cell behaviours Jeon and colleagues employ this device to study the effects of soluble biomolecule gradients on neutrophil migration, neural stem cell differentiation, breast cancer cell chemotaxis and rat intestinal cell migration (Chung BG et al., 2005; Gunawan RC et al., 2006; Lin F et al., 2005). The device has also been used to create substrate-bound biomolecule gradients to direct the growth of hippocampal neurons and examine cell cycle progression and exit in intestinal cells. Robert Langer group first fabricated a gradient PEG hydrogel using this kind of device (Burdick JA et al., 2004). Two PEG macromer/initiator solutions were injected into this device so that a polymer solution gradient was generated in the outlet chamber and then photo-

polymerized into hydrogel under UV light. The fabricated PEG hydrogel can also form a gradient mechanical strength if the inlets have different PEG concentrations. Zaari N and Wong JY have used PEG hydrogel with gradient mechanical properties to study the influence of mechanical property gradient on vascular smooth muscle cells. Results show that PEG hydrogel surface with higher mechanical strength promote the cells attachment and proliferation (Zaari N et al., 2004).

The above research works indicate the gradients fabricated from microfluidic devices are very useful in cells related research. The gradient PEG hydrogel is fabricated in our project to realize the control of specific interaction with RGD peptide. The microfluidic device is used as the platform to achieve concentration gradient profiles of RGD peptide. Moreover, the gradient PEG hydrogel in previous research works is only used for cell culture on the surface. If cells like MSCs can be seeded into the PEG hydrogel in situ, it will be more useful to study the interaction of cells with biomaterials, such as cells proliferation and differentiation.

Chapter 3 Simulations of Microfluidic Gradient Generator

Abstract

A microfluidic gradient generator for generation of PEG-RGD continuous gradient is designed. CFDRC finite volume computational fluid dynamics software was used to simulate the generation of RGD gradient in PEG solution and derive the optimal parameters for rapid generation of stable bio-molecule gradient. Simulation results show that the diffusion coefficient of fluid and the pump driving velocity have important impacts on gradient profiles. Large diffusion coefficient could enhance the mixing process and make the concentration profiles in the final cell culture chamber more linear. A high driving velocity could generate step concentration profiles at the end of the cell culture chamber due to insufficient mixing process, while a lower one could generate a more linear profile.

3.1 Introduction

The microfluidic gradient generator was first proposed by Whitesides (Jeon NL et al., 2000). This kind of microfluidic device could generate large concentration gradients over small length scales. Generally, the microfluidic device consists of several channels connected to a chamber in which the molecule concentration gradient is generated. Laminar flows of liquids with different concentrations flow side-by-side along the channels. In the flow process, diffusive mixing occurs in the continuous laminar flow system perpendicular to the flow direction.

In our project, a microfluidic gradient pattern was designed using CAD software. The microfluidic gradient design was shown in Figure 3.1. There were two inlets and one outlet in the pattern. Seven branched microchannels were connected to an outlet chamber. The width of the microchannel was 100 μm, while the total width of the chamber was 1700 μm. The height of the channel was 150 μm. With the microfluidic gradient pattern, Computational fluid dynamics simulations was done to explore the generation of biomolecule gradient and the effects of different parameters such as diffusion coefficient and the driving velocity on the generation of rapid and stable gradient.

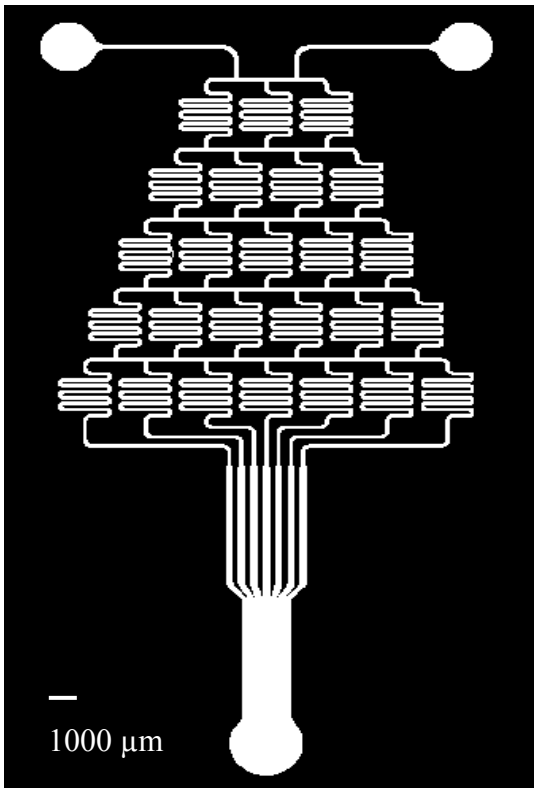

Figure 3.1 Microfluidic gradient generator pattern

3.2 Fluid Simulation Model

The simulation of the microfluidic gradient generation system was analyzed using computational fluid dynamics simulations. Figure 3.2 shows the 2D microfluidic model. This model consisted of the following elements: seven inlets (microchannels), one cell culture chamber for gradient generation, and one outlet. A finite volume software CFDRC was used for the simulations. The CFDRC software contained several modular programs such as CFD-GEOM, CFD-ACE, CFD-VIEW, CFD-MICROMESH and CFD-VISCART. Three of these programs, namely CFD-GEOM, CFD-ACE and CFD-VIEW were used.

The CFD-GEOM program was used to create the model geometry. The grid density

was set as 10,000/mm^2, which was an optimal value. If the grid density was more than 10,000/mm^2, it took more time for the simulation and there was no difference in the simulation results (Within 0.1%). If the grid density was less than 10,000/mm^2, the simulation results were less accurate. Hence, the grid density 10,000/mm^2 was selected.

The geometry created in CFD-GEOM was then imported into the CFD-ACE program for the simulation. Two application modules of the CFD-ACE program were selected for this CFD-simulation, namely the flow module and chemistry/mixing module. The flow module enabled the type of flow motion to be determined and the velocity profile to be computed using the Navier-Stokes equations for an isothermal incompressible fluid. The second module allowed the PEG-RGD concentration gradient with diffusion coefficient *D* to be calculated through Fick's law, using the velocity calculated from the Navier-Stokes equations as an input. The system was approximated to a 2D system since all of the microchannels were about 100 μm deep. The equations used for fluid dynamic analysis of the system were:

$$\rho\left(\frac{\partial u}{\partial t} + u \cdot \nabla u\right) = -\nabla p + \eta \nabla^2 u + f$$

$$\nabla \cdot u = 0$$

where u is the velocity vector, ρ is the fluid density, η is the dynamic viscosity, p is the pressure, f represents body forces (per unit volume) acting on the fluid and ∇ is the *del* operator. The first equation is the momentum balance, and the second is the equation of continuity for incompressible fluids. And the equation used for concentration analysis was:

$$\frac{\partial C}{\partial t} + \nabla \cdot (-D\nabla C) = -u \cdot \nabla C$$

where C is PEG-RGD's concentration and u is the velocity vector calculated in the Fluid module.

In the CFD-ACE program, the temperature was set to 300 K. In literature, the diffusion coefficient (D) of PEG was around 1×10^{-10} m^2/s (Costin CD et al., 2003). The exact value depends on the PEG molecular weight and experimental parameters. Therefore, diffusion coefficient 1×10^{-10} m^2/s was used in CFD-ACE. In the literature, the viscosity of PEG solution was around 24 mpa.s (Kirincic S et al., 1999). Then, the seven input concentrations C_i (i=1, 2, 3, 4, 5, 6, 7) were initially set at 0mM, 0.125mM, 0.25mM, 0.375mM, 0.5mM, 0.625mM, and 0.75mM to enable the effects of the PEG-RGD diffusion coefficient on the concentration profile to be evaluated. At the same time, various simulations were carried out with different values of D ranging from 1×10^{-7} to $1\times10^{-10}m^2/s$ at the same flow rate $5\times10^{-3}m/s$. Next, the average velocity was set as the following five values - $5\times10^{-4}m/s$, $2.5\times10^{-3}m/s$, $5\times10^{-3}m/s$, $1\times10^{-2}m/s$ and $2.5\times10^{-2}m/s$ with the same D $1\times10^{-10}m^2/s$. The fluid dynamic boundary conditions imposed within CFDRC were slip at all walls and zero pressure or resistance to flow at the outlet of the device. The convergence point was 10^{-4} with the average iterative times 30.

The simulation results obtained from the CFD-ACE module were then studied using the CFD-VIEW program. A line was drawn across the channel and then the gradient profiles on the line were plotted.

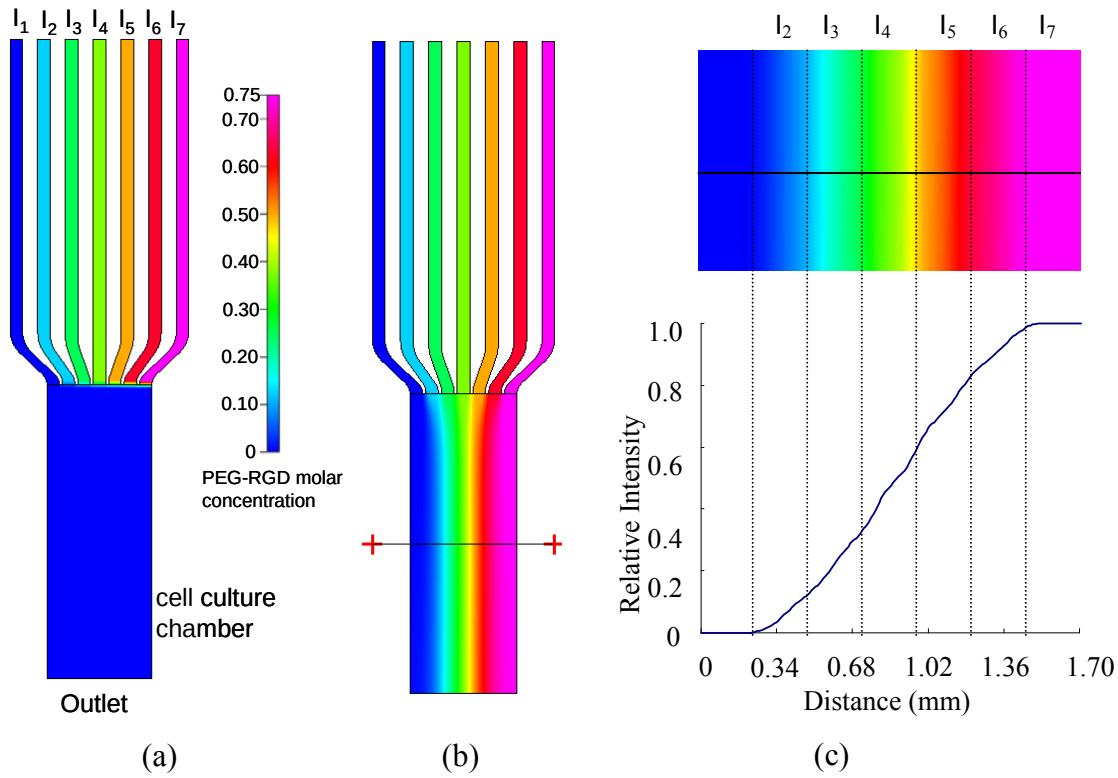

Figure 3.2 CFD-simulation (a) Grid model and boundary conditions used for 2D CFD-simulation, I_i (i=1, 2, 3, 4, 5, 6, 7) represented seven different inlets, (b) Simulation of relative intensity profiles of gradient formation with the velocity of 8×10^{-3} m/s and the diffusion coefficient of 10^{-8} m^2/s, (c) The gradient curve of PEG-RGD concentrations according to the distance across the cell culture chamber.

3.3 Results and discussion

3.3.1 Mixing effect

Using CFDRC software, the velocity profiles and diffusion efficiencies in the microfluidic system were analyzed in details. Figure 3.2 shows the simulation result of relative intensity profiles of gradient formation with the velocity of 5×10^{-3} m/s and the diffusion coefficient of 1×10^{-10} m^2/s. The mixing effect was affected by several parameters, such as, the diffusion coefficient of fluid, fluid velocity, and the

number of cycles of curving microchannels. Our analysis here is mainly focused on the effects of the diffusion coefficient (D) and fluid velocity.

3.3.2 Gradient development

In the simulation, the gradient development of PEG-RGD solution was first studied as shown in Figure 3.3. When the effect of inletting velocity was much larger than that of diffusion, PEG-RGD in the right channel could not immediately squeeze out the buffer near the side wall until later. Simulation results of the PEG-RGD concentration distribution in the culture chamber at different time were described in Figure 3.3(a), and the relative intensity profiles at the end of the chamber were shown in Figure 3.3(b). Initially, PEG-RGD concentration in the center of the chamber was quite high, and in time PEG-RGD with different concentrations presented themselves, in the chamber with the settled track. Meanwhile, PEG-RGD apparently would diffuse into the near buffer. Finally, the smooth concentration gradient of PEG-RGD would become stable at the defined time.

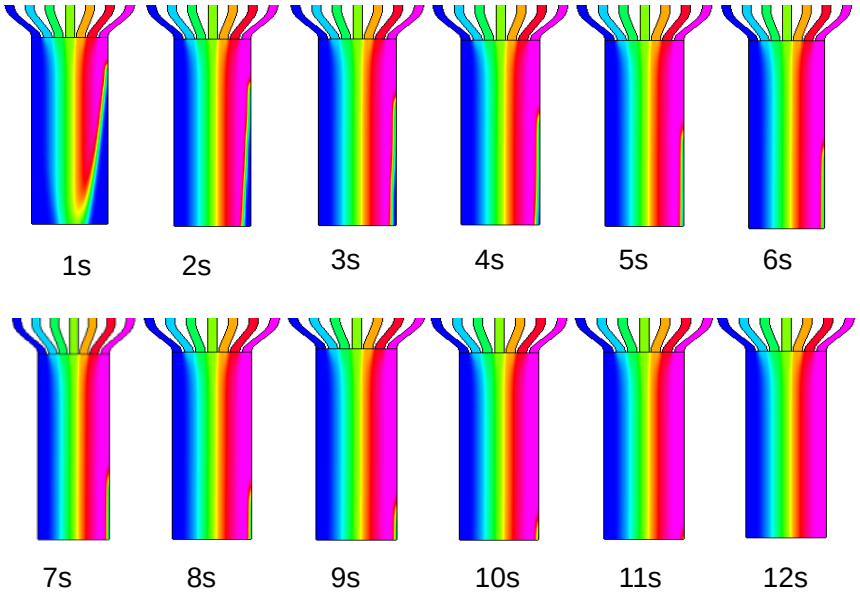

(a)

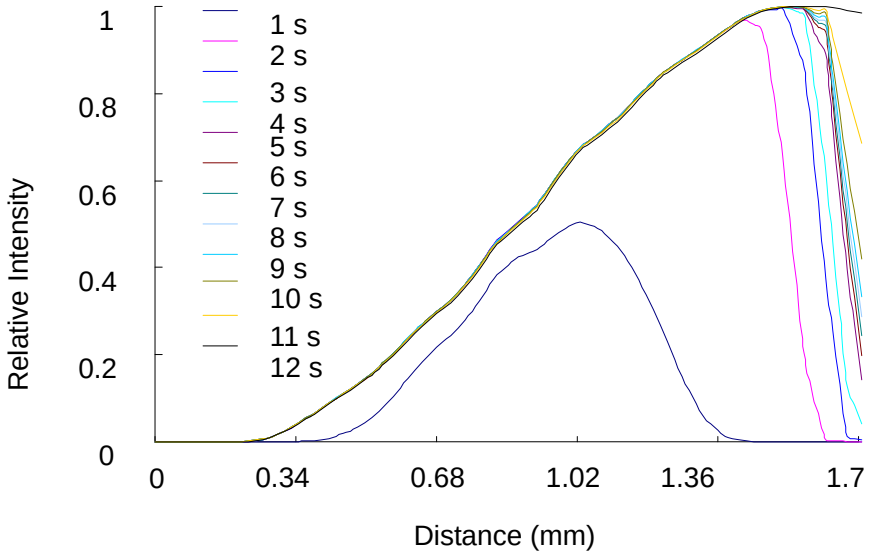

(b)

Figure 3.3 Gradient development with the inletting velocity of 5×10^{-3} m/s and the diffusion coefficient of 1×10^{-10} m^2/s. The inlet concentrations were 0 and 0.75mM respectively, and the abscissa represents the distance across the cell culture chamber. (a) Images of time sequence, (b) Relative intensity profiles according to time sequence.

3.3.3 Effect of diffusion coefficient

In the simulation, it was found that the diffusion coefficient (*D*) had important impact on gradient profiles. The simulation was done using different D ranging from 1×10^{-7} to 1×10^{-10} m^2/s as shown in Figure 3.4. Among the four diffusion coefficients, the largest value 1×10^{-7} m^2/s generated a relatively smaller and flatter gradient profile, which was due to the over mixing of PEG solution. The other three diffusion coefficients generated somewhat larger linear gradient profiles. Similar results were obtained by Dertinger et al. (Dertinger SKW et al., 2001) and Tirella et al. (Tirella A et al., 2008) using numerical methods.

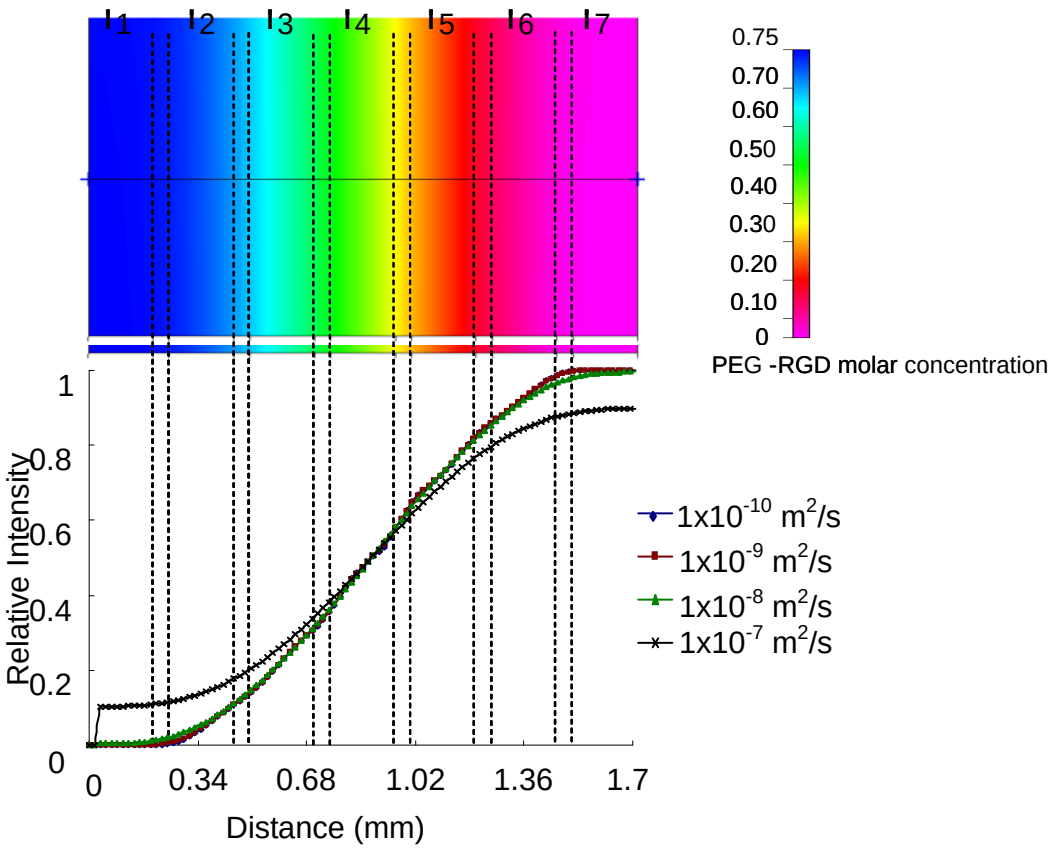

Figure 3.4 Modeled relative intensity profiles in the cell culture chamber 1.7mm from the microfluidic inlets for various values of the diffusion coefficient, *D* in m^2/s. The inlet concentrations were 0 and 0.75mM respectively, and the abscissa represented the distance across the cell culture chamber. The velocity here is 5×10^{-3} m/s

3.3.4 Velocity effect

Besides the diffusion coefficient, the velocity also had the important impact on gradient profiles. The velocity effects on the gradient generation were then explored. The simulation results with different velocities were shown in Figure 3.5. The Reynolds number was also calculated basded on the equation $Re=\rho VL/\mu$, where ρ is the density, V is the velocity, L is the characteristic length and μ is the viscosity. The calculated value of Reynolds number ranged from 0.094 to 4.7. As the Reynolds number was very small, the flow in the channel should be laminar. As shown in Figure 3.5, higher velocity larger than 5×10^{-3} m/s could generate a concentration profile with more obvious step-like structure, while a lower one could generate a more linear profile. It took more time for solution with lower velocity completing the channel. So the solution with lower velocity had more time for the mixing and more linear gradient can be generated.

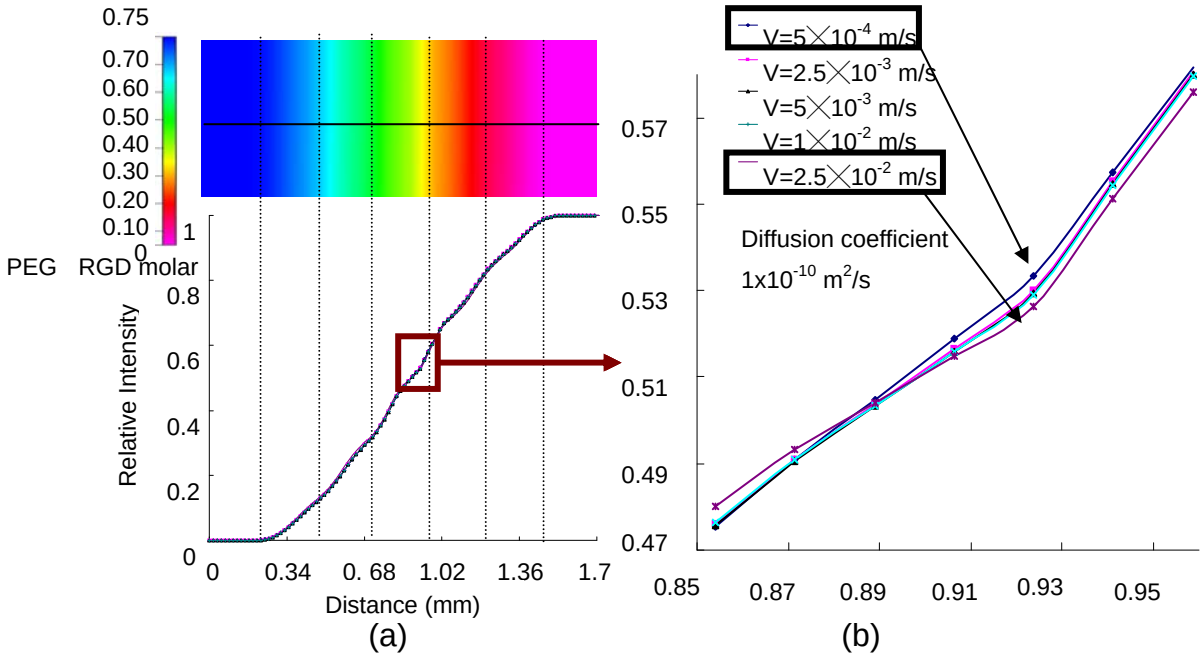

Figure 3.5 Modeled relative intensity profiles in the cell culture chamber 1.7mm from the microfluidic inlets for various values of the inletting velocities, V in m/s. The inlet concentrations were 0 and 0.75mM respectively, and the abscissa represented the distance across the cell culture chamber. The diffusion coefficient D : 1×10^{-10} m^2/s

3.3.5 Peclet number effect

Peclet number (Pe) is a dimensionless number. Pe is defined as LV/D, where L is the characteristic length, V is the velocity and D is the diffusion coefficient. As discussed in 3.3.3 and 3.3.4, the diffusion coefficient and velocity have important impact on gradient profiles. The combined effects of diffusion coefficient and velocity can be represented by peclet number. Different peclet numbers would generate different gradient profiles. The effect of Pe numbers on gradient profiles is shown in Figure 3.6. We studied the effect of five Pe numbers, ranging from 1.5×10^2 to 1.5×10^6. If the Pe number is less than 1.5×10^4, more linear gradient profiles can be generated. If the Pe number is larger more than 1.5×10^5, the gradient profiles have some step-like

appearance, which are resulted from inadequate mixing.

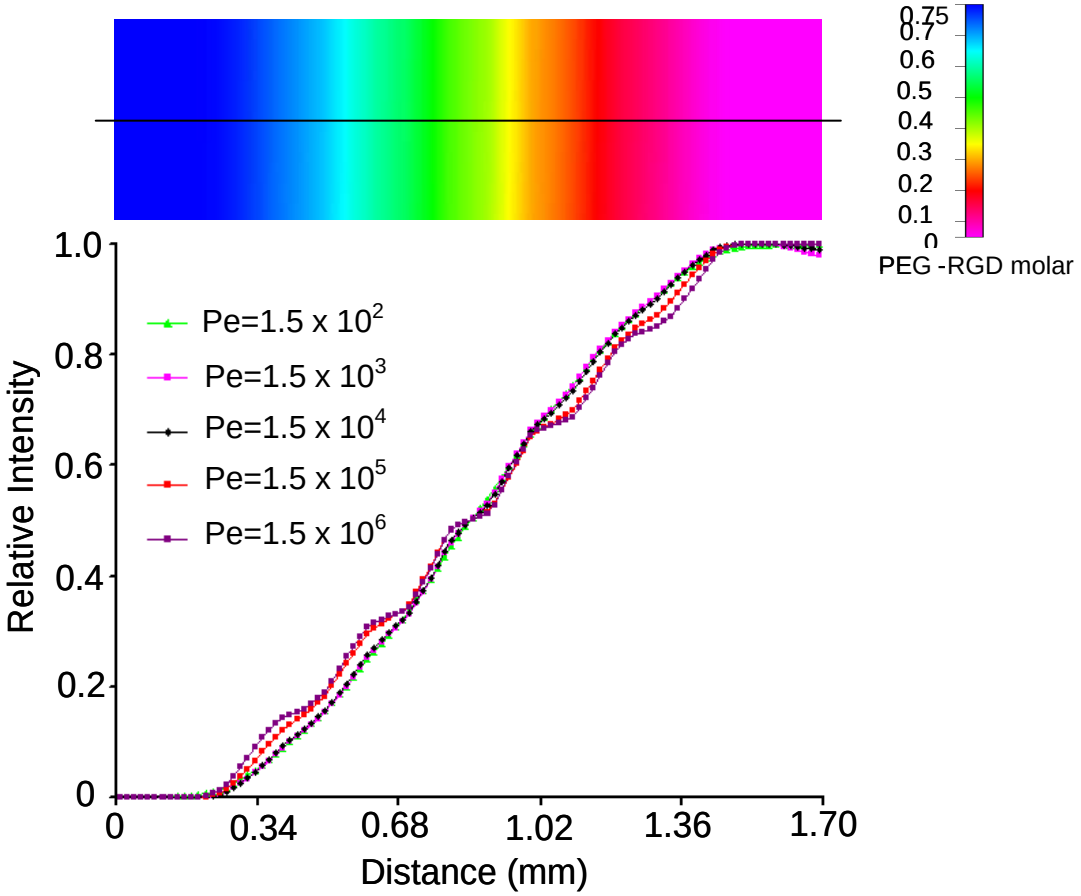

Figure 3.6 Effect of Peclet number (Pe) on gradient profiles across the cell culture chamber

Chapter 4 Fabrication of Microfluidic Device

Abstract

Microfabrication methods including photolithography and soft lithography were used to fabricate the microfluidic device. Negative photoresist Su-8 was used to fabricate the master on Si wafer using photolithography method. The Su-8 master on Si wafer was then used to fabricate the PDMS microfluidic gradient generator mold with soft lithography method. Glass slides were surface modified with silane to make the surface reactive, which could covalently bond with the PEG hydrogel in the photo-crosslinking step. The surface modification was characterized by water contact angle measurement and X-ray photoelectron spectroscopy (XPS) measurement. The PDMS and modified glass slides were finally covalently bonded by plasma treatment.

4.1 Introduction

4.1.1 Microfabrication

Microfabrication describes the fabrication process of miniature structures of micrometer sizes or smaller. Microfabrication is increasingly important in modern science and technology which is widely applied in the fabrication of sensors, microreactors, microelectromechanical systems and microanalytical systems (Qin D et al., 1998; Xia Y, 1998). The important techniques of microfabrication include photolithography and soft lithography, which were used in this project, to fabricate the PDMS based microfluidic gradient generator.

4.1.2 Photolithography

Photolithography is a process to transfer geometric patterns from a mask to the surface of a substrate. The steps involved in photolithography are wafer cleaning; spin coating of photoresist; soft baking; mask alignment; exposure; post baking; development and hard baking (Jones SW, 2000). These steps are introduced below.

4.1.2.1 Wafer cleaning

In the first step, silicon wafers can be cleaned by chemicals to remove any contaminants such as organic impurities on the surface. After cleaning, silicon wafers are further baked at a high temperature such as more than 200 ℃ to evaporate water on the surface.

4.1.2.2 Spin coating of photoresist

Photoresists can be divided into two categories: positive and negative. For positive photoresist, it can become soluble in the developer after exposure to UV light. The exposure to UV light can change the chemical structure of positive photoresist so that it can be then washed away by the developer, leaving the bare substrate. Negative photoresist has the opposite manner. The exposure to UV light can crosslink the resist to become non soluble in the developer. Therefore, the negative resist after exposure can remain on the surface after developing while the resist without UV exposure can be developed. In this project, SU-2050 photoresist is chosen for the experiments.

4.1.2.3 Soft baking

Soft baking is the step to remove the solvents from the photoresist coating. Soft baking plays an important role in photolithography. The temperature of soft baking was around 94 ℃ for 5 min. Over soft baking can decrease the photosensitivity and reduce the solubility of photoresist in developer while under soft baking can not fully remove the solvents.

4.1.2.4 Mask alignment and exposure

Mask alignment is an important step in the photolithography. A photomask is a square glass plate with patterned metal film on one side. The pattern in the mask can be transferred onto the wafer surface. After alignment of photomask on the wafer surface, the photoresist on the wafer can be then exposed to UV light through the pattern.

4.1.2.5 Post baking

Post baking is a bake step after exposure but prior to developing. Post baking is performed at 10 ℃ to 20 ℃ above the soft baking temperature. Post baking can improve critical dimension control, exposure latitude and enhance the photoresist profile.

4.1.2.6 Development

The negative photoresist after exposure can remain complete in the developer solution. The photoresist pattern on the silicon wafer surface transferred from the photomask can be developed in the developer.

4.1.2.7 Hard baking

Hard baking is the final step in the photolithography. This step is necessary to harden the photoresist, decrease the internal stress and improve the adhesion of photoresist to the Si wafer.

4.1.3 Soft lithography

Soft lithography refers to a family of techniques for fabricating microstructures and nanostructures based on printing, molding and embossing (Weibel DB et al., 2007; Xia Y, 1998). Soft lithography was developed as an alternative to photolithography. As the technique is based on using a patterned elastomeric polymer as a mask and stamp, it is called “soft lithography”. There are many technologies included in soft

lithography such as micro contact printing (μCP), replica molding (REM) and microtransfer molding (μTM) (Xia Y, 1998).

Poly(dimethylsiloxane) (PDMS) is widely used as the elastomer in the soft lithography techniques. The PDMS elastomer can be fabricated by mixing two kits: liquid silicone rubber base and curing agent. After mixing, the liquid solution will be poured over the master, and heated to curing. After curing, the mixed liquid will become a solid, crosslinked elastomer. There are several advantages for the use of PDMS in soft lithography (Xia Y, 1998). PDMS can make conformal contact with surfaces over relatively large areas and can be released easily from masters. PDMS has low interfacial free energy and good chemical stability. PDMS is hydrophobic and does not swell with water. PDMS has good thermal stability and gas diffusion property. PDMS is also optically transparent.

PDMS has been widely used in fabricating microfluidic devices which is one application in soft lithography (McDonald JC et al., 1999; Whitsides GM, 2006). The microfluidic devices are formed by placing PDMS layer with a glass surface. The microfluidic channels can be formed by conformal contact between two layer surfaces.

PDMS surface contains methyl groups ($-CH_3$), which makes PDMS hydrophobic. But its surface can be rendered hydrophilic by exposure to a plasma of air or oxygen to generate hydroxyl group (-OH). If the oxidized PDMS contacts oxidized glass,

they will form an irreversible bonding through the covalent crosslinking. And the irreversible bonding between PDMS and glass makes it possible to from sealed microfluidic device. The liquids can flow in the microfluidic channels in a laminar way (Weibel DB et al., 2007).

4.2. Experimental

4.2.1 Fabrication of Su-8 master on Si wafer by photolithography

A high resolution printer was used to generate a transparency photomask from a CAD files. The transparency photomask was then used to fabricate Su-8 pattern on Si wafer. The process is shown in Figure 4.1 and described below.

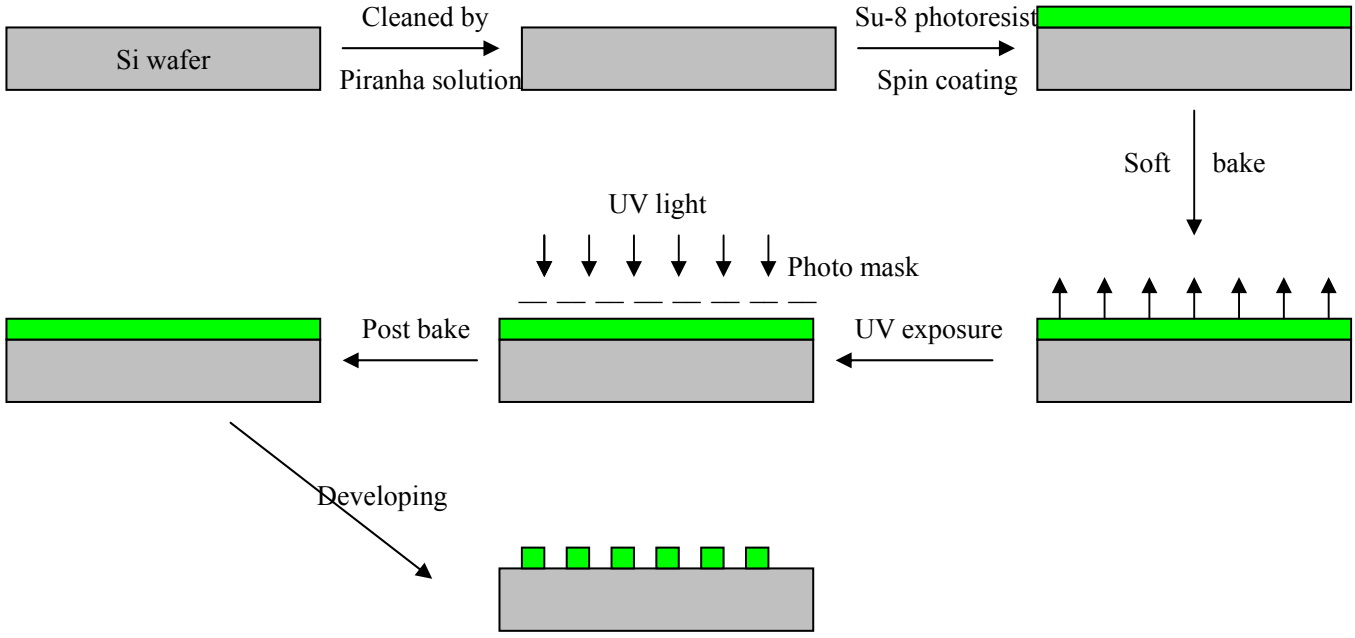

Figure 4.1 Fabrication of Su-8 master on Si wafer

The Si wafer was cleaned by a piranha solution with 98% sulphuric acid/30% hydrogen peroxide (V/V=4:1) for 1 hr at 200 ℃ to remove any contaminants. The

cleaned Si wafer was then washed with distilled water and baked at 200 ℃ for 1 hr before use. Negative photoresist su-8 2050 (MicroChem Corp., Newton, MA) was spin coated on the Si wafer for 30 s at a speed of 1500 rpm. The thickness of the coated su-8 2050 was about 150 μm. The Si wafer was then soft baked for 9 min at 95 ℃. The soft bake can evaporate the solvent from the photoresist. The photomask was then placed on the surface of Si wafer with photoresist and subjected to UV exposure at 365 nm (EXFO S1000). The total exposure energy was about 750 mJ/cm^2. The Si wafer was post baked at 95 ℃ for 7 min. The post bake can minimize the internal stress of Su-8 pattern on Si wafer. The Si wafer was developed in Su-8 developer, followed by isopropanol (IPA). Subsequently, tap water was used to rinse the Si wafer. The Su8 master on Si wafer was finally hard baked at 200 ℃ for 2 hr. The Su-8 pattern on Si wafer was observed under microscope.

4.2.2 Fabrication of PDMS mold by soft lithography

The Su8 master on a silicon wafer was used as a mould for fabricating a PDMS mould. The Su8 master was placed into a chamber so that it was capable of holding the PDMS solution.

The fabrication process is shown in Figure 4.2 and the description is as follow. PDMS and its curing agent (Sylgard 184 silicone elastomer kit, Dow Corning) were mixed at a ratio of 10:1. It was then stirred thoroughly for 10 minutes, and then degassed in vacuum desiccators for an hour as to remove bubbles. The mixed solution is then poured into the chamber of the Si-Su8 wafer mask. The chamber was

placed into vacuum desiccators again until no air bubbles appeared in PDMS solution, the chamber was placed in an oven at 80 ℃ for 3 h. The PDMS was solidified. The PDMS was then peeled off from the Si wafer carefully. The PDMS piece was cleaned by DI water followed by ethanol for 15 minutes and rinsed with DI water again. The PDMS was then undergone nitrogen blowing and finally baked in an oven for an hour at 65 °C.

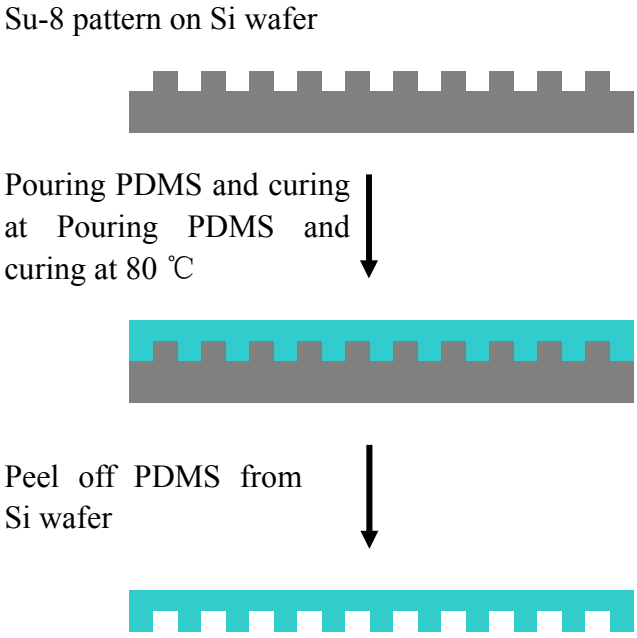

Figure 4.2 Fabrication of PDMS mold by soft lithography

4.2.3 Surface modification of glass slides

In the project, glass slides were used to bond with PDMS to form the microfluidic device. PEG hydrogels were then fabricated. In order to make the PEG hydrogel attach to the glass slides, the glass slides were surface modified in advance.

The glass slides were treated with a piranha solution composed of H_2SO_4 and H_2O_2 (V:V=4:1) for 1 hr to remove any contaminants and expose the reactive hydroxyl

group on the surface. The treated glass slides were dried by nitrogen blowing and then immediately subjected to a toluene solution with 10% 3-(Trimethoxysilyl)propyl methacrylate(TPM). The silanization was performed at 60 ℃ for 24 h. Subsequently, the glass slides were washed with methanol, followed with distilled water to eliminate toluene and unreacted TPM. Then the glass slides were gently dried under nitrogen gas and cured in an oven at 120 ℃ for 1 h. The fabrication of TPM graft glass slides was shown in Figure 4.3.

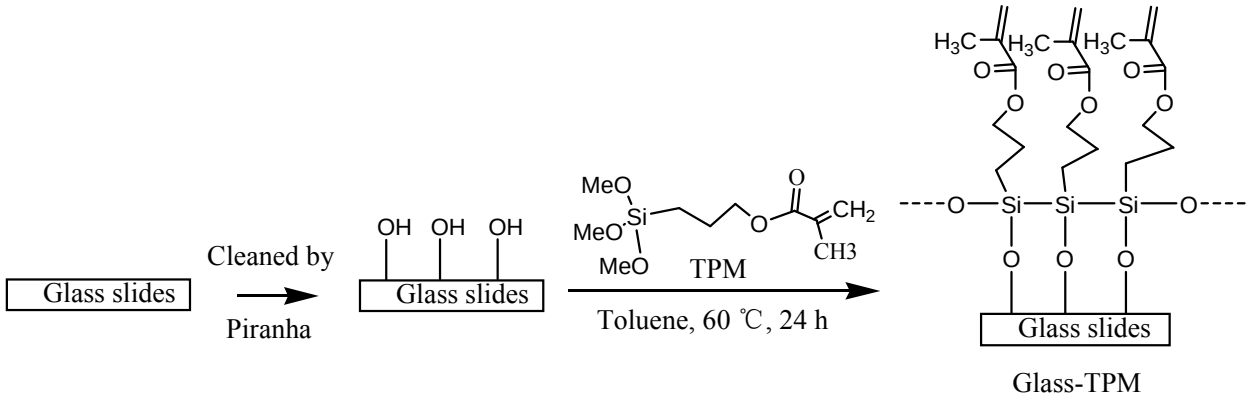

Figure 4.3 Surface modification of glass slides with TPM

The TPM graft on glass slides was demonstrated by X-ray photoelectron spectroscopy (XPS) measurement. The XPS used in the experiment was a Sengyang SKL-12 electron spectrometer equipped with a VG CLAM 4 MCD electron energy analyzer while X-ray source was a dual anode source from VG (type XR3E2). Mg Kα radiation (1253.6 eV) at a current of 15 mA was used. The surface modification was also characterized by water contact angle (Rame-hart 250-F1 standard goniometer with dropimage advanced 2.1 user guide, NJ, USA). Drops of about 30 μl distilled water were deposited onto the glass surfaces, and then the static contact angles after 20 s were recorded. The reported values were the average of 6 measurements.

4.2.4 Plasma bonding of PDMS with glass slides

The purpose of performing plasma was to create the hydroxyl (–OH) group on both of the surface of glass slide and PDMS. The hydroxyl (–OH) group allowed covalent interaction between the two surfaces and which leading to a firm bonding. The combination of the two surfaces then created a channel for liquid passing through.

Holes were punched in the inlet and outlet of PDMS using 12 gauge needles. PDMS and TPM treated glass slides were first cleaned in ultrasonic acetone and methanol, followed by distilled water. Oxygen plasma was then used to bond PDMS and glass slides. The plasma bonding was a kind of irreversible bonding, which is caused by the covalent interaction of PDMS and glass. However, reversible bonding was needed in the experiment, as PEG hydrogel must be approached for further characterization.

A method was used to solve this problem. Selected areas covering the microchannel network were for plasma, rather than the whole areas of PDMS. The gradient chamber part was not for plasma treatment. In this case, the inlet and microchannel network of PDMS had strong bonding with glass slides while the gradient channel can be easily peeled off. The whole process for plasma preparation and treatment was shown in Figure 4.4, 4.5 and 4.6. Figure 4.4 shows the partially oxygen plasma preparation. Figure 4.5 shows that -OH group was produced on the PDMS surface after oxygen plasma. Figure 4.6 shows the cross-section of the PDMS microfluidic

device.

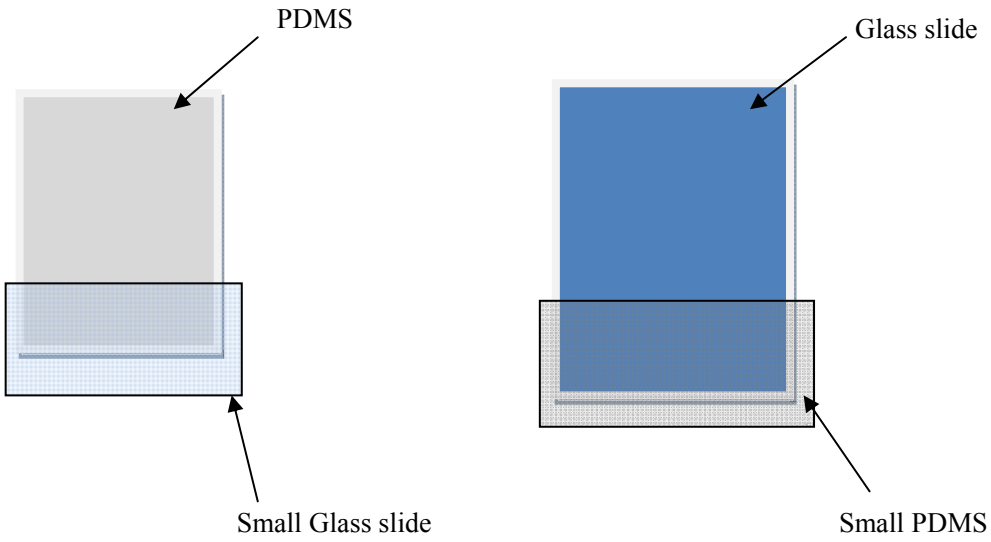

Figure 4.4 Oxygen plasma preparation process

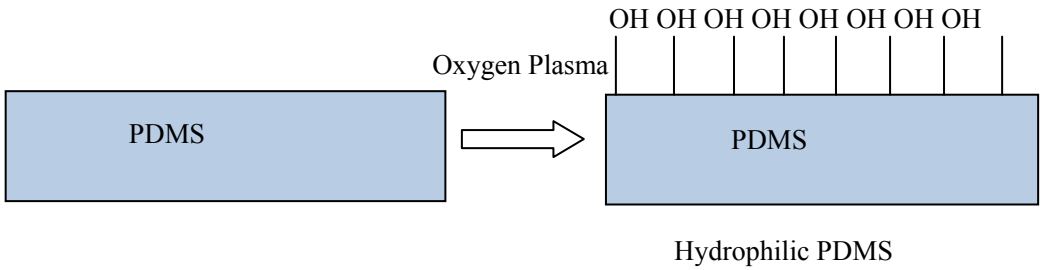

Figure 4.5 Oxygen plasma surface modifications of PDMS

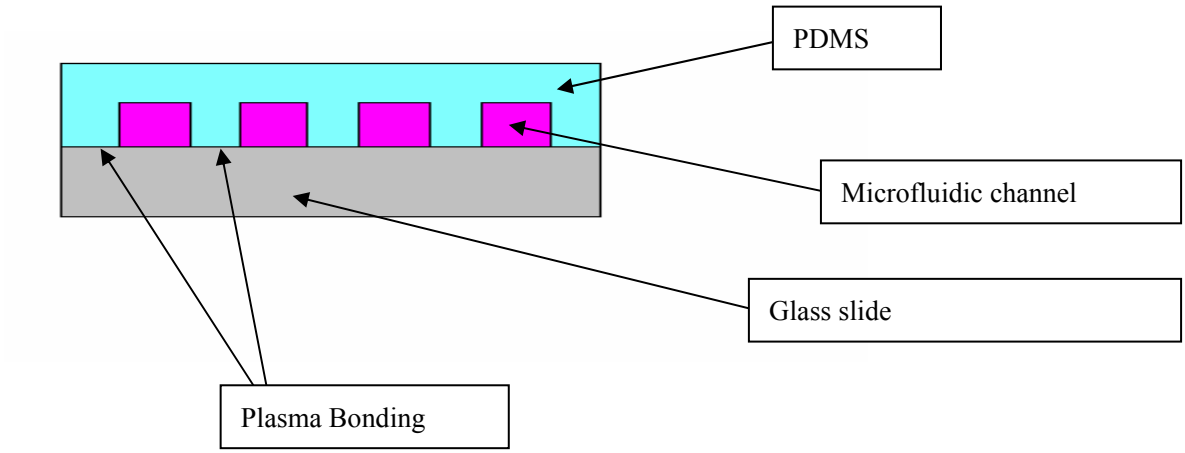

Figure 4.6 Integration of the PDMS microfluidic device

4.3 Results

4.3.1 *Fabrication of Su-8 master*

Figure 4.7 shows the fabricated Su-8 master on Si wafer. There were two inlets and one outlet. The width of the microchannel in the front part was 100 μm, while the width of gradient chamber in the back part was 200 μm. The gradient chamber connected to the outlet was 1700 μm in width. The height of the pattern can be changed from 50 μm to 150μm.

As the Su-8 pattern on the Si wafer had a relatively high height, it was difficult to fabricate and special attention should be paid to spin coating, UV exposure and developing. The speed for spin coating was 1500 rpm or even lower. No air bubbles should exist after spin coating. The total UV energy should be 750 mJ/cm^2 or more. Less time was needed in the developing. If it was developed for a long time, the Su-8 pattern can be easily detached from the Si wafer.

The fabricated Su-8 master generally had internal stress, which could make the master easily destroyed in use. In order to eliminate the internal stress, it should be careful in the post bake process. The Si wafer was first baked at 95 ℃ for 7 min. The temperature was then decreased gradually at about 10 ℃ / 30 min. If the temperature decreased sharply, internal stress would exist in the Su8 pattern. The hard bake time should be at least 2 hr at 200 ℃. After hard baking, the temperature was also decreased gradually at about 30 ℃ / 30 min.

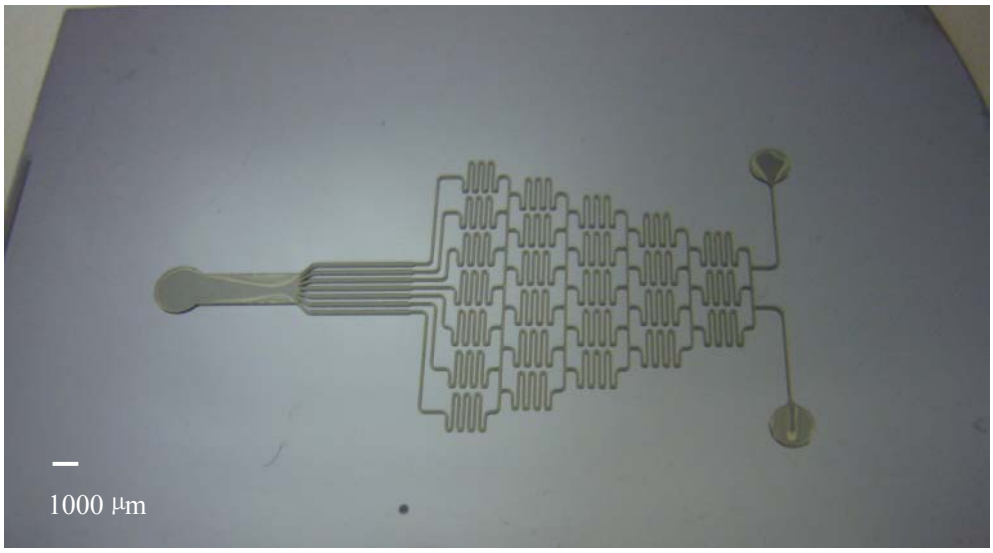

Figure 4.7 Su-8 master on Si wafer

4.3.2 Surface modification of glass slides

In this project, glass slides were used as the substrates o bond with PDMS mold to form the microfluidic gradient generator. PEG hdyrogels with RGD gradient were then fabricated within the PDMS microfluidic gradient generator. In order to make the PEG hydrogel attach to the glass slides, the glass slides must be surface modified in advance.

The glass slides were treated with the silane, 3-(Trimethoxysilyl)propyl methacrylate(TPM). TPM has the chemical group MeO-Si-O- which can react with the –OH group of glass. TPM molecule also had vinyl group -C=C-, which can polymerize with vinyl group of PEGDA. Therefore, The PEG hydrogel can attach to the glass slides by covalent bonding. The modified glass slides were characterized by XPS measurement. The XPS result is shown in Figure 4.8.

In Figure 4.8, the long band which ranged from 0 eV to 1000 eV was the general

band including all the elements on the surface and the narrow band from 280 eV to 300 eV described the binding energy for the core element carbon. Compared with the binding energy of carbon in Figure 3.8(a), the Figure 3.8(b) shows a secondary peak, which was higher in binding energy than the main peak from 287 eV to 291 eV attributed to the carbon in C-H and C-O. This peak was resulted from the chemical group C=O in TPM. Since the information depth of XPS is 10nm (Steffens GCM et al., 2002), the result confirmed the existence of TPM on glass surface.

The water contact angles, which are indicators of the wettability of surfaces, were measured for glass and glass-TPM, and are shown in Figure 3.9. In Figure 3.9, the contact angle for glass was about 49°. After TPM was grafted on the glass surface, the contact angle increased to about 72°. The TPM molecules had the chemical group C=C-(C=0)-O-, which was relatively hydrophobic than glass. Therefore, the TPM layer grafted on the glass-TPM surface can increase the hydrophobicity of glass surface. The improved hydrophobicity can increase the water contact angle on glass surface. The water contact results also demonstrated the successful surface modification of glass by TPM molecule.

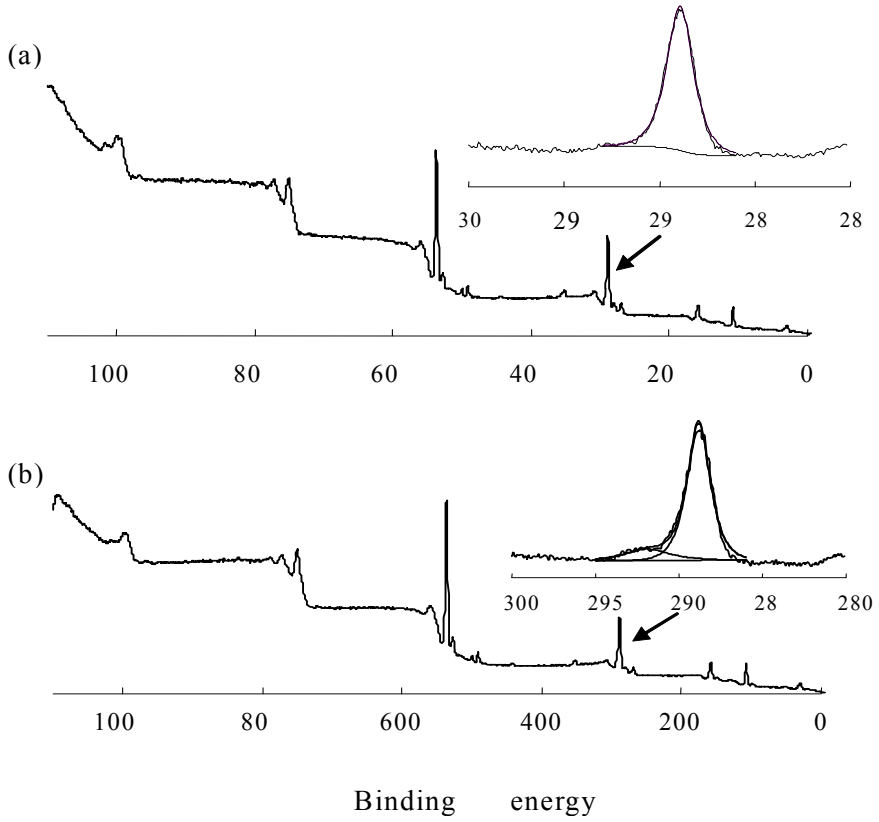

Figure 4.8 XPS spectra for (a) glass and (b) glass-TPM

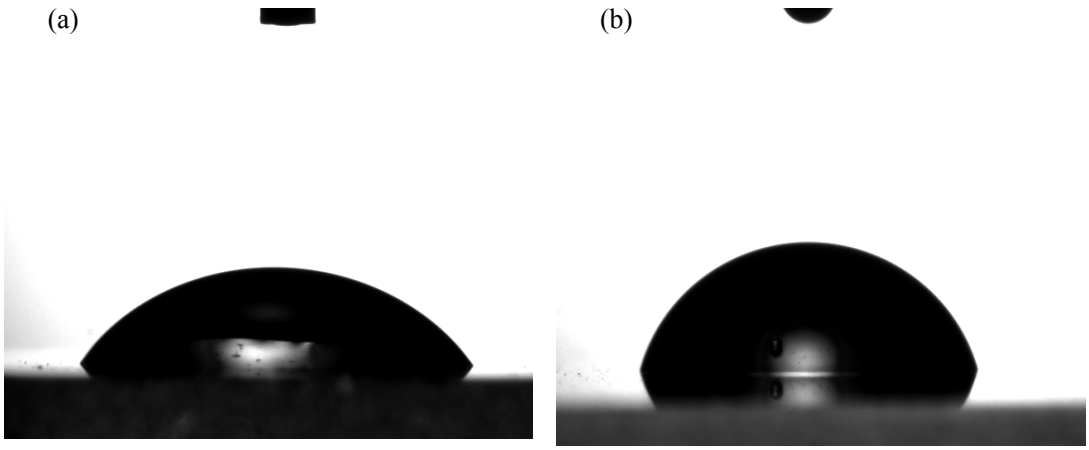

Figure 4.9 Water contact angles of (a) glass and (b) glass-TPM (Data are expressed ±SD, n=6)

4.3.3 PDMS mold fabricated by soft lithography

PDMS mold was fabricated against the Su8 master on Si wafer by soft lithography. Holes were then punched in the inlet and outlet of PDMS using 12 gauge needles. The fabricated PDMS mold is shown in Figure 4.10.

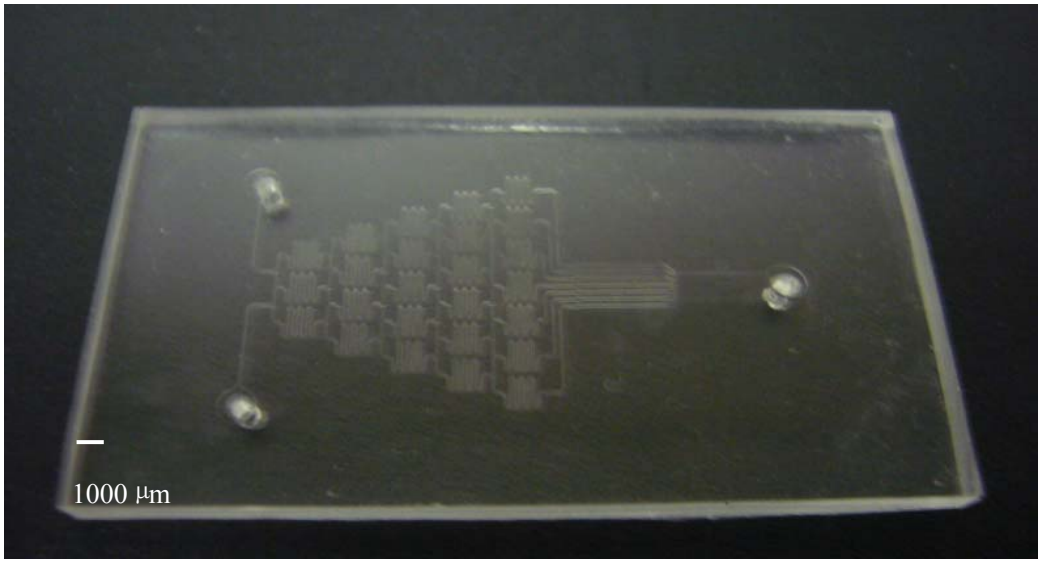

Figure 4.10 PDMS mold fabricated by soft lithography

In the experiment air bubbles were often found in the PDMS mold. In order to eliminate the air bubbles, more time such as 1 hr was needed for degassing in the vacuum. The rigidity of PDMS mold was determined by the ratio of PDMS monomer and its crosslinking reagent. The normal ratio was 10:1. If the ratio was more than 10:1, the PDMS mold had less rigidity and showed more flexibility. If the ratio was less than 10:1, the PDMS mold would have more rigidity. In my experiment, the ratio more than 10:1, such as 13:1, was used. This is due to the easy punching of PDMS and plasma bonding of PDMS with glass.

4.3.4 Plasma bonding of PDMS with glass slides

PDMS and glass slides were bonded by oxygen plasma. Selected areas covering the

microchannel network were for plasma, rather than the whole areas of PDMS. The gradient channel part was not for plasma treatment. Therefore, the PDMS in the gradient channel after plasma can be still uncovered. The picture of fabricated device is shown in Figure 4.11.

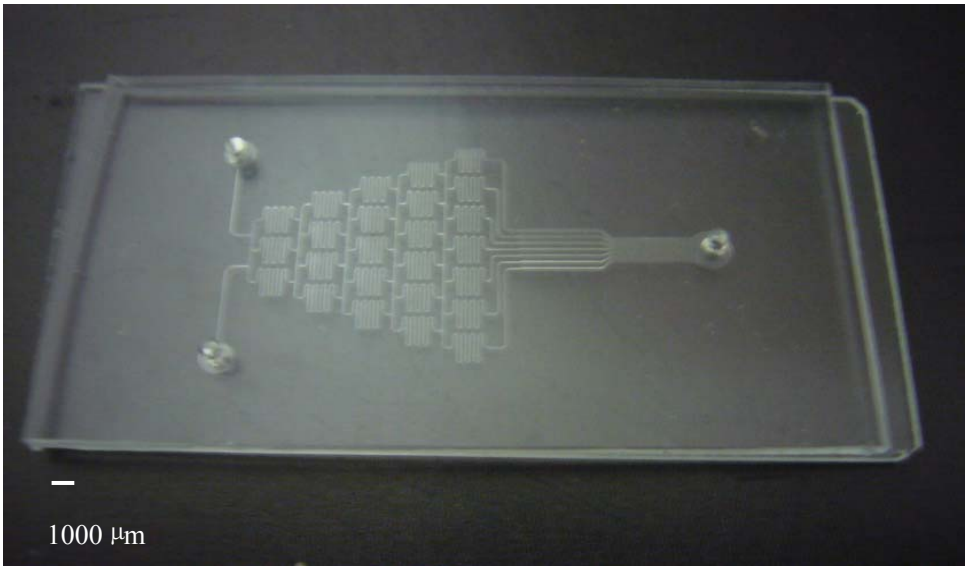

Figure 4.11 Microfluidic device fabricated by plasma bonding of PDMS and glass slides

Chapter 5 Characterization of Microfluidic Gradient Generator

Abstract

Blue dye solution and fluorescence polymer microbeads were used to test the performance of the fabricated microfluidic gradient generator for color and beads gradient generation. Four flow rates 0.1, 0.5, 1 and 2 (ml/hr) were chosen to evaluate the effects of flow rate on the gradient generation. With the increase of the flow rate, the time for solution completing the channel decreased. The flow rates of 0.1 and 0.5 (ml/hr) showed better effect to form gradient, the concentration of which increased gradually and constantly. For solution with fluorescence beads at flow rate of 0.5 ml/hr, it also formed an approximately linear distribution along the channels.

5.1 Introduction

The PDMS microfluidic gradient generator shown in Figure 5.1 was successfully fabricated by photolithography and soft lithography discussed in Chapter 4. This microfluidic gradient generator had two inlets. One inlet was connected to DI water and another inlet was connected to DI water with certain agent concentration. The two solutions were injected into the inlets simultaneously by a microfluidic syringe pump. As the solutions flowed into the microchannels, they were repeatedly split, mixed, and recombined. After several rounds of branched channels, all branched channels containing different proportions of infused solutions were brought together into a single chamber. As predicted by the FEM simulation result, a concentration gradient profile was generated within the microfluidic device by laminar flow and diffusion mixing in the outlet chamber. The flow rates of infused solution could have important effects on the shape and quality of gradient distribution. In this chapter, the solutions with color dye and fluorescent polymer microbeads were used to characterize the gradient effect of the microfluidic device.

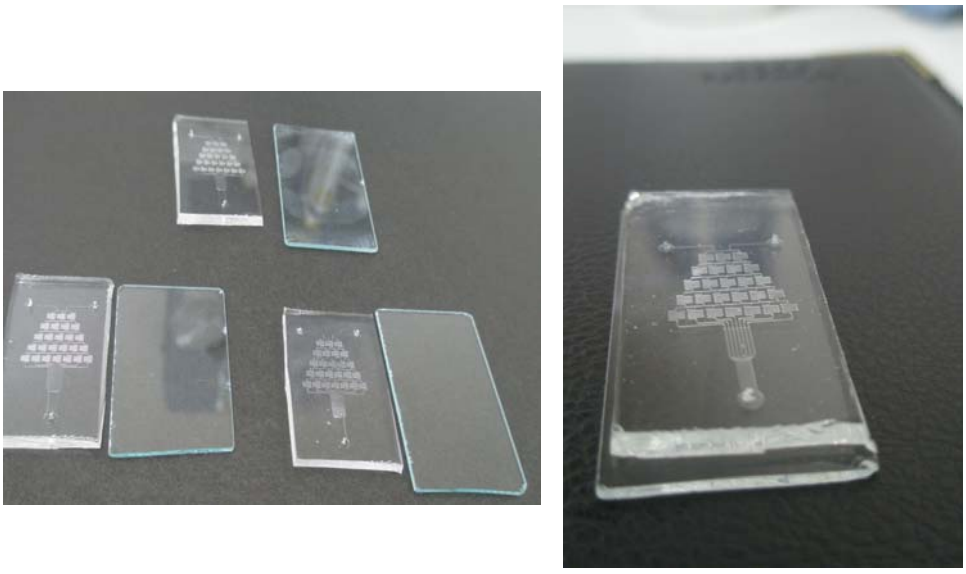

Figure 5.1 Microfluidic devices used in the experiment

5.2 Experimental

5.2.1 Generation of dye gradient

The two inlets of the microfluidic gradient generator were first filled with ethanol. Dropper was placed at the outlet in order to fill the microchannel fully with ethanol until no air bubbles was observed. After that, distilled (DI) water was used to replace the ethanol using the same method.

Polyethylene tubing with steel needles was inserted into the inlet holes to make the fluidic connections. The piece of tubing was then connected to a syringe pump. Blue dye solution was prepared and filled in one syringe while the other was filled with distilled water. The needles of the syringes were inserted into the inlets separately. The flow rate was first adjusted to 0.1 ml/hr. Several minutes later, the blue solution and transparent distilled water were mixed, split and mixed along the channel again. The flowing process inside the device was captured at a fixed period of duration by a digital camera. Ultimately, a dye gradient was formed in the microfluidic channel. The gradient was observed and analyzed under an optical microscope. Micropump flow rate of 0.1 ml/hr, 0.5 ml/hr, 1 ml/hr and 2 ml/hr were used to repeat the experiment procedures. Finally, all the images were analyzed using Matlab programming.

5.2.2 Generation of gradient of fluorescence polymer microbeads

The gradient of dye solutions could give a direct impression of gradient formation. But it was difficult to simulate cells movement in microfluidic channel. So the

fluorescence polystyrene microbeads were used for generating the fluorescence intensity distribution in order to simulate cells distribution. The polystyrene microbeads were about 2-3 μm in diameter and modified with carboxyl group, which could inhibit the deposition in solution. The process for generating gradient of polymer beads was similar to that of dye gradients. Briefly, one inlet was injected with solution of fluorescence polymer beads while another inlet was injected with distilled water. A fluorescence microscope was used to observe the distribution of fluorescence microbeads.

5.3 Results

5.3.1 Generation of dye gradient

Figure 5.2 shows the flowing process with flowing speed of 0.1 ml/hr. There were two inlets containing distilled water (left) and blue dye solution (right). As the streams traveled into the network, they were repeatedly split at the nodes, combined with neighboring streams, and allowed to mix by diffusion in the separate channel. In each layer, neighboring streams carrying different concentrations of blue dye were mixed in proportions equal to the splitting ratios at each node. At the end of flow, all streams carrying different concentrations of blue dye solution combined in a single channel. As shown in Figure 5.2, 570 sec was needed for filling the microchannel. 750 sec was needed to attain stable condition. As a result, 660 sec in average was needed for flow rate of 0.1 ml/hr to run through the channel.

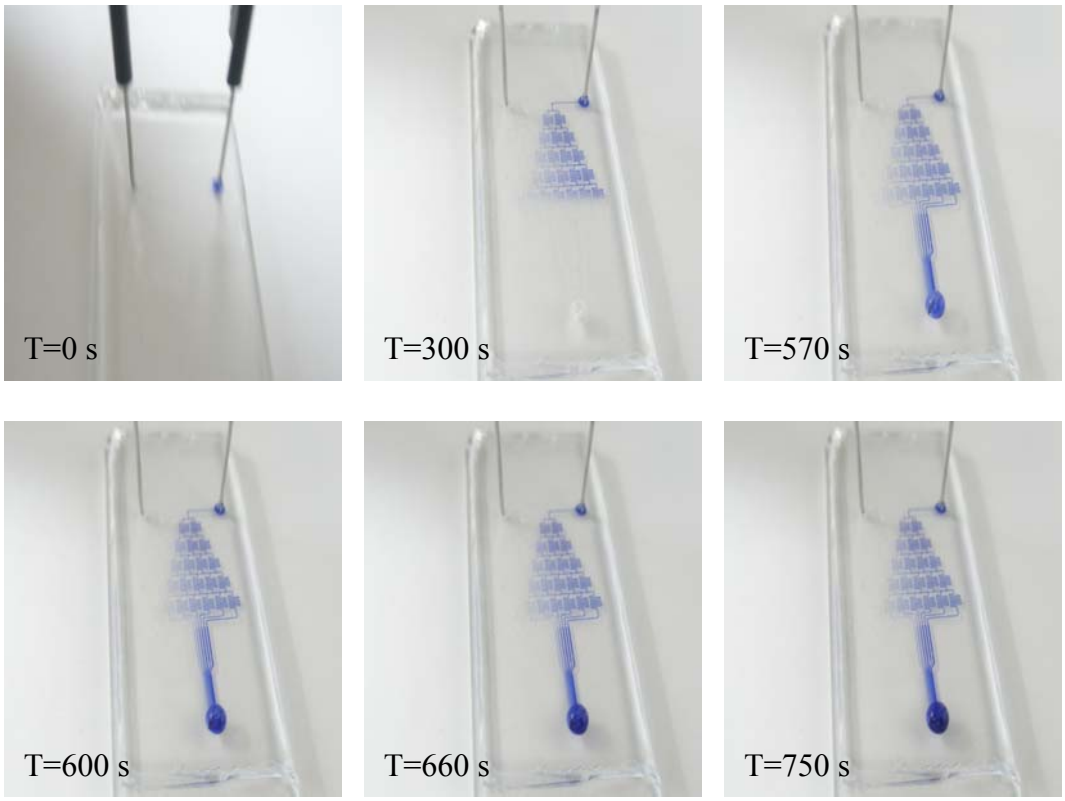

Figure 5.2 Flowing process of 0.1ml/hr

The flowing process of 0.5 ml/hr is shown in Figure 5.3. It took about 160s for a complete flow, and about 200s for maintaining a stable condition. Therefore the average time needed for flow rate 0.5 ml/hr was 180s. Compared with the flow rate of 0.1 ml/hr, less time was need to completing the channel. A stable flowing was achieved, which was similar to that of 0.1 ml/hr.

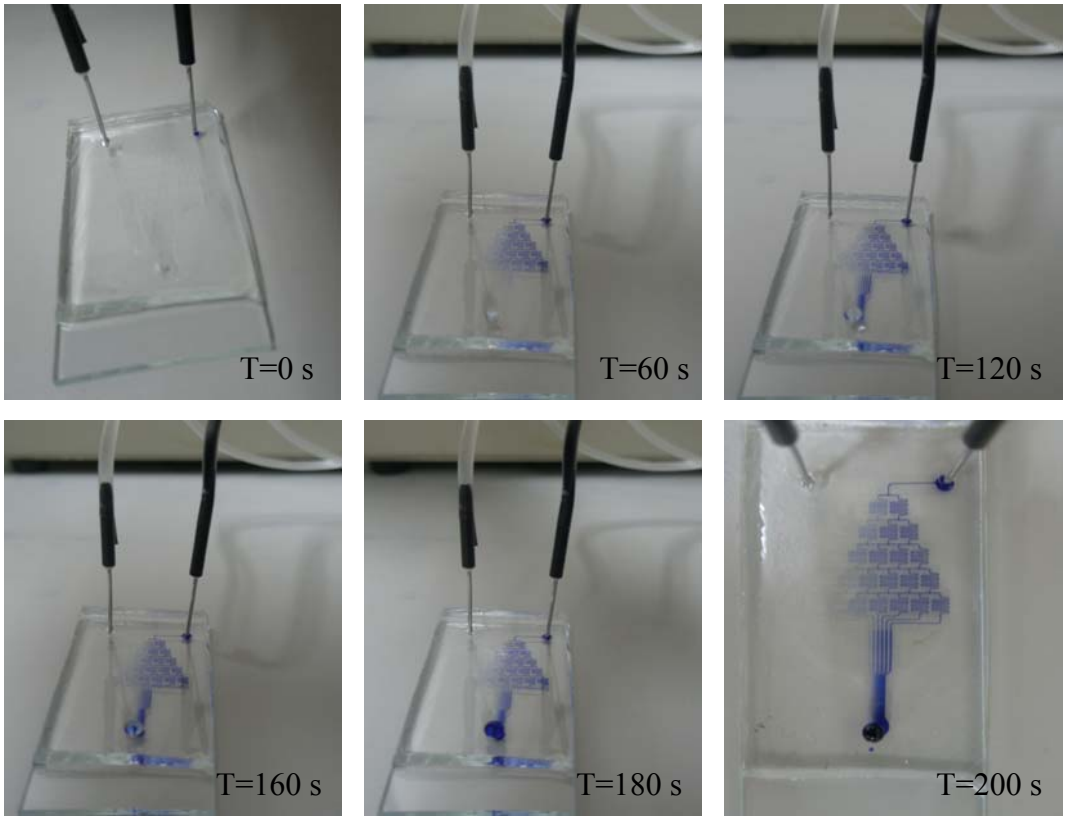

Figure 5.3 Flowing process of 0.5 ml/hr

Figure 5.4 shows the flowing process of 1 ml/hr. At time 40s and 80s, some unstable flowing was found. Each layer of the microchannels had some inconstant blue color distribution. This may be resulted from the relative faster flow rate compared with 0.1 ml/hr and 0.5 ml/hr. 120s was needed to complete the channel. 140s was needed to attain a stable condition. As a result, the average time needed for flow rate of 1 ml/hr to run through the channel was 130s.

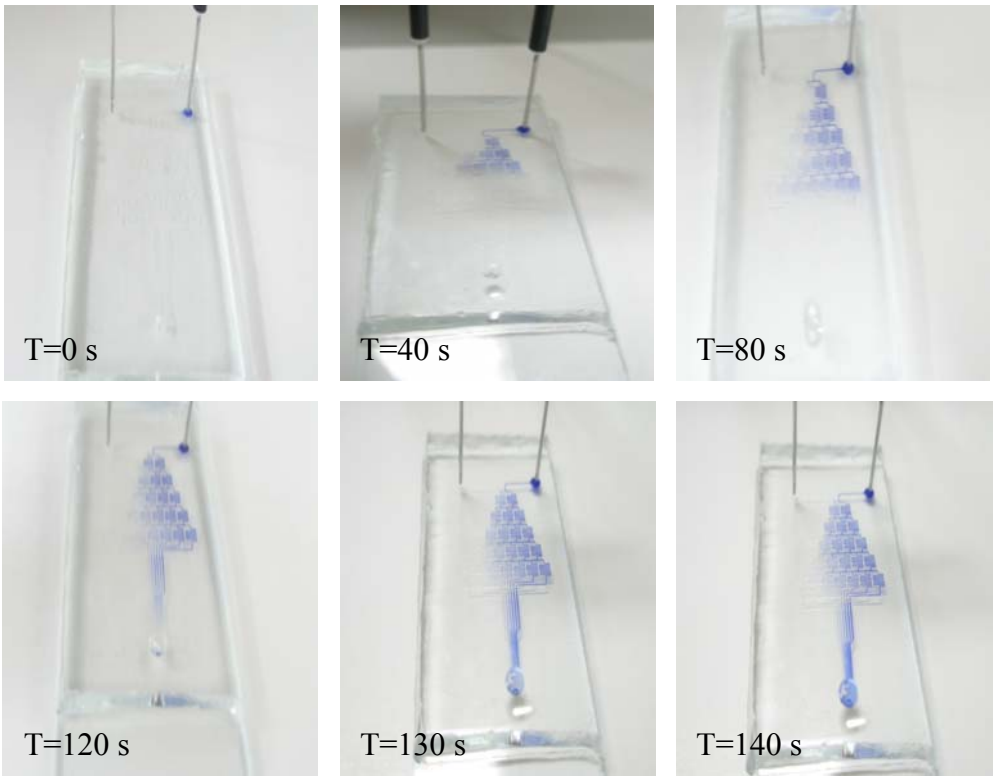

Figure 5.4 Flowing process of 1ml/hr

Figure 5.5 shows the graph of the relationship between the flow rate (ml/hr) with the average completion time (s) of the microfluidic device flowing process. The completion time was defined as the time for solution runnig through the microfluidic device. A trend line was added. The completion time decreased sharply as the flow rate increased from 0.1 ml/hr to 0.5 ml/hr. Then the complete time decreased slowly from 0.5 ml/hr to 1 ml/hr.

Figure 5.6 shows the regions of interest in the microfluidic network for gradient quality analysis. The first interested region was the mixing of the blue dye solution and the distilled water. The occupational ratio of blue dye solution can indicate the flowing stability. The color change of blue dye solution and the distilled water in the microchannels can show the mixing effect of the two solutions. The other interested

region was the gradient channel. The gradient channel can show the blue color distribution along the channel.

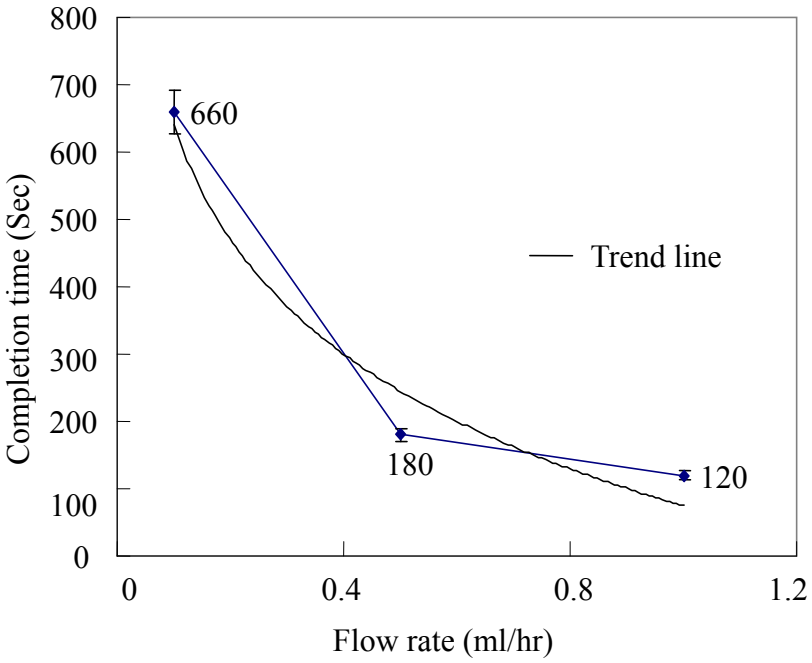

Figure 5.5 Relationship between flow rate and average completion time in microfluidic device

Figure 5.7 shows the first mixing channel of the microfluidic network of flow rate 0.1 ml/hr. It can be observed that the mixing process of the first channel was very stable and both dyed and transparent solution occupied 50% of the channel width. The blue dye solution and the distilled water were also mixed well. After being brought together, the two solutions became a uniform solution gradually. Figure 5.8 shows the gradient analysis region. A blue color gradient was observed. The bottom area had lighter blue color while the top area had deeper blue color. And the blue color exhibited a gradient change across the channel.

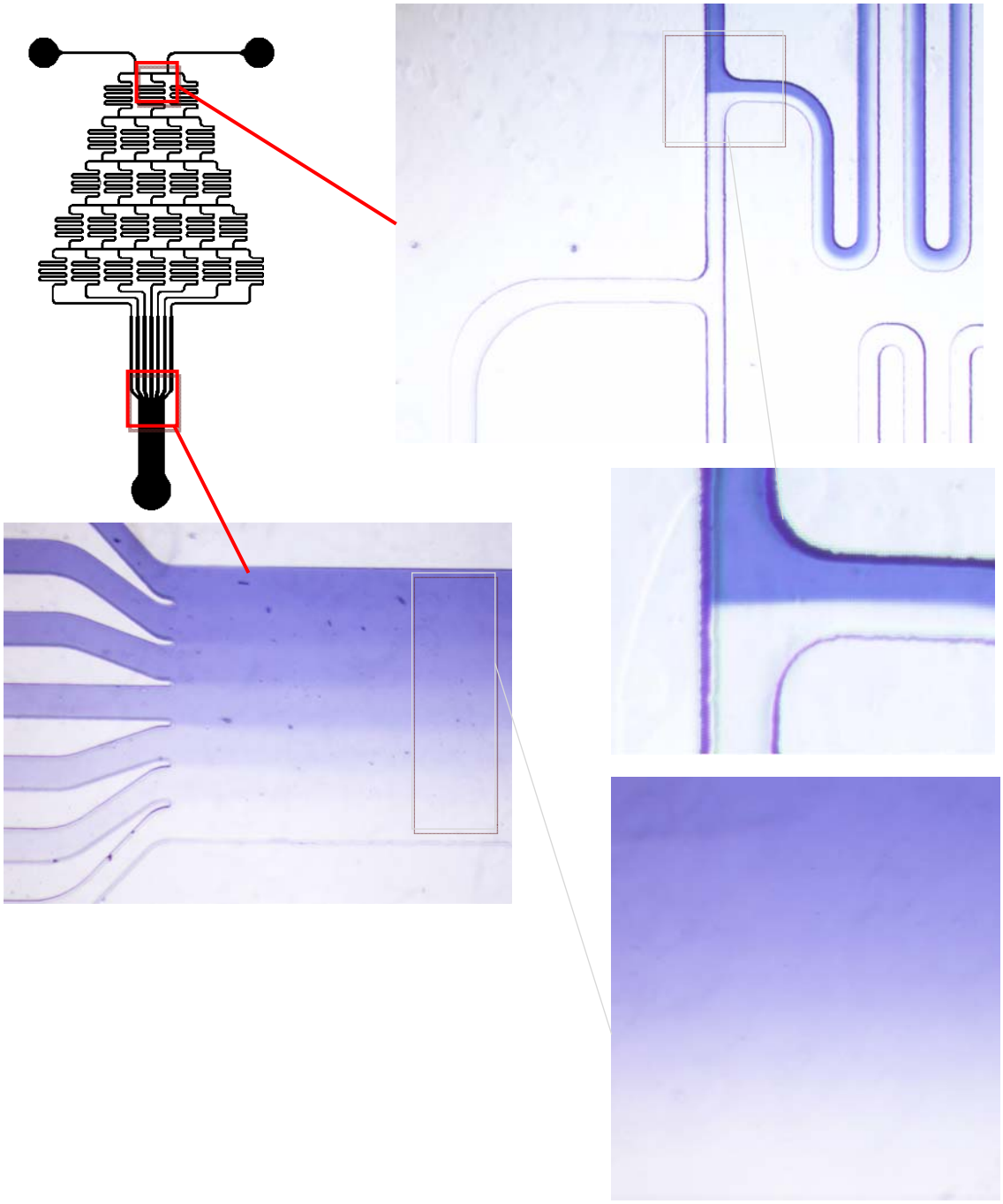

Figure 5.6 Several regions in the microfluidic network chosen for gradient quality analysis

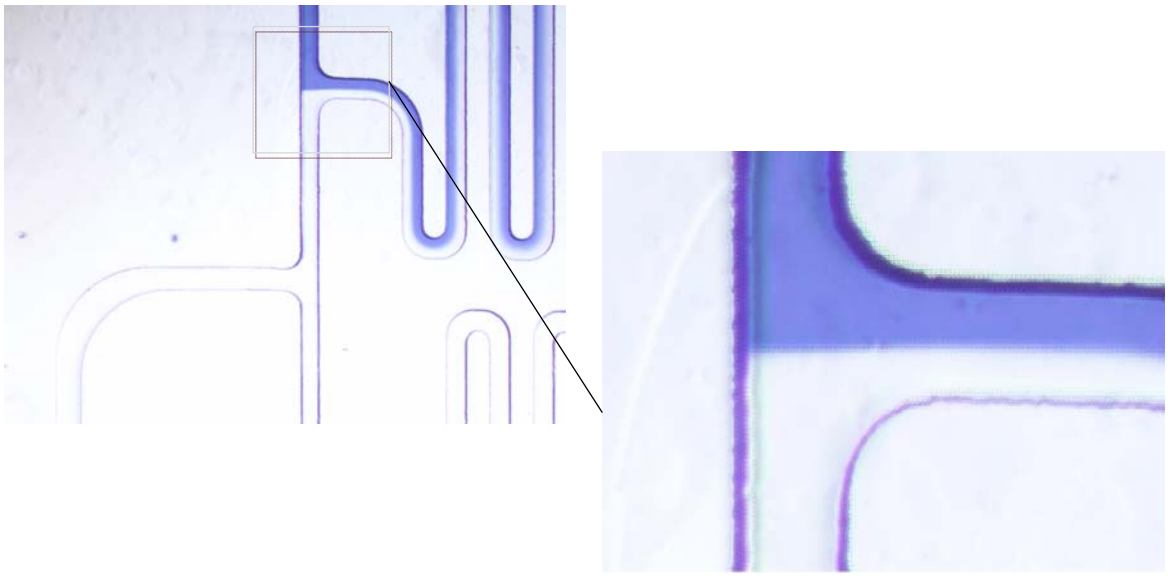

Figure 5.7 Mixing channel in the microfluidic network of flow rate 0.1 ml/hr

Figure 5.8 Gradient in the microfluidic network of flow rate 0.1 ml/hr

Figure 5.9 shows the first mixing channel of the microfluidic network of flow rate 0.5 ml/hr. It can be observed that the mixing process was very stable and still occupied 50% of the channel width as 0.1 ml/hr. Figure 5.10 shows the gradient analysis region. The gradient was also similar to that of 0.1 ml/hr. the blue color exhibited a gradient change across the channel.

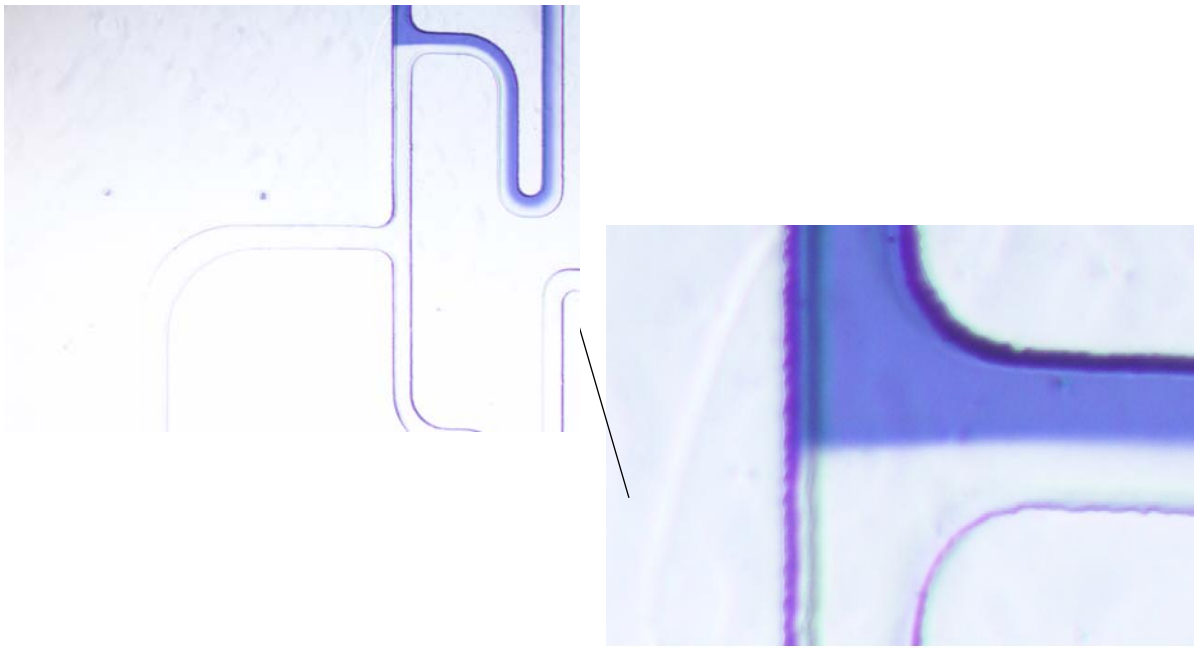

Figure 5.9 Mixing channel in the microfluidic network of flow rate 0.5 ml/hr

Figure 5.10 Gradient in the microfluidic network of flow rate 0.5 ml/hr

Figure 5.11 shows the first mixing channel of the microfluidic network when we used flow rate of 1 ml/hr. It can be observed that the mixing process for 1 ml/hr was no longer 50/50. This was resulted from the relative higher flow rate compared with 0.1 ml/hr and 0.5 ml/hr. Higher flow rate can result in the unstable flowing. Figure 5.12 shows the gradient analysis region. The blue color in the gradient changed with

fluctuations in step, which was different from the case of using 0.1 ml/hr and 0.5 ml/hr. It is well known the gradient formed in this kind of situation was formed by controlling the laminar flow rate and the molecular diffusion (Dertinger SKW et al., 2001). With a constant molecular diffusion, higher flow rate of the laminar flowing would induce incomplete mixing of solutions of different concentrations. Thus the incomplete mixing formed the gradient with some fluctuations and step-like pattern.

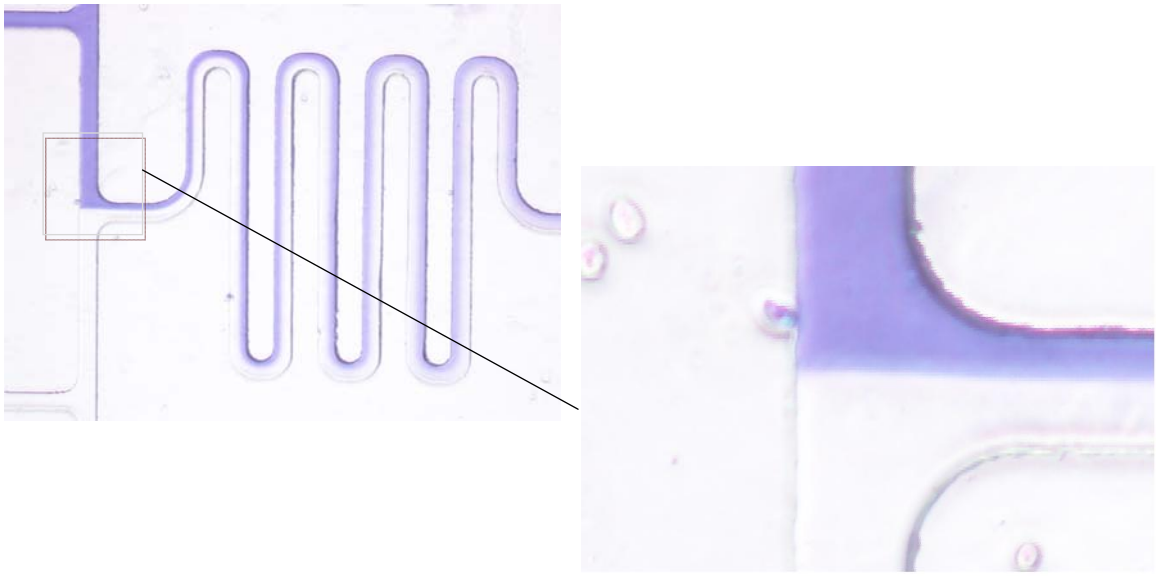

Figure 5.11 Mixing channel in the microfluidic network of flow rate 1 ml/hr

Figure 5.12 Gradient in the microfluidic network of flow rate 1 ml/hr

Figure 5.13 shows the first mixing channel of the microfluidic network of flow rate 2 ml/hr. It can also be observed that the mixing process for 2 ml/hr was similar to 1 ml/hr. The occupation of the mixing channel for the solution was no longer 50/50. Moreover, the mixing of the blue dye solution and the distilled water in the microchannels was incomplete. They still behaved as two separate solutions after mixing in the microchannels. Figure 5.14 shows the gradient flow region. The gradient had some fluctuations and step-like pattern which was similar to that of 1 ml/hr. The difference between 2 ml/hr and 1 ml/hr was that the blue color changed sharply from light to deep in the middle of gradient of 2 ml/hr. This was caused by the incomplete mixing in the microchannels mentioned above. When there was incomplete mixing in the microchannels, the concentrations of the solutions brought together into the gradient channel changed unevenly with a break increase in the middle two solutions.

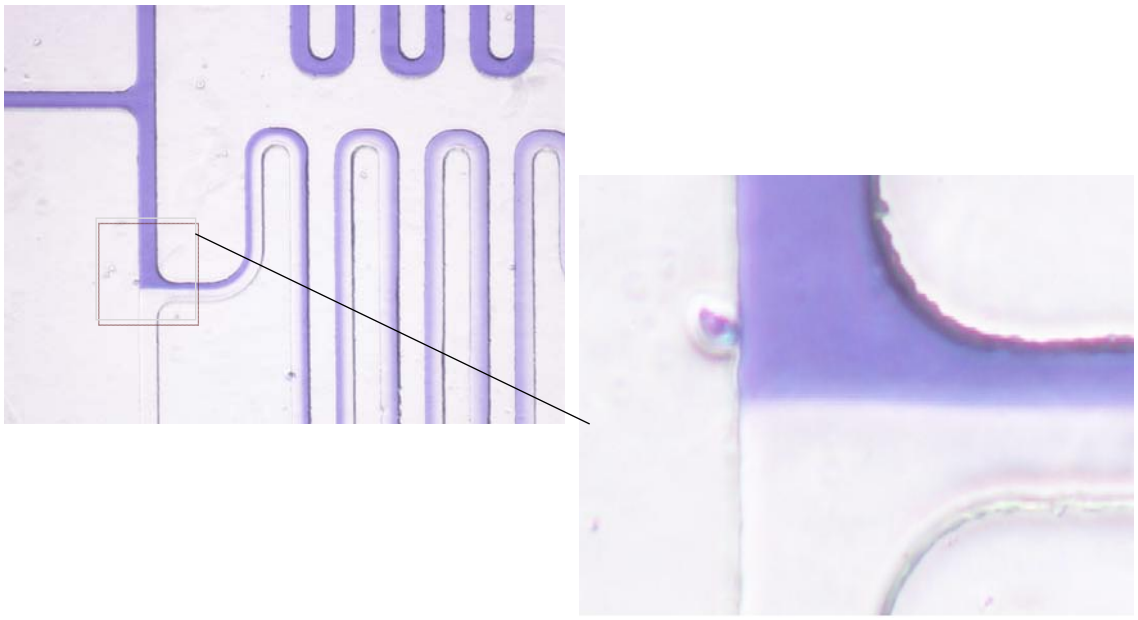

Figure 5.13 Mixing channel in the microfluidic network of flow rate 2 ml/hr

Figure 5.14 Gradient in the microfluidic network of flow rate 2 ml/hr

In flow rate 2 ml/hr, failure flowing process was often observed. Figure 5.15 shows the failure case of the microfluidic network. The circled part was the unsatisfactory region. As the flow rate of 2 ml/hr was relatively higher, the solution flowed unstable. The unstable flowing caused the failure.

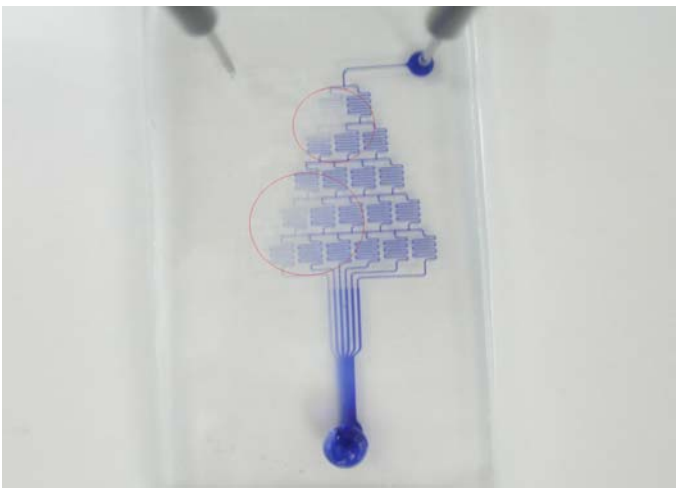

Figure 5.15 Failure case of flow rate 2 ml/hr

Images of the concentration gradient of different flow rate which were created by a

transparent and a dye solution were captured by digital camera attached to the microscope. MATLAB program was used to analyze the color intensity of these photos.

Figure 5.16 shows the gradient analysis graph of 0.1 ml/hr. The graph indicates that the concentration along the interested region was approximately linear. This implies the color concentration increased gradually. The concentration gradient of flow rate 0.5 ml/hr is shown in Figure 5.17. The graph shows a similar pattern to 0.1 ml/hr which implied that the concentration gradient was also in linear. Figure 5.18 shows the gradient analysis graph of 1 ml/hr. The graph shows a different pattern from the previous result. The curve was not linear; fluctuation was presented along the curve. There were seven flat stages in the curve. This implied the concentration gradient along the investigated region did not increase gradually. The seven stages were resulted from the incomplete mixing of the seven concentrations of color solution, which was mentioned above.

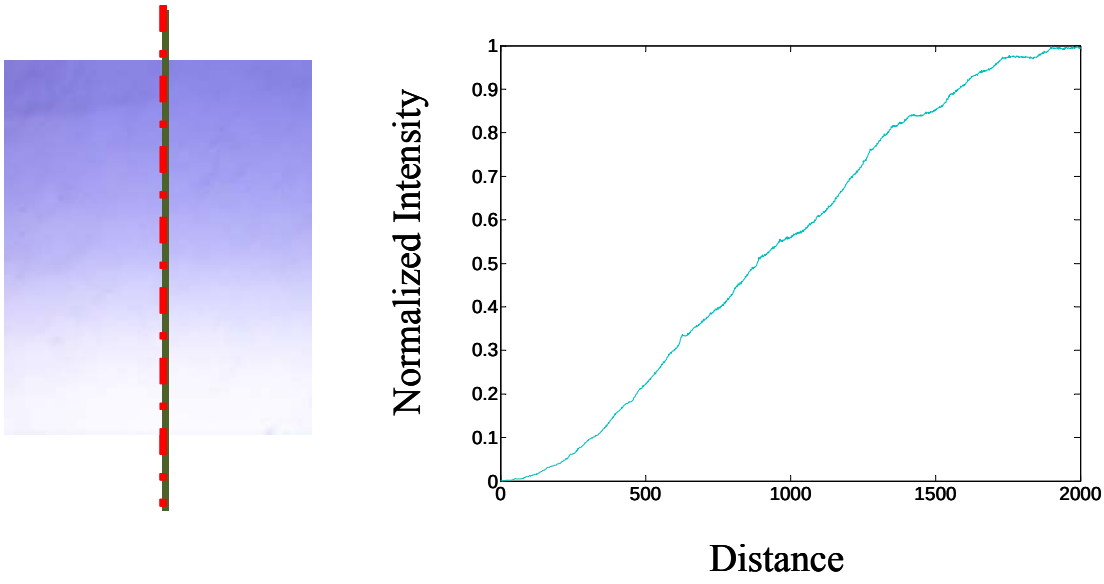

Figure 5.16 Gradient analysis of 0.1 ml/hr

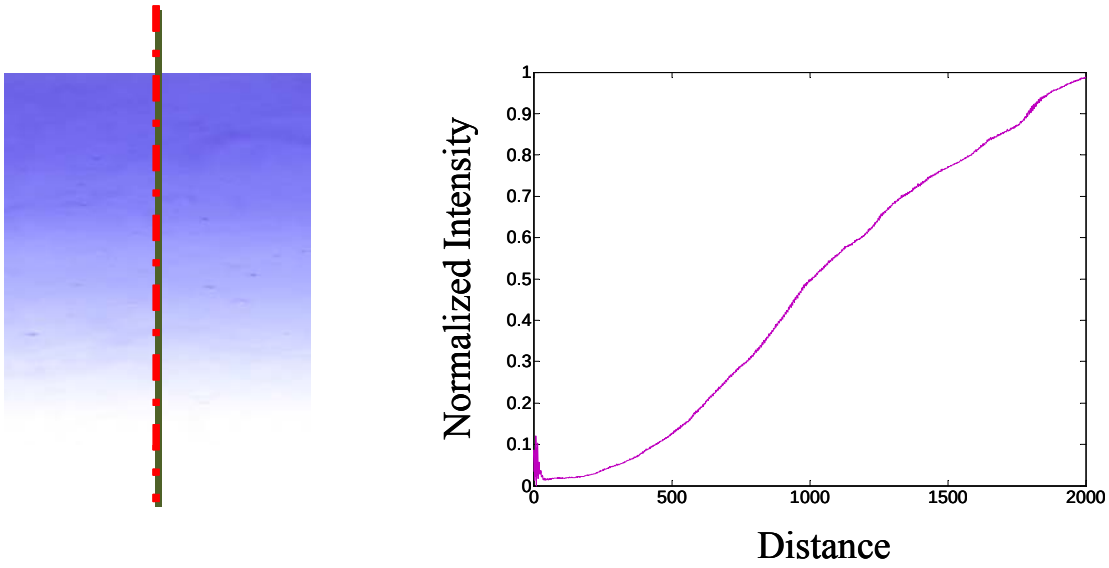

Figure 5.17 Gradient analysis of 0.5 ml/hr

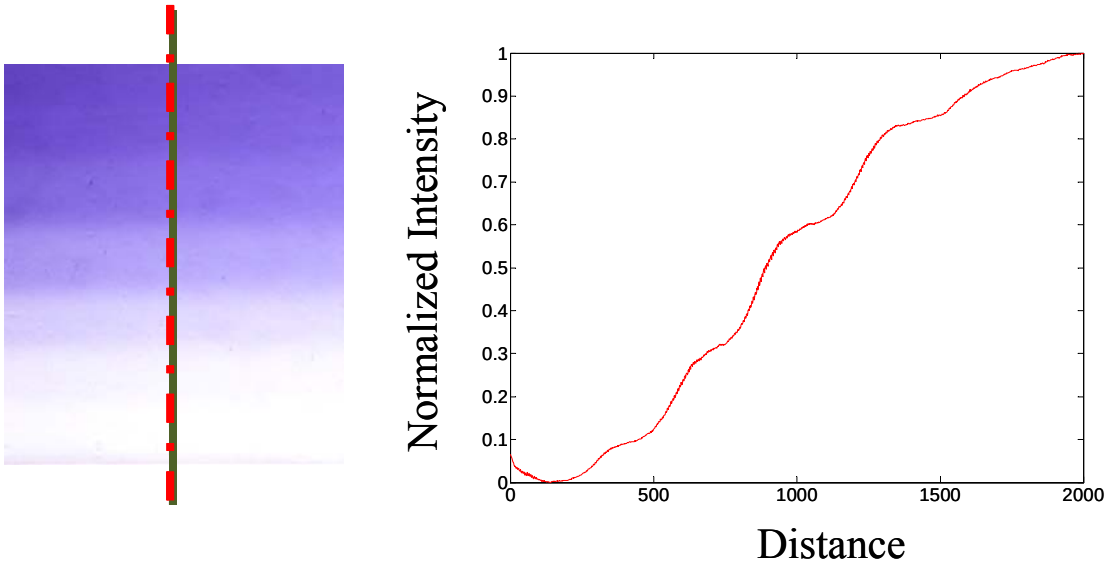

Figure 5.18 Gradient analysis of 1 ml/hr

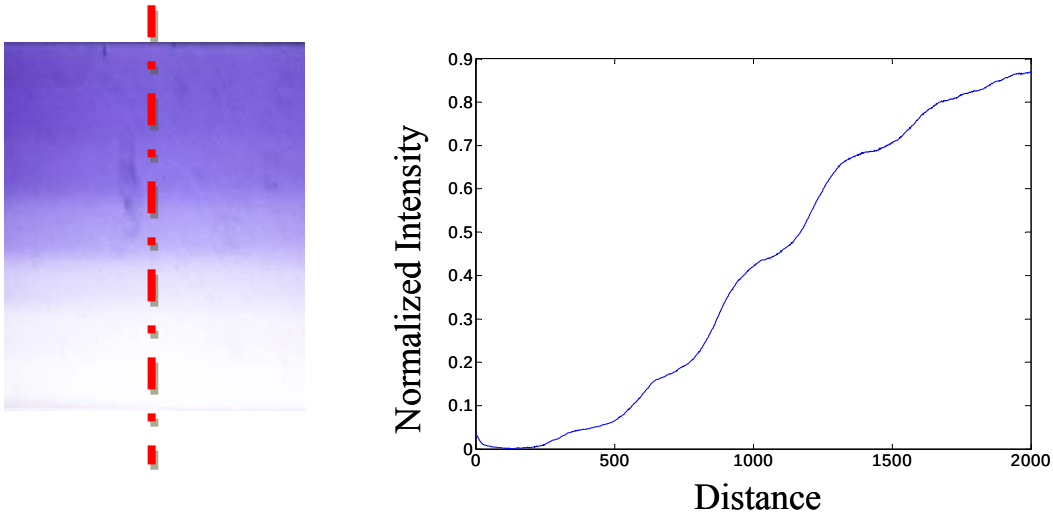

Figure 5.19 Gradient analysis of 2 ml/hr

The concentration analysis graph for 2 ml/hr is shown in Figure 5.19. The curve shows a similar pattern to 1 ml/hr. Fluctuation and step-like pattern were present in the cure. There were also seven flat stages in the curve. The stages occupied longer distance than that of 1 ml/hr. Therefore the concentration between two neighboring stages increased more sharply. It was obvious that the mixing of 2 ml/hr was more incomplete than 1 ml/hr.

Figure 5.20 shows the integrated comparison analysis between all flow rates (0.1, 0.5, 1 and 2 ml/hr). The flow rate of 0.1 ml/hr and 0.5 ml/hr show relatively linear gradients while the flow rate of 1 ml/hr and 2 ml/hr show gradients with fluctuations and step-like patterns.

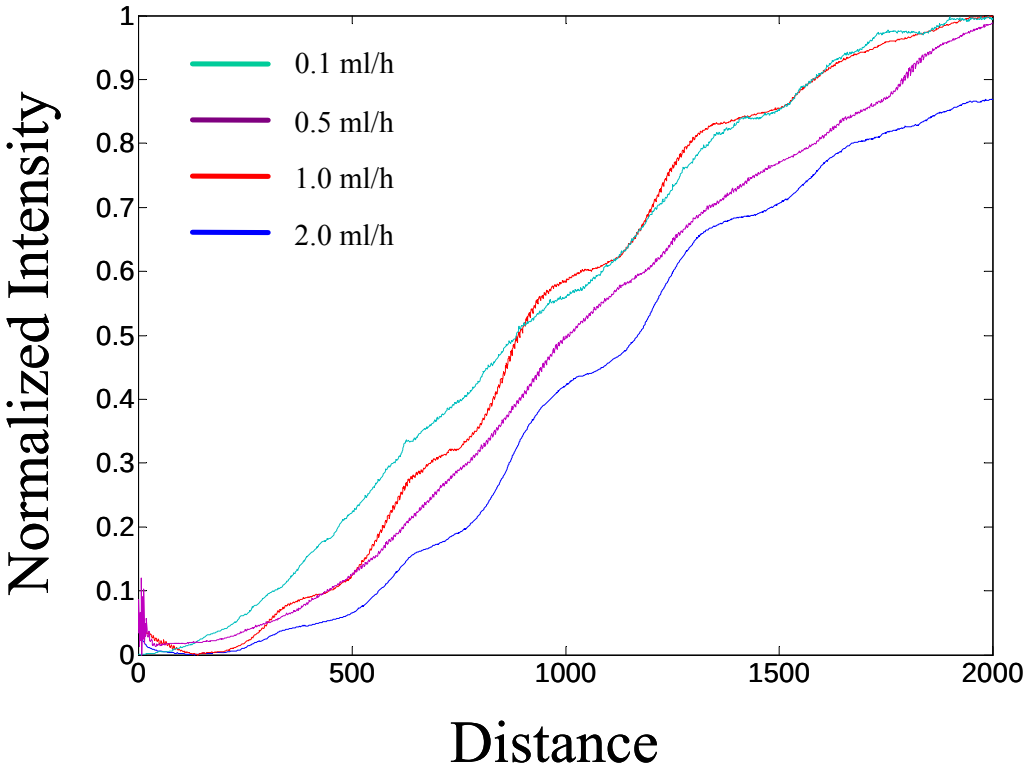

Figure 5.20 Gradient profiles comparison with different flow rates

5.3.2 Generation of gradient of fluorescence polymer beads

Fluorescence polystyrene beads were used to generate gradients of polymer beads to simulate cells movement in microfluidic channel. One inlet was connected to syringe that contained solution of polymer beads while the other inlet was connected to syringe that contained solutions without polymer beads. The flow speed of the two inlets was controlled at 0.5 ml/hr. Fluorescence microscope equipped with Micro-PLV was used to observe and record video of the movements of fluorescence polymer beads. The images of the gradient of polymer beads were then captured. Figure 5.21 shows two micrographs. Figure 5.21(b) shows a junction where two streams were first brought together. Figure 5.21 (c) shows the generated gradient of fluorescence beads. It can be observed that the mixing process was stable and the solution of fluorescence beads occupied 50% of the channel width in the mixing part.

In the gradient channel, the quantity of the polymer beads increased from left to right.

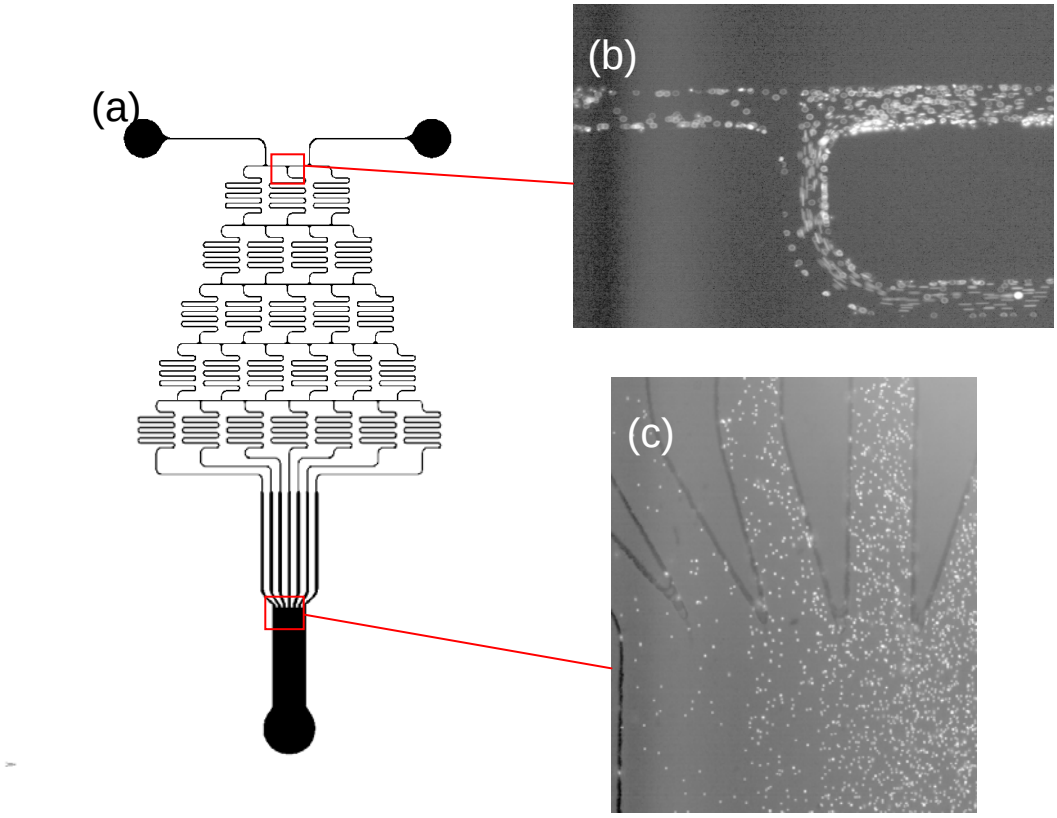

Figure 5.21 Micrographs of a junction where two streams of fluorescence beads were brought together and the generated gradient of beads

5.4 Discussion

5.4.1 Relationship between flow rate and time for complete the channel

According to the graph results of the relationship between the flow rate (ml/hr) with the average complete time (s) of the microfluidic device flowing process of Figure 5.5, it can be deduced that the relationship of the flow rate and the flowing time was not liner and directly proportional. From the trend line in Figure 5.5, it can be estimated that the time of completion was inversely exponentially proportional to the flow rate. However, there were several possible errors in the flow rate this experiment.

There was a random time lag in the starting step after the needle was being inserted into the inlets. The lower the flow rate, the longer the time lag. This error would affect the time parameter. It is suggested to start recording time when dyed solution was observed in the first channel. The integrity of the inlets may be damaged by repetitive practice of in and out of the needles; this may result in the leakage of solution.

5.4.2 Relationship between flow rate and concentration gradient quality

From Figures 5.6 to 5.14, it can be summarized that the mixing channel of the microfluidic network of flow rate 0.1 ml/hr and 0.5 ml/hr was in a steady flow. Both of the transparent and dyed solutions occupied 50% of the channel's width. The flow rate of 0.1 ml/hr and 0.5 ml/hr were ideal and under control. For flow rate of 1 ml/hr and 2 ml/hr, it was found that the first mixing channel occupied uneven distribution of the solution so the flowing process was unstable and not under control.

In the part of concentration gradient analysis, referenced to Figure 5.20, flow rate of 0.1 ml/hr and 0.5 ml/hr showed a very similar pattern. Both of the curves were very smooth and direct linear. It implies that the concentration of the investigated region increased gradually and constantly. For flow rate of 1 ml/hr and 2 ml/hr, the curves were quite different from 0.1 ml/hr and 0.5 ml/hr. Fluctuations and step-like pattern can be observed. It implies that some part of the investigated region had the same concentration. The concentration along the region did not increased gradually and

constantly. The concentration gradient quality of 0.1 ml/hr and 0.5 ml/hr were more acceptable than 1 ml/hr and 2 ml/hr.

The above analysis shows that the injecting velocity 1 ml/hr was a critical velocity for forming the linear gradient. The injecting velocity 1 ml/hr was then conversed into the solution velocity in the seven branched channel. As the branched channel had a width 200 μm and height about from 75μm to 100 μm, the calculated velocity value was about 5.3×10^{-3} m/s. This velocity value was close to the theoretical simulated value 8×10^{-3} m/s which was discussed in chapter 3. In the simulation, linear gradient can be formed below velocity 8×10^{-3} m/s. Therefore, the practical result was consistent with the theoretical simulated result.

However, there were various possible errors in the flow rate quality analysis experiment. Firstly, the integrity of the inlets may be damaged by repetitive practice; leakage of solution may exist during the experiment. Control of the leakage of solution was especially difficult in transparent solution. Secondly, the analysis photo captured by microscope may contain contaminants such as dust, dirt or even air or water droplets on the surface of PDMS. Such contaminants could affect the color analysis by the MATLAB program. It is suggested to capture the same region for data analysis in order to reduce error. However, if contaminant was presented in the photo being analyzed, a clear region should be selected.

5.4.3 Generation of gradient of fluorescence polymer beads

The flow rate of 0.5 ml/hr was chose due to the relative better performance in generating gradient, which was discussed above. Figure 5.21 shows that the fluorescence polymer beads can form a gradual gradient distribution along the channel which was consistent with the results of dye solution. As the size of the fluorescence beads was similar to that of the cells, it is also possible that the cells can move well in the microchannels.

Chapter 6 RGD Incorporated 2D PEG Hydrogel Surface for Mesenchymal Stem Cells (MSC) Culture

Abstract

RGD peptide was incorporated to PEG polymer chain by chemical grafting. Different concentration RGD peptide was polymerized with PEG diacrylate to form RGD incorporated PEG hydrogel. Fourier-transform infrared spectroscopy (FTIR) was used to characterize this chemical grafting reaction. The characterization results showed that RGD was successfully incorporated to PEG. MSCs were then cultured on the 2D PEG hydrogel surface incorporated with RGD concentration of 0, 0.25mM, 0.5mM and 0.75mM. Actin and nucleus staining of MSCs were done to characterize stem cell adhesion and spreading. With the increase of RGD concentration in PEG hydrogel, both cell density and adherent cell area increased.

6.1 Introduction

6.1.1 RGD incorporation into biomaterials

Biomaterials such as synthetic polymers usually have enough mechanical properties and stability. However, these biomaterials often do not have adequate interaction between materials and cells, which results in foreign body reactions. There are many methods to improve bioactivity properties of biomaterials, such as surface modification with cell adhesion proteins or peptides to obtain controlled interaction between cells and biomaterial interfaces (Lin YC et al., 2009; Sargeant TD et al., 2008; Zhang H et al., 2000).

The RGD sequence is a ligand for integrin-mediated cell adhesion (Ruoslahti E et al., 1987). If the RGD sequence can be immobilized to the biomaterial's surface, it will promote cell adhesion. However RGD is chemically inactive, it is difficult to immobilize RGD to the biomaterials' surface directly.

Although RGD is chemically inactive, it can still react with some chemical groups, such as hydroxyl, amino and carboxyl groups in special conditions (Hersel U et al., 2003; Niu X et al., 2005). As many types of biomaterials do not have these active chemical groups, surface modification methods should be used to make surface active. Physical blending and chemical grafting have been widely used to introduce the functional chemical groups.

Physical blending means to blend some special material with certain functional

groups onto biomaterial surface. For example, polyethersulfone (PES) membrane can be modified by blending with a copolymer of acrylic acid (AA) and N-vinyl pyrrolidone (VP). The acrylic acid has the functional group carboxyl acid. The carboxyl acid group can further react with the amino group of peptide and proteins. The modified PES membrane has better biocompatibility than unmodified PES membrane (Liu Z et al., 2009). Physical blending is a simple method. However it may have some problem such as miscibility between the two materials. Moreover, the blending effect is often not stable and the blended components can be eluted into the fluids during the cell culture process.

Compared with physical blending, chemical grafting can introduce more stable functional groups. For example, PLLA is a kind of biodegradable polymer, which is widely used in tissue engineering (Freed LE et al., 1993; Ma PX et al., 2001). However, PLLA has poor cell-adhesive property. To improve the cell-adhesive property, various approaches have been developed. One approach is surface modification with grafting acrylic acid (AA) by polymerization, which can be ready for further immobilization with peptides. The immobilized peptides can promote cell adhesion (Jung HJ et al., 2008). Some other methods such as oxidation and plasma deposition can also introduce functional groups on the biomaterials' surface. In these cases, carboxyl group can be introduced on the polystyrene surface by plasma treatment (Sasai Y et al., 2008). The introduced functional groups have the ability to immobilize biomolecules.

In these cases, there are many functional groups such as hydroxyl, amino and carboxyl groups in the biomaterials, the RGD sequence can be easily incorporated. RGD sequence is mostly incorporated to biomaterials by a stable covalent amide bonding. This is mostly completed by the reaction between activated carboxyl acid group and the N-terminus of RGD sequence. The carboxyl acid can be firstly activated by 1-ethyl-3-(3-dimethylaminopropyl)-carbodiimide (EDC). The activated carboxyl acid can then be stabilized by NHS. Finally, RGD reacts with the activated carboxyl acid forming the amide bond (Grabarek Z et al., 1990). The reaction scheme is shown in Figure 6.1.

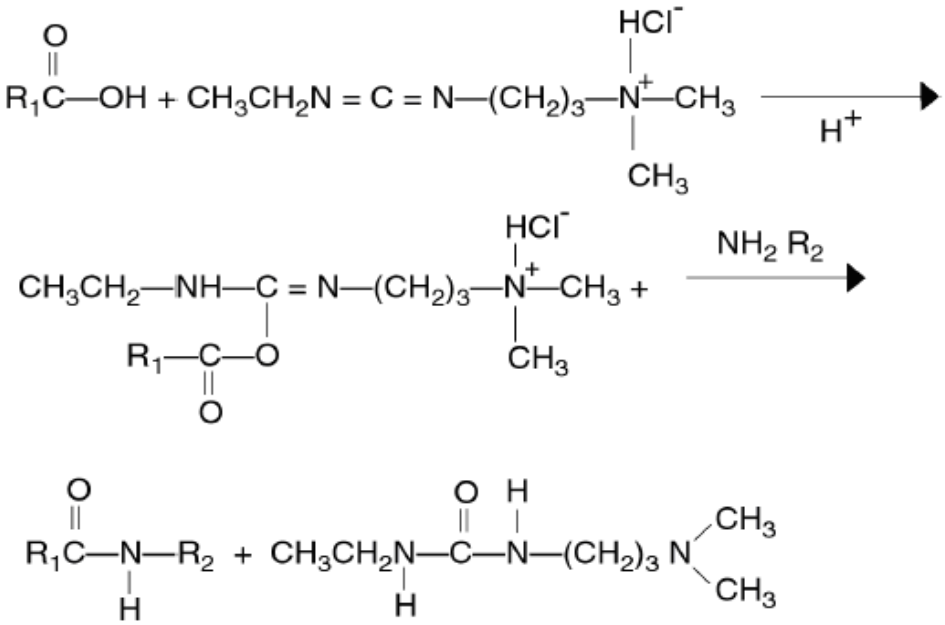

Figure 6.1 Reaction scheme for EDC and peptide

Some biomaterials often do not have carboxyl acid groups. For instance they have amino groups or hydroxyl groups. In this case the modification method will be different for incorporation. Amino groups can be treated with anhydride to generate carboxyl groups which can then react with RGD sequence (Morpurgo M et al., 1999). Biomaterials with hydroxyl groups can be treated with N,N'-disuccinimidyl

carbonate or similar groups to obtain active groups which can further react with the peptide (Morpurgo M et al., 1999).

6.1.2 Photopolymerization mechanism

Photopolymerization is a method to covalently crosslink monomer or macromer solution to a three-dimensional network via chain polymerization mechanism. Photopolymerization has been utilized in wide applications ranging from integrated circuits to polymeric dental fillings. Photopolymerizations can be performed with low energy input, which is spatially and temporally controlled at room temperature. Due to the mild reaction conditions, photopolymerization has been widely used in fabrication of biomaterials.

The first step in the photopolymerization is the initiation of photoinitiator, which can adsorb light in ultraviolet (200-400 nm) or visible light (400-800 nm) range. After adsorbing light, the photoinitiator can produce radicals in two ways. One is to dissociate into primary radicals and the other is to react with a second species (A-H) via hydrogen abstraction to form secondary radicals ($R^{\cdot}$) (Bryant SJ et al., 2005). The reaction scheme is shown in Figure 6.2. The radicals $R^{\cdot}$ then react with vinyl groups C=C to start the photopolymerization.

There are many kinds of photoinitiators such as aromatic carbonyl compounds, benzoin derivatives, benziketals, acetophenoe derivatives and hydroxylphenones (Nguyen KT et al., 2002). The most widely used photoinitiator is the aromatic

carbonyl compounds such as phtotoinitiator 2,2-dimethoxy-2-phenylacetophenone (Irgacure 651) and 4-(2-hydroxyethoxy)phenyl-(2-hydroxy-2-propyl)ketone (Irgacure 2959) which are commonly used in fabricating hydrogel scaffold (Williams CG et al., 2005).

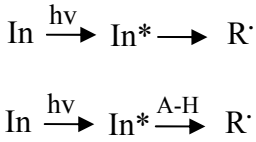

Figure 6.2 Reaction scheme of photo initiation

The radicals produced in the above step then react with the added monomers by vinyl groups (C=C). This stage is the second step, also called propagation. In propagation, there are two processes which are auto-acceleration and auto-deceleration. As the monomer solution is converted into a 3D polymer network, the solution viscosity increases dramatically. With the increase of solution viscosity, the radical mobility will decrease. This decrease would further cause an increase in radical concentration. The increased radical concentration can further lead to a polymerization rate increase. This phenomenon is the auto-acceleration. Close to the maximum polymerization rate, the increase of solution viscosity will make the mobility of vinyl groups difficult. Then, the decrease of vinyl groups' mobility results in the decrease of polymerization, which is regarded as auto-deceleration. The overall rate of polymerization can be controlled by the changes of concentrations of photoinitiator and monomers. The increase of concentrations of photoinitiator and monomers generally leads to an increase of polymerization rate (Bryant SJ et al., 2005).

6.2 Methodology

6.2.1 Incorporation of RGD peptide to PEG molecule

Arg-Gly-Asp (RGD) peptide (Sigma-Aldrich, Inc., Louis, MO 63103 USA) was incorporated into PEG molecule by reacting the –NHS group of Acryl-PEG-NHS (3400 Da, Laysan Bio Inc., AL, USA) with $–NH_2$ of the peptide, as shown in Figure 6.3.

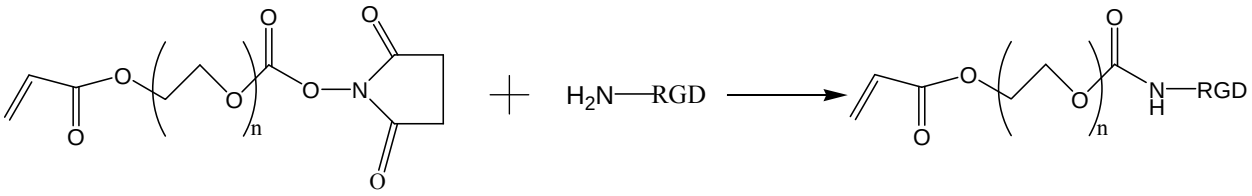

ACRL-PEG-NHS RGD peptide ACRL-PEG-RGD

Figure 6.3 Chemical reaction scheme of ACRL-PEG-NHS with RGD peptide

RGD and ACRL-PEG-NHS powder were mixed at a ratio of 1: 2.5, and added into 10 mM sodium bicarbonate buffer solution to react for 6 hrs at room temperature. Excessive ACRL-PEG-NHS was used to make RGD peptide react completely. The reaction product was named as ACRL-PEG-RGD. Then dialysis tube was used to dialysis the incorporated solution for one day. Small molecules such as sodium bicarbonate would pass through the membrane into periphery solution, while ACRL-PEG-RGD molecules would remain within the tube. Finally, ACRL-PEG-RGD solution was evaporated in freeze drying vacuum for seven hours, and the ACRL-PEG-RGD powder was well prepared. Fourier-transform infrared spectrometer (FTIR) was used to characterize ACRL-PEG-NHS and ACRL-PEG-RGD. The ACRL-PEG-RGD was also dissolved into phosphate buffer

solution (PBS) to store at -20 ℃ with the concentration of 10 mM for later usage.

6.2.2 Mesenchymal stem cells culture

The rat bone marrow derived mesenchymal stem cells were obtained from Lonza PT-2505. . The stem cells were cultured in a culture flask and incubated in a humidified incubator supplemented with 5% CO_2 at 37 ℃. The non-adherent cells were removed after two days culture, leaving the mesenchymal stem cells in the culture flask. Cells were passaged with 0.025% trypsin–EDTA. Passage 3 cells were trypsinized, centrifuged and used for culture on PEG hydrogel.

6.2.3 Fabrication of PEG hydrogel for two dimentional (2D) cell culture

Poly(ethylene glycol) diacrylate (PEGDA, 500 Da, Sigma-Aldrich, Inc., Louis, MO 63103 USA) was dissolved into PBS solution at a ratio of 30:70 (V/V). Photoinitiator Irgacure 2959 (Ciba Specialty Chemicals Inc., Switzerland) was dissolved into ethanol at a concentration of 10% (W/V). The photoinitiator solution was then added into the PEGDA solution with a concentration 0.1% (W/V). Stock ACRL-PEG-RGD solution (10 mM) was finally added into the PEGDA solution to prepare the solution with RGD concentration of 0 mM, 0.25 mM, 0.5 mM and 0.75 mM. Poly(ethylene glycol) diacrylate (PEGDA, 3400 Da, Laysan Bio Inc., AL, USA) was also used to fabricate PEG hdyrogel. The preparation procedure of PEG (3400 Da) solution was the same to PEG (500 Da) described above.

PEG hydrogel was fabricated by photopolymerization using an UV spotter source (EXFO S1000, USA). For photopolymerization of PEG hydrogel, a PDMS chamber on a glass slide was first fabricated. The glass slides were surface modified with a hydrophobic silane TPM, which was also used to fabricate the gradient device discussed in Chapter 4. To form the chamber, the PDMS mold was attached closely onto the glass surface. As there was no plasma bonding between the two surfaces, the PDMS mold can be easily detached from the glass surface. PEG solution was injected into the chamber between PDMS and glass slides through the hole in the PDMS. Then the glass slides with PEG solution in the PDMS chamber was placed under UV light (365nm, 200 mW/cm^2) for 1 min to cure the solution forming PEG hydrogel. Details of the process are illustrated in Figure 6.4.

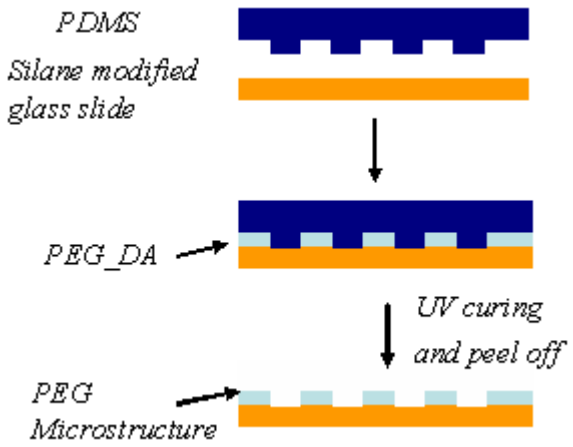

Figure 6.4 Fabrication of PEG hydrogel

The PEG hydrogel on glass slide was put into a petri dish, which was filled with PBS solution. The petri dish was then sterilized under UV light for 5 hrs. After sterilization, PBS solution was removed and low-glucose Dulbecco's modified Eagle

medium supplemented with 10% FBS, 1% penicillin/streptomycin, 0.25% gentamicin, and 0.25% fungizone was added into the petri dish. Passage 3 MSCs were seeded onto the PEG hydrogel. The cells seeding density was about $6x10^4$ cells/cm^2. The petri dish was incubated in a humidified incubator supplemented with 5% CO_2 at 37 ℃. Cell culture medium was changed every two or three days.

6.2.4 Actin and nucleus staining

For actin and nucleus staining, 4% paraformaldehyde was added onto the samples for 15min. Then the media in petri dish was removed and the samples were washed gently with PBS solution. 0.01%Triton-X 100 was then added into PBS for 1 min, which was used to destroy the cell wall so that dye could permeate into cells. Then, the solution inside the petri dish was removed again following by PBS washing. Phalloidin–Tetramethylrhodamine B isothiocyanate P1951 (Sigma-Aldrich, Inc., USA), which was used to stain cell backbone, was diluted and added to each of the samples for 30 min. Diluted 4',6-diamidino-2-phenylindole, dihydrochloride (DAPI) D1306 (Invitrogen Corporation, USA) was then added to each sample for 5 min. DAPI was used for staining the cell nuclei. A few drops of n-propyl gallate were added for extending dyeing time. N-propyl gallate was a kind of anti-fading agent which can decrease the rate of decolorization. Fluorescence images of stained cells were recorded by a fluorescence microscope.

6.3 Results

6.3.1 Incorporation of RGD peptide to PEG chain

RGD molecule was incorporated to PEG chain by the reaction of -NH_2 group of RGD with –NHS group of ACRL-PEG-NHS. The incorporated molecule was then characterized by FTIR. Figure 6.5 shows the FTIR spectra of ACRL-PEG-NHS and ACRL-PEG-RGD. The adsorption band 1640 cm^{-1} arises from the C=O stretching vibration. Comparing ACRL-PEG-NHS with ACRL-PEG-RGD, ACRL-PEG-RGD had a stronger adsorption band at 1640 cm^{-1}. This was due to the widely distributed C=O groups in RGD incorporated within PEG. Another difference was 1735 cm^{-1}, at which ACRL-PEG-NHS had a stronger adsorption band than ACRL-PEG-RGD. This adsorption band resulted from -(C=O)-NHS group. After incorporation, -NHS group was replaced by –NH_2 group. Therefore, the adsorption band 1735 cm^{-1} decreased after incorporation reaction. The FTIR results demonstrated the successful incorporation of RGD to PEG..

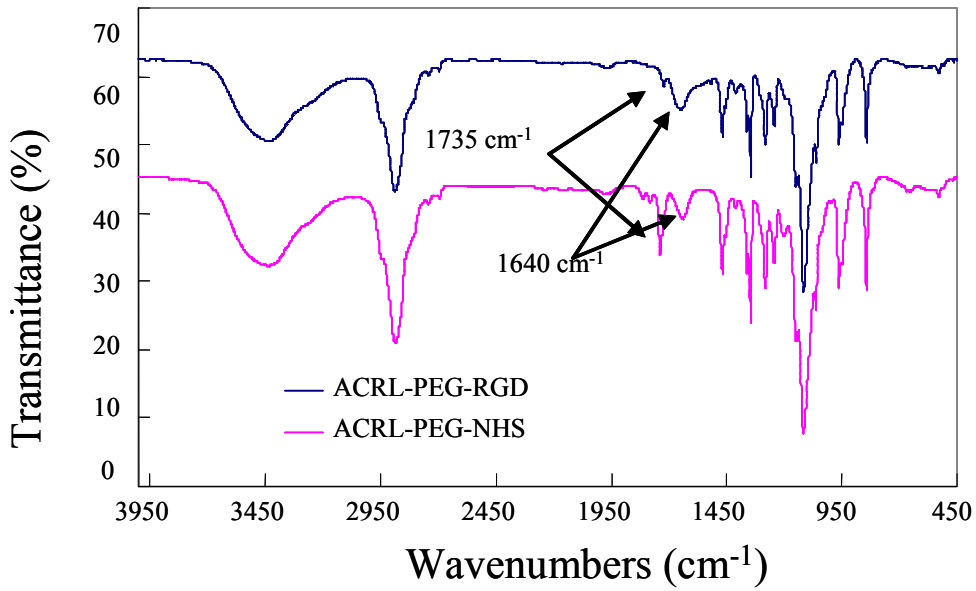

Figure 6.5 FTIR spectra of ACRL-PEG-NHS and ACRL-PEG-RGD

6.3.2 PEG hydrogel for 2D MSCs culture

6.3.2.1 PEG hydrogel with molecular weight 500Da

Firstly, PEG hydrogel with molecular weight 500Da was fabricated for 2D MSCs culture. An optical microscope was used to take images of MSCs which are shown in Figure 6.6.

Figure 6.6 shows the adhesion and morphology of MSCs cultured on 2D PEG hydrogel surface with different RGD concentrations of 0, 0.25 and 0.5 mM. It can be seen that the cells clearly show different adhesion densities and morphologies. As shown in in Figure 6.6(a) and Figure 6.6(b), MSCs cultured on PEG hydrogel without RGD had no adhesion and the cell morphology was round without any spreading. As shown in Figure 6.6(c) and 6.6(d), MSCs cultured on PEG hydrogel with 0.25 mM RGD can adhere on the surface and showed a flattened morphology with spreading spikes. As shown in Figure 6.6(e) and 6.6(f), more cells can adhere on the hydrogel with 0.5 mM RGD compared with 0.25 mM RGD. The cells were mostly spreading with ruffling of peripheral cytoplasm. The results indicated that RGD can promote MSCs adhesion and spreading.

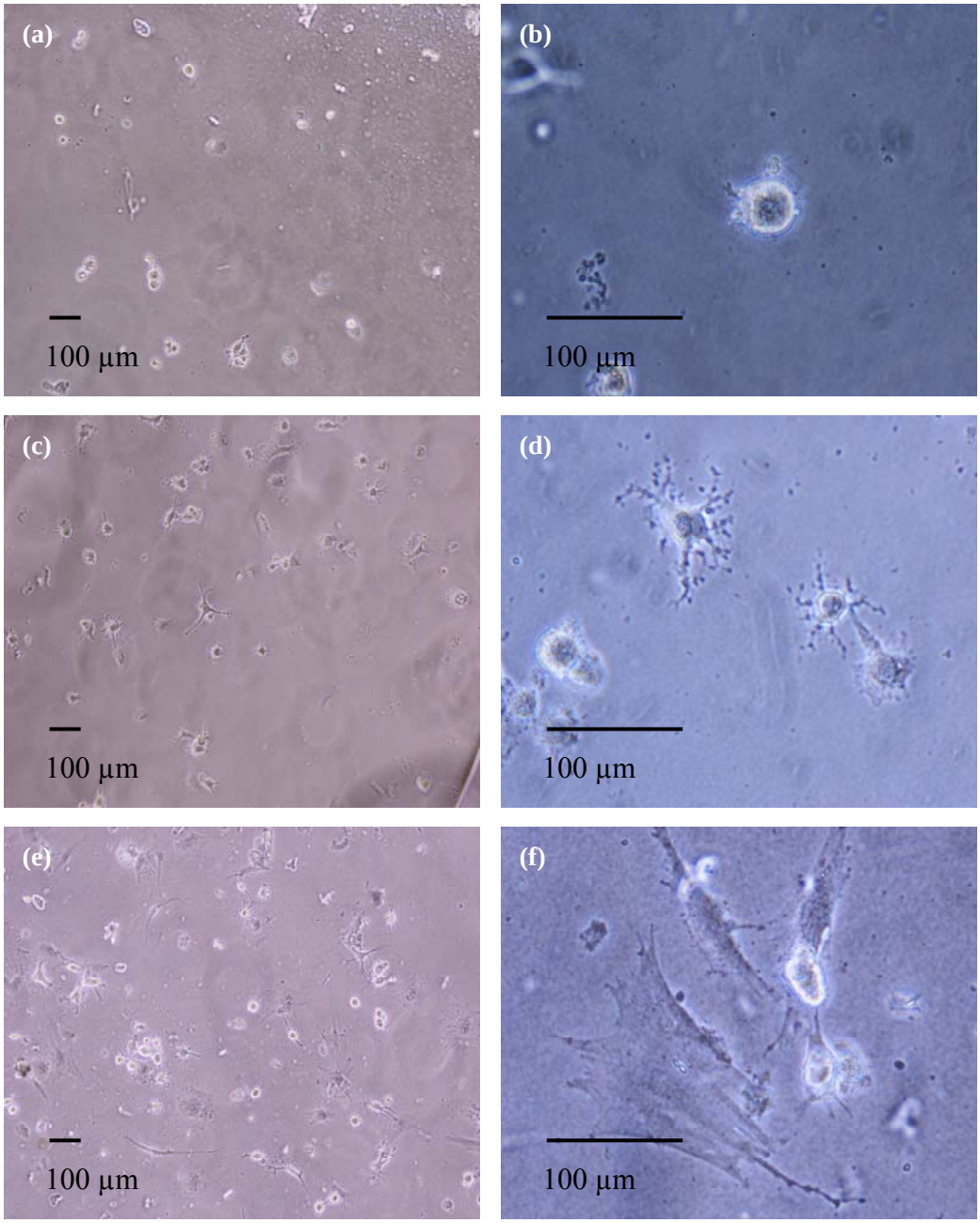

Figure 6.6 MSCs cultured for 1 day on 30% (w/v) PEG (500 Da) hydrogel with different RGD concentrations. (a) 0 mM, 10×; (b) 0 mM, 40×; (c) 0.25 mM, 10×; (d) 0.25 mM, 40×; (e) 0.5 mM, 10×; (f) 0.5 mM, 40×.

Actin and nucleus staining were also done to characterize MSCs adhesion and spreading. Fluorescence images were taken and shown in Figure 6.7. The red color was actin while the blue color was nucleus. From Figure 6.7, it can be seen that more cells can adhere on the PEG hydrogel with 0.5 mM RGD than that without RGD.

The cells on PEG hydrogel without RGD had a round shape while the cells on 0.5 mM RGD hydrogel had a spreading shape.

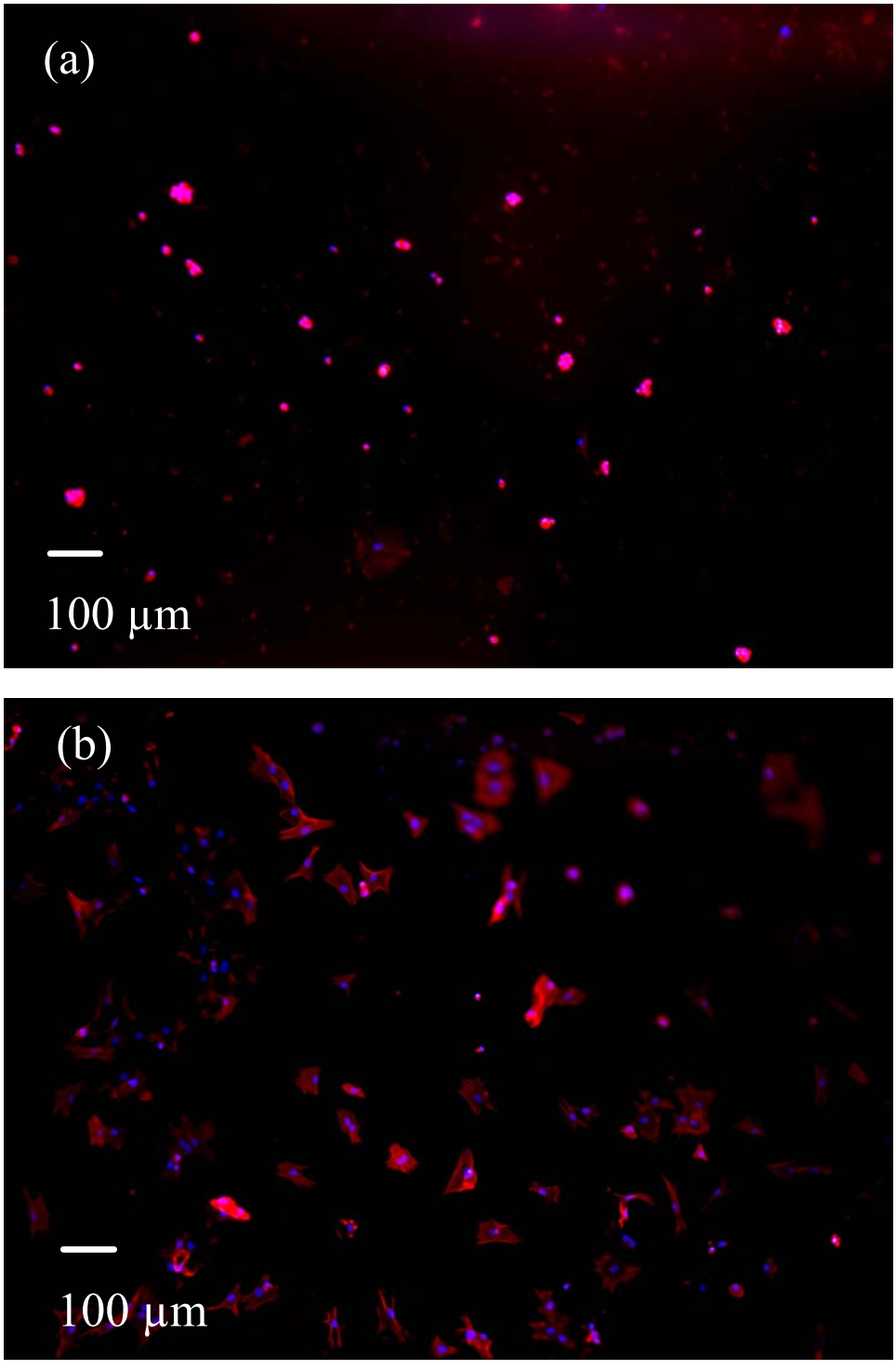

Figure 6.7 Fluorescence images of MSCs cultured for 1 day on 30% (w/v) PEG (500 Da) hydrogel with different RGD concentrations. (a) 0 mM, 10×; (b) 0.5 mM, 10×.

The cell adhesion density was calculated according to the optical and fluorescence images of cells on PEG hydrogel. The cell adhesion density was illustrated in Figure 6.8. For half day culture and one day culture, the cell adhesion density both increased with the increase of RGD concentration. After a half day culture, the number of cell adhesion was similar between 0.25 mM RGD and 0.5mM RGD, but after one day of culture, the number of cell adhesion was similar between 0.5 mM RGD and 0.75 mM RGD. The results indicated that higher RGD concentration would promote more cell adhesion, and this phenomenon is in line with the receptor mediated cell adhesion mechanism of RGD (Chen CS et al., 2003).

From the above results, it can be seen that MSCs cultured on hydrogels with different RGD concentration had different spreading shape. Therefore, the cell adhesion area was also different. The single cell adhesion area was calculated and the results were shown in Figure 6.9. Figure 6.9 shows that the single cell adhesion area increased with the increased RGD concentration. PEG hydrogel with 0.75 mM RGD had the largest cell adhesion area, which was about 4000 μm^2. The results of cell adhesion area indicated that RGD can promote cell spreading.

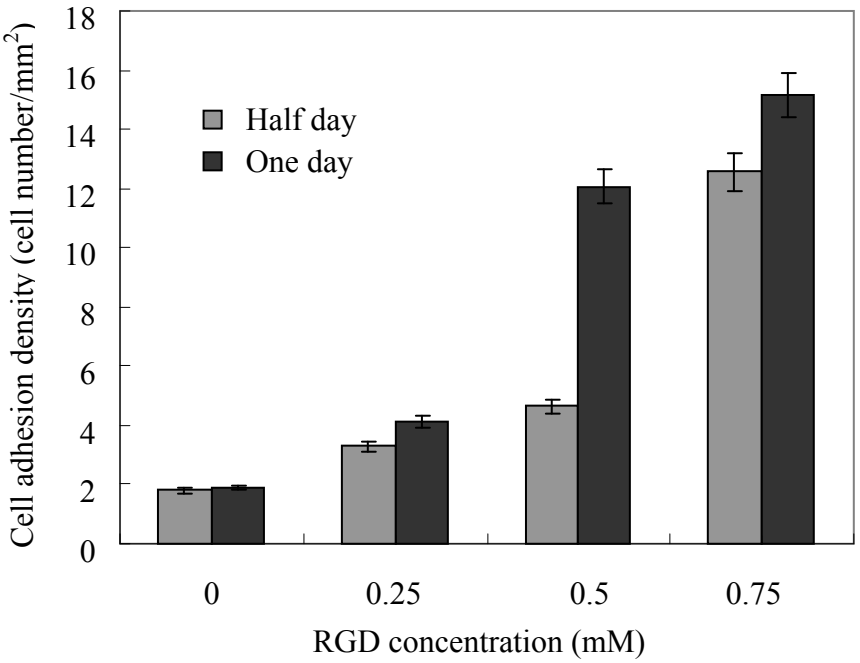

Figure 6.8 MSCs adhesion densities on PEG (500 Da) hydrogel with different RGD concentrations 0 mM, 0.25 mM, 0.5 mM and 0.75 mM after half day and one day culture

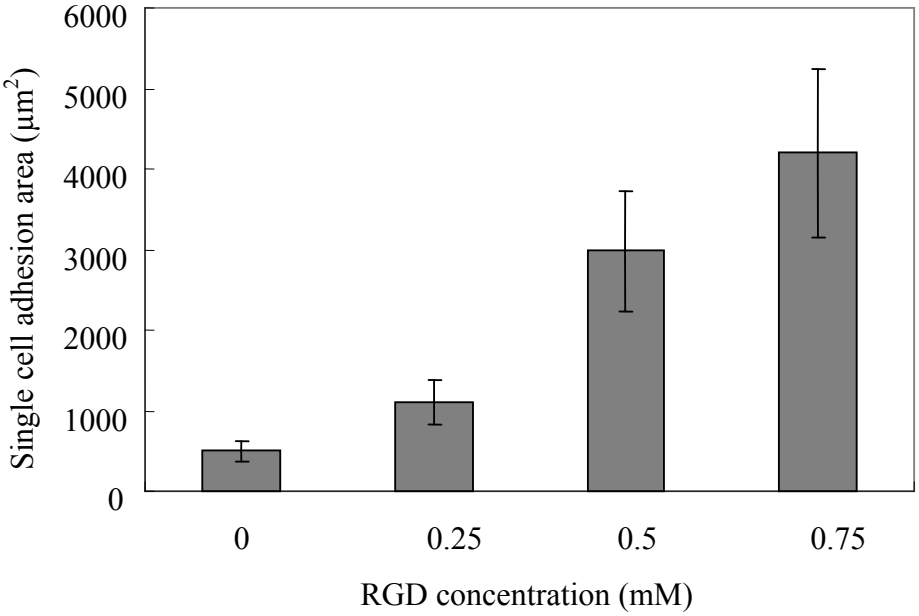

Figure 6.9 Single MSCs adhesion area on PEG (500 Da) hydrogel with different RGD concentrations 0 mM, 0.25 mM, 0.5 mM and 0.75 mM, cells cultured for one day

6.3.2.2 PEG hydrogel with molecular weight 3400Da

It was found that 500 Da PEG hydrogel was easily detached from glass slides surface after one day culture. This may be due to the high cross-linking degree of PEG hydrogel 500Da. In order to observe cell adhesion and spreading in a long time, 3400 Da PEGDA was chosen. The 3400 Da PEGDA had less vinyl groups (C=C) compared with the same amount of 500 Da PEGDA. Therefore, it had less cross-linking degree which resulted in a long term cell culture.

The hydrogel which was made from 3400 Da PEG had higher stability and was not easy to detach from the glass slides surface. MSCs were then cultured on 3400 Da PEG hydrogel surface. Optical microscope was used to observe the MSCs morphology. Cell adhesion density was calculated for cell culture of one day and two days. The cell adhesion density was shown in Figure 6.10. With the increase of RGD concentration, the cell adhesion density also increased. The cell adhesion density of two days culture was slightly higher than that of one day culture. So there was no significant difference for between one day and two days culture. The results indicated that one day culture was enough for MSCs adhesion.

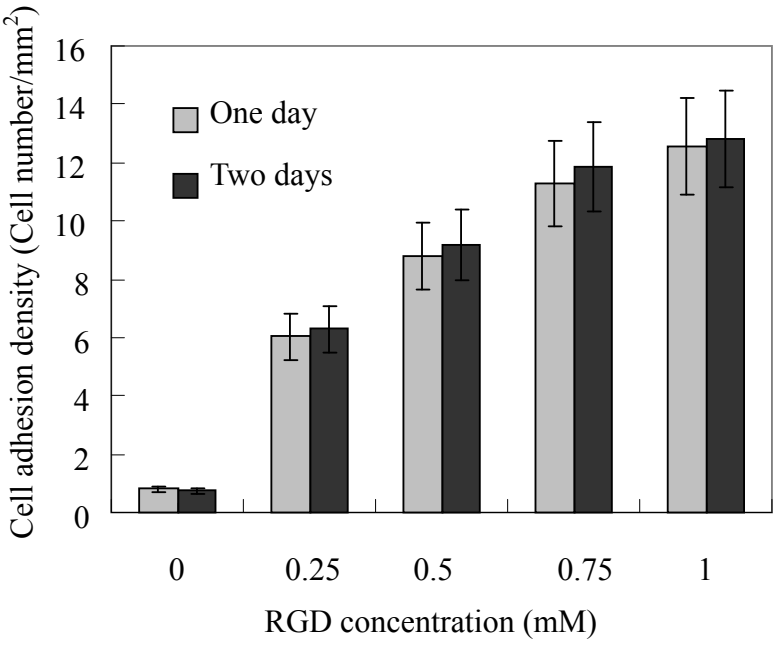

Figure 6.10 MSCs adhesion densities on PEG (3400 Da) hydrogel with different RGD concentrations 0 mM, 0.25 mM, 0.5 mM, 0.75 mM and 1 mM after one day and two days culture

6.4 Discussion

In this project, RGD was chemically incorporated to PEG molecule. The incorporation reaction was done in water solution at room temperature. As it is known PEG is a bio-inactive material which has no interaction with cells, some biomolecules can be incorporated to PEG to study the specific interaction between cells and the specific biomolecules. RGD biomolecule is the ligand for integrin-mediated cell adhesion which is used to study the interaction of RGD and MSCs in our project. Besides RGD, other biomolecules such as heparin and collagen can also be incorporated to PEG to study the specific interaction (Benoit DS et al., 2005; Lee HJ et al., 2006). These incorporation reactions were also based on the reaction of –NHS and $–NH_2$ in water solution at room temperature.

RGD was chemically incorporated to PEG hdyrogel, so it will not be released from PEG hydrogel during cell culture. With the increase of RGD concentration, more RGD sites were ready on the PEG hydrogel surface, which resulted in more cell adhesion sites on PEG hydrogel surface. Therefore, more cells could be adhered on the PEG hydrogel surface with higher RGD concentration.

For cell culture half day on PEG (500 Da) hydrogel, the cell adhesion density has a large jump from 0 mM to 0.75 mM. This jump suggests that this concentration range from 0 mM to 0.75 mM is a critical window for cell adhesion of half day. For cell culture one day on the PEG (500 Da) hydrogel, the cell adhesion density has a jump from 0 mM to 0.5 mM. This jump also suggests that the concentration range from 0 mM to 0.5 mM is a critical window for cell culture of one day.

For cell culture one day and two days on PEG (3400 Da) hydrogel, there was no significant difference of cell adhesion density. This can be explained by the saturation of cell adhesion. The cells have occupied all the RGD sites on the PEG surface after one day. Therefore, there is no obvious difference of cell adhesion between one day and two days culture.

Chapter 7 RGD Gradient 2D PEG Hydrogel Surface for Mesenchymal Stem Cells (MSC) Culture

Abstract

PEG hydrogel with RGD gradient was fabricated using PDMS microfluidic gradient generator. MSCs were then cultured on the gradient PEG hydrogel surface. Actin and nucleus staining were done to characterize cells adhesion and spreading. It was found that cells adhesion density and spreading area increased with increase of RGD concentration in the gradient. And there was a critical RGD concentration below which fewer cells adhered on the surface and above which more cells can attach.

7.1 Introduction

In Chapter 6, MSCs were cultured on PEG hydrogel with different RGD concentrations. MSCs had different responses to different RGD concentrations. With the increase of RGD concentration, more cells can adhere and spread on the PEG hydrogel. However, cells *in vivo* are often in a gradient environment of certain molecule. Gradients play essential roles in many phenomena including development, inflammation, and wound healing. Interest in these phenomena has led to the development of numerous *in vitro* methods for exposing cells to gradients (Liu L et al., 2007; Luhmann T et al., 2009).

In this chapter, a PDMS microfluidic gradient generator was used to fabricate 2D RGD gradient PEG hydrogel. The design and fabrication of this microfluidic device were discussed in Chapter 4. From the results of simulations and practical testing in Chapter 3 and Chapter 5, gradient could be successfully generated in this kind of microfluidic device. PEG solution with different RGD concentrations was then injected into the microfluidic device. After formation of stable RGD gradient, the whole device was exposed to UV light to crosslink the PEG solution into hydrogel. Thus, RGD gradient PEG hydrogel could be fabricated. Compared with the conventional method to fabricate PEG hydrogel with different RGD concentrations, this microfluidic device integrated the concentration control into one piece of gradient PEG hydrogel. The gradient hydrogel had a continuous concentration variation which can not be achieved in conventional method. Moreover, this device can also be used to fabricate gradient PEG hydrogel with different RGD

concentration profiles by changing the solution injecting velocity.

MSCs were then cultured on the RGD gradient PEG hydrogel. In Chapter 6, MSCs had different responses to PEG hydrogel with different RGD concentrations. In high RGD concentration area, more cells adhered on PEG hydrogel surfaces. On this RGD gradient PEG hydrogel, MSCs may also have similar behavior. However, there may be some new phenomena. In Chapter 6, the cell adhesion density had a jump in a certain concentration window. However, we did not know the exact concentration point for the jump. With this kind of gradient PEG hydrogel, the concentration point for the jump may be found. By changing the injecting velocity, different gradient profiles can be achieved. The different gradient profiles may also have different impacts on cells' behaviors.

7.2 Methodology

7.2.1 Generation of RGD gradient PEG hydrogel

The two inlets of the microfluidic gradient generator were first filled with ethanol. Dropper was placed at the outlet in order to fill the microchannel fully with ethanol until no air bubbles present. After that, phosphate buffer solution (PBS) was used to replace the ethanol by using the same method. This method can prevent air bubbles in the microfluidic device. If PBS solution was directly injected into the device, there were many air bubbles due to the hydrophobicity of PDMS.

Poly(ethylene glycol) diacrylate (PEGDA, 500 Da, Sigma-Aldrich, Inc., Louis, MO

63103 USA) was dissolved into PBS solution at a ratio of 30:70 (V/V). Photoinitiator Irgacure 2959 was dissolved into ethanol at a concentration of 10% (W/V). The photoinitiator solution was then added into the PEGDA solution with a concentration of 0.1% (W/V). Stock ACRL-PEG-RGD solution (10 mM) was finally added into the PEGDA solution to prepare the solution with RGD concentration 0.25 mM and 0.5 mM.

Polyethylene tubing with steel needles was inserted into the inlet holes of the microfluidic device to make the fluidic connections. The piece of tubing was then connected to a syringe pump. Prepared PEG solution without RGD was filled in one syringe while the other was filled with PEG solution with RGD 0.25 mM, 0.5 mM, 1 mM or 2 mM. The needles of the syringes were inserted into the inlets separately. The flow rate was firstly adjusted to 0.5 ml/hr. Several minutes later, the PEG solution with RGD and without RGD were mixed, split and mixed along the channel again. Ultimately, a RGD gradient PEG solution was formed in the microfluidic channel. The RGD gradient PEG solution in the microfluidic device was then placed under UV light (365nm, 200 mW/cm^2) for 1 min for photo-polymerization of RGD gradient PEG hydrogel. The hydrogel was then put into a petri dish filled with PBS solution.

7.2.2 MSCs culture on RGD gradient PEG hydrogel

The PEG hydrogel in the petri dish was then sterilized under UV light for 5 hrs. After sterilization, PBS solution was removed and low-glucose Dulbecco's modified Eagle

medium supplemented with 10% FBS, 1% penicillin/streptomycin, 0.25% gentamicin, and 0.25% fungizone was added into the petri dish. Passage 3 MSCs were seeded onto the PEG hydrogel. The cells seeding density was about 60,000 cells/cm^2. The petri dish was incubated in a humidified incubator supplemented with 5% CO_2 at 37 ℃. Cell culture medium was changed every two or three days.

7.2.3 Actin and nucleus staining

The MSCs cultured on RGD gradient PEG hydrogel were observed by optical microscope. After one day culture, actin and nucleus staining were also done for the MSCs. The protocol for the staining was the same to that discussed in Chapter 6.

7.3 Results

MSCs were cultured on the RGD gradient PEG hydrogel. An optical microscope was used to observe the cells. Figure 7.1 shows the images of 0-0.25 mM RGD gradient PEG hydrogel for one day cell culture. Figure 7.1(a) shows the MSCs cultured on the whole RGD gradient PEG hydrogel. With the increase of RGD concentration from 0 mM to 0.25 mM, more cells adhered on the hydrogel surface. Figure 7.1(b) is the 10× image showing MSCs on the partial area of the RGD gradient PEG hydrogel. On PEG hydrogel with low RGD concentration, fewer cells attached on the surface and the cell shape was round. On PEG hydrogel with high RGD concentration, more cells attached on the surface and the cells had a spreading shape. Figure 7.1(c) is the 20× picture, which shows the middle area of the gradient PEG hydrogel. It more clearly indicated the cell adhesion change from low RGD concentration to high RGD

concentration. The MSCs had more spreading spikes on high RGD concentration area.

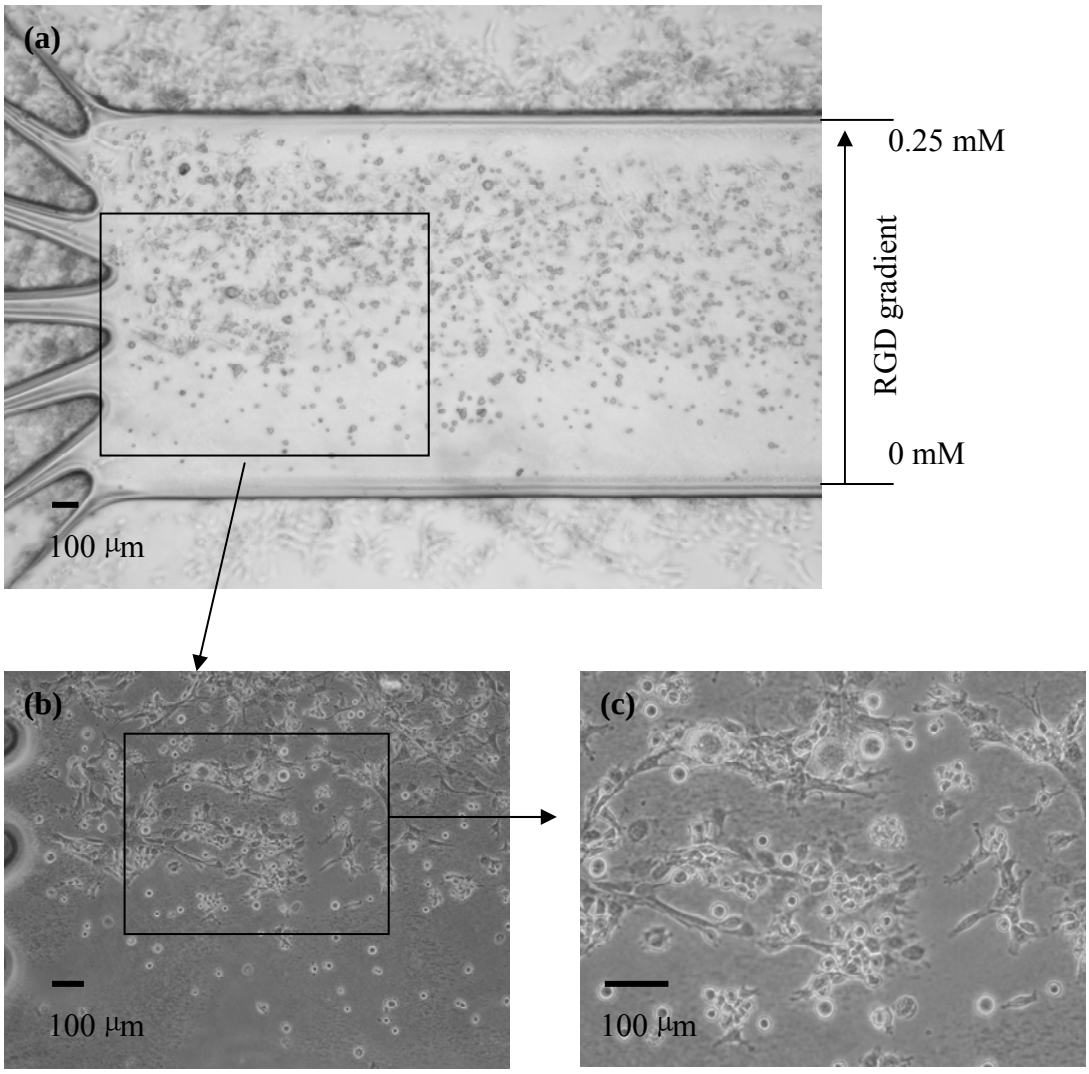

Figure 7.1 MSCs cultured on RGD gradient PEG hydrogel (0-0.25 mM) for 1 day. (a) 4×, (b) 10×, (c) 20×

Different gradient profiles may have different impacts on stem cells behaviors. In our research, other RGD gradient PEG hydrogels were also fabricated with 0-0.5 mM, 0-1 mM and 0-2 mM. Figure 7.2 shows the images of 0-0.5 mM RGD gradient PEG hydrogel for one day cell culture. In Figure 7.2(b) and 7.2(c), MSCs can adhere

on the low RGD concentration area, which was different from Figure 7.1(b) and 7.1(c). This was due to the relatively higher RGD concentration in 0-0.5 mM gradient that in 0-0.25 mM on the same area. This RGD concentration in low concentration area of 0-5 mM RGD gradient was also enough for MSCs adhering on the surface.

Comparing the two cases of 0-0.25 mM and 0-0.5 mM RGD gradient PEG hydrogl, there are similar characteristics. The adherent cell number generally increased from the low RGD concentration to high RGD concentration area. However, there are also some different characteristics. Compared with Figure 7.2(a), Figure 7.1(a) had a more obvious trend which showed that the cell adhesion number increased from low RGD concentration to high RGD concentration. From these results, it can be concluded that MSCs on 0-0.25 mM RGD gradient had largest distribution difference of cell adhesion. It means that MSCs were mostly sensitive to this RGD gradient profile.

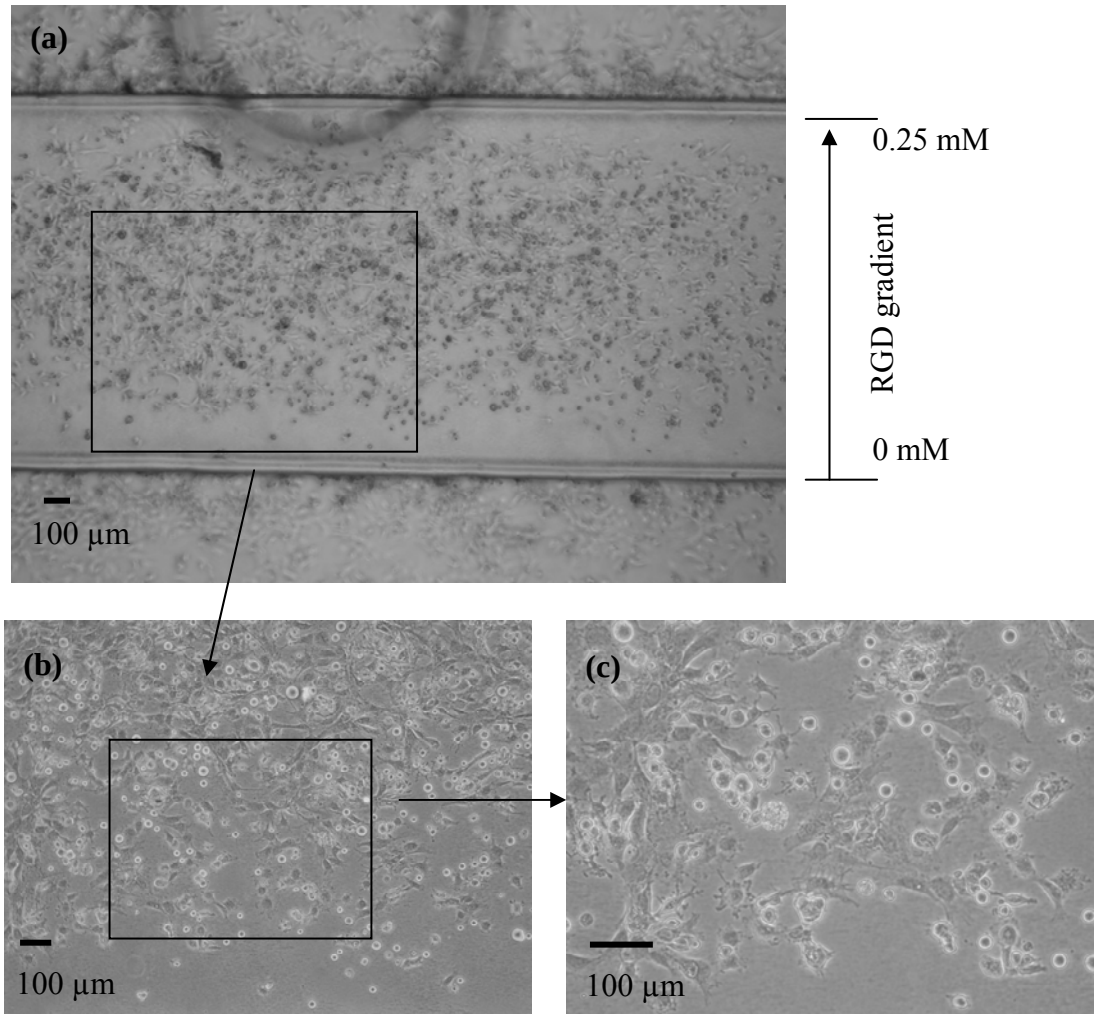

Figure 7.2 MSCs cultured on RGD gradient PEG hydrogel (0-0.5 mM) for 1 day. (a) 4×, (b) 10×, (c) 20×

Figure 7.1 and 7.2 show the optical images of MSCs on RGD gradient PEG hydrogel. However, the optical images were somewhat not very clear. In order to observe cells adhesion and spreading more clearly, actin and nucleus staining were performed. The actin and nucleus staining can clearly indicate cells adhesion and spreading.

Figure 7.3 shows the fluorescence images of actin and nucleus staining of MSCs on different RGD gradient PEG hydrogel. Figure 7.3(a) and 7.3(b) are PEG hydrogel with 0-0.25 mM RGD gradient. Figure 7.3(c) and 7.3(d) are PEG hydrogel with 0-0.5 mM RGD gradient. Figure 7.3(e) and 7.3(f) are PEG hydrogel with 0-1 mM

RGD gradient. Figure 7.3(g) and 7.3(h) are PEG hydrogel with 0-2 mM RGD gradient. The nucleus staining results shows that the adherent cell number generally increased with the increase of RGD concentration on PEG hydrogel. For all the four samples, the cell adhesion number on 0-0.25 mM RGD gradient hydrogel increased mostly dramatically. The actin staining results indicated the cell spreading on PEG hydrogel. The cells on low RGD concentration area generally had round shape while the cells on high RGD concentration area had spreading shape. The cells on 0-0.25 mM RGD gradient showed big difference for cell spreading shape change from low RGD concentration to high RGD concentration. The cells on 0-1 mM and 0-2 mM RGD gradient were almost spreading thoroughly from low RGD concentration to high RGD concentration area.

The actin and nucleus staining pictures in Figure 7.3 indicates that the MSCs have different responses to different RGD gradient profiles. However, Figure 7.3 just shows 4× pictures, which can not indicate the detailed information of cell adhesion and spreading. Images of higher magnification were also taken which were shown in Figure 7.4 and Figure 7.5.

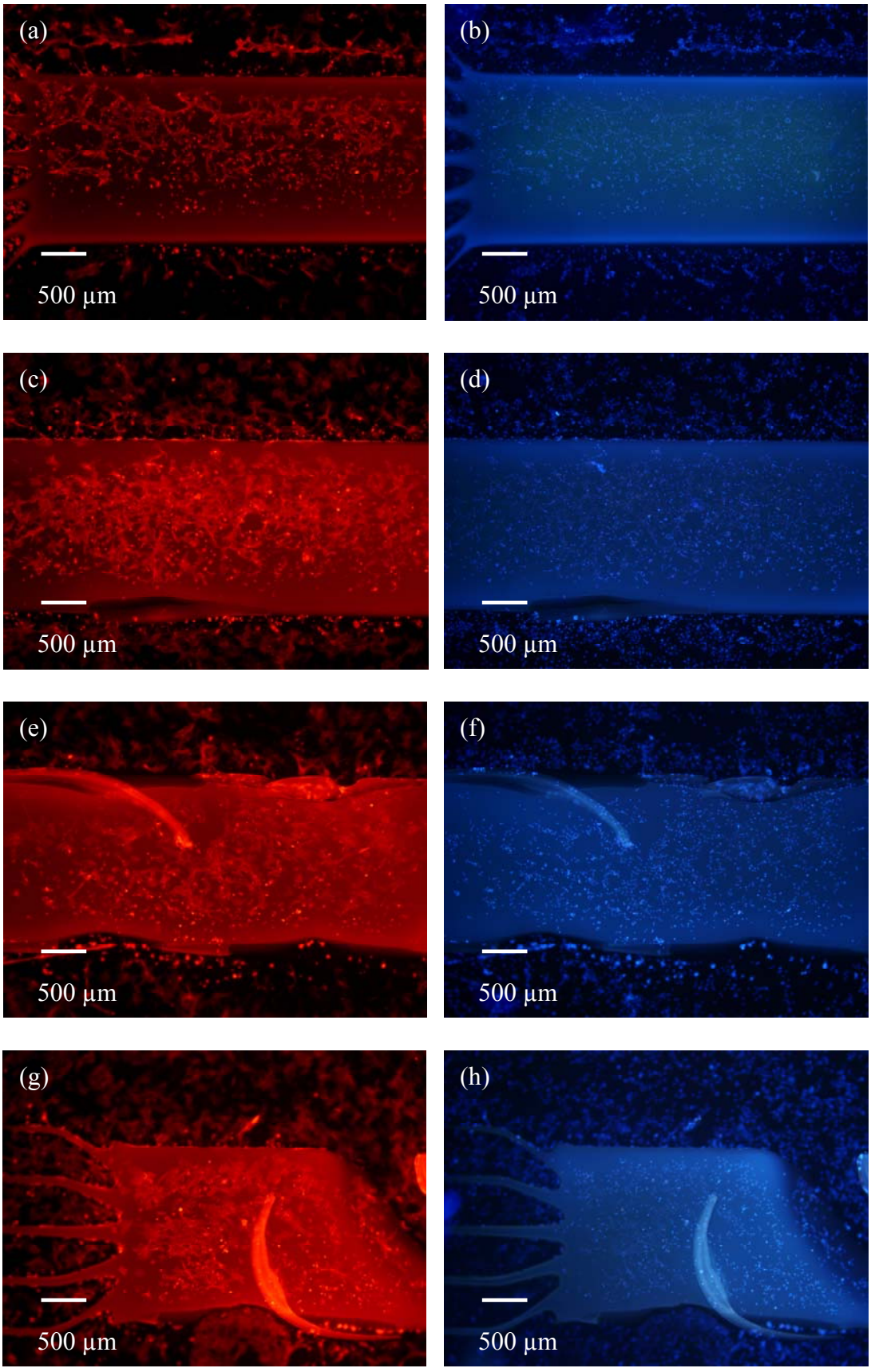

Figure 7.3 MSCs cultured on different RGD gradient PEG hydrogel for 1 day (4×). (a) 0-0.25 mM, actin staining, (b) 0-0.25 mM, nucleus staining, (c) 0-0.5 mM, actin staining, (d) 0-0.5 mM, nucleus staining, (e) 0-1 mM, actin staining, (f) 0-1 mM, nucleus staining, (g) 0-2 mM, actin staining, (h) 0-2 mM, nucleus staining

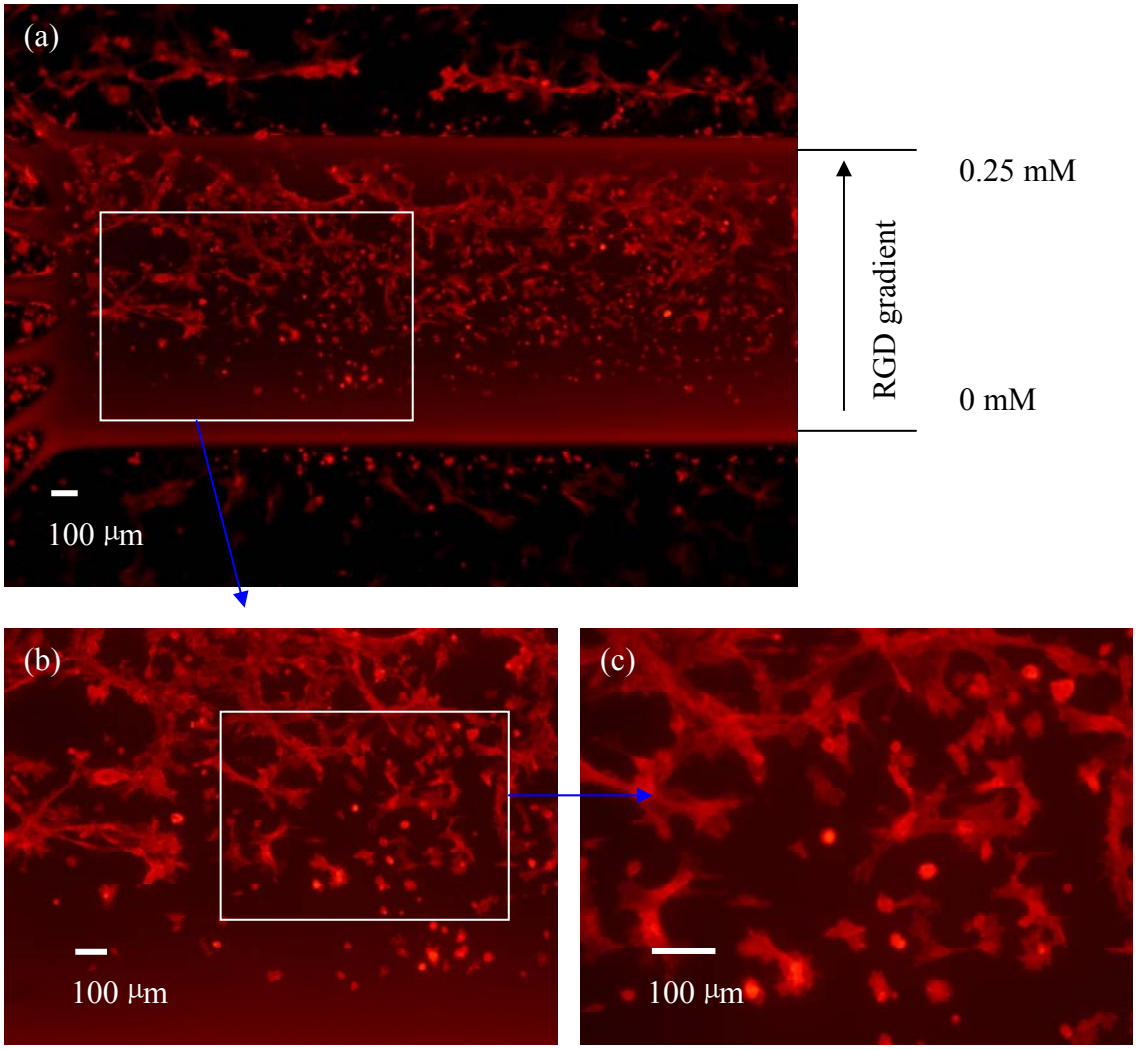

Figure 7.4 Actin staining of MSCs cultured on RGD gradient PEG hydrogel (0-0.25 mM) for 1 day. (a) 4×, (b) 10×, (c) 20×

Figure 7.4 is actin staining of MSCs cultured on PEG hydrogel with 0-0.25 mM RGD gradient for 1 day. Figure 7.4(a) is 4× image, which shows the actin staining of cells on the whole gradient PEG hydrogel. On the low RGD concentration area (bottom area of the PEG hydrogel), there were no cells adhered on the surface. With the increase of RGD concentration, more cells could adhere and spread on the surface. On the top area of hydrogel with the highest RGD concentration, the cells could fully spread on the surface. Figure 7.4(b) is 10× image, which shows cells on partial area of the whole PEG hydrogel. Figure 7.4(c) is from partial area of Figure 7.4(b). It more clearly indicated the cell morphology change, which was from round

to full spreading. The cells on high RGD concentration area in Figure 7.4 connected with each other and had many adhesion fibers on the surface. The cells on high RGD concentration hydrogel covered more adhesion area than the cells on low RGD concentration hydrogel.

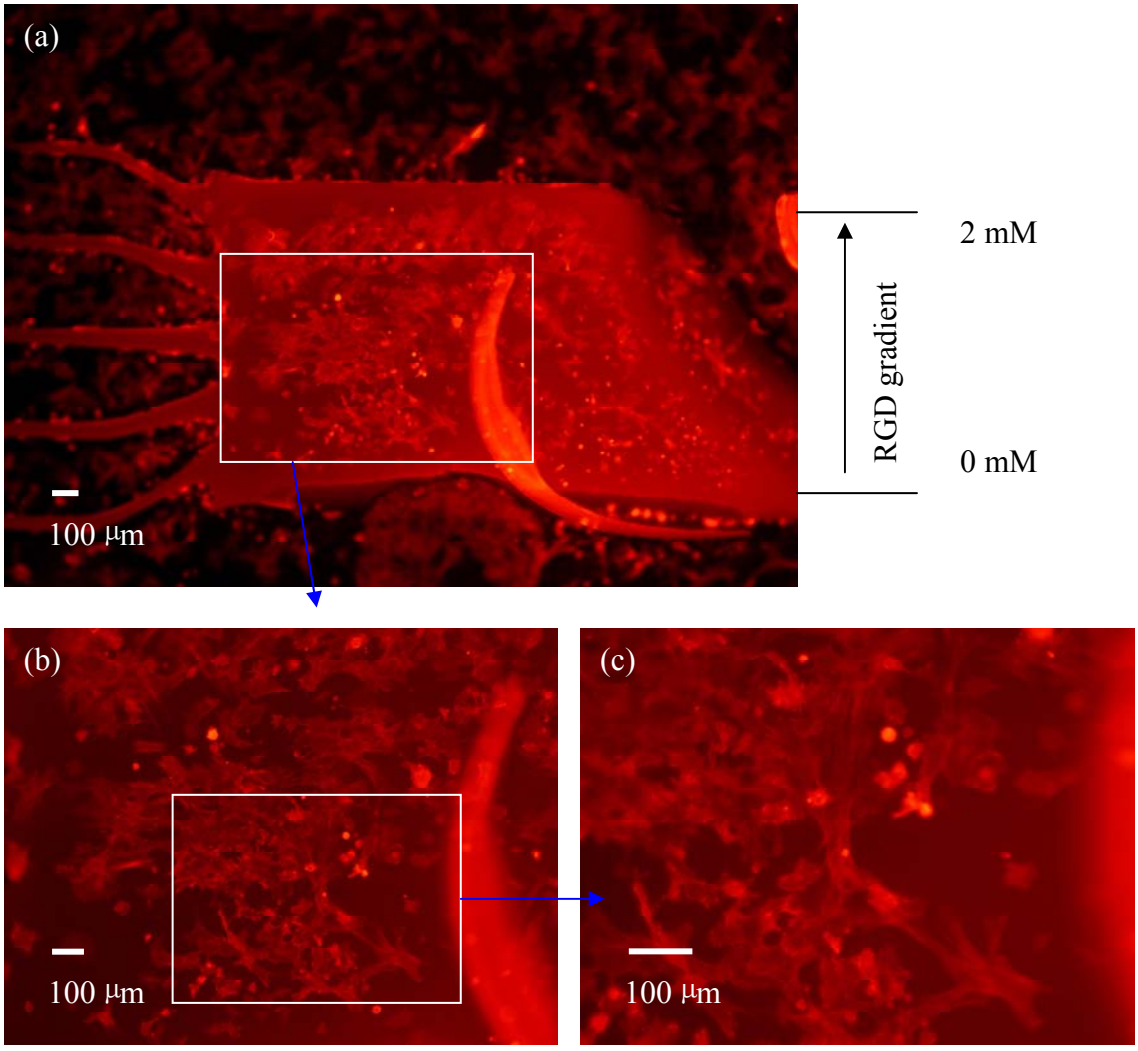

Figure 7.5 Actin staining of MSCs cultured on RGD gradient PEG hydrogel (0-2 mM) for 1 day. (a) 4×, (b) 10×, (c) 20×

Figure 7.5 shows another RGD gradient 0-2 mM, which was the largest gradient profile across the hydrogel in our experiment. Figure 7.5(a) has a different distribution of cells compared with Figure 7.5(a). The cells on low RGD concentration area in Figure 7.5(a) can also adhere on the surface and had a spreading morphology. The cells in Figure 7.5(b) and 7.5(c) adhered well on any area

of hydrogel surface and had a spreading morphology. Therefore, the gradient effect of cell adhesion on 0-2 mM RGD concentration hydrogel was not obvious compared with the 0-0.25 mM RGD gradient PEG hydrogel.

The nucleus staining of cells on RGD gradient PEG hydrogel could be used to calculate the cell adhesion density. Figure 7.6 shows the cell adhesion density on 0-0.25 mM RGD gradient PEG hydrogel. The hydrogel was divided into 7 bins, which was indicated in Figure 7.6(a). The bin “1” represented the highest RGD concentration while the bin “7” had the lowest RGD concentration. Then the cell adhesion number was counted on each bin. The results of cell adhesion number are shown in Figure 7.6(b). From Figure 7.6(b), it can be seen that the cell adhesion number on bin “7” was nearly zero. With the increase of bin “2” to bin “6”, the cell adhesion number decreased, which meant that the cell adhesion density decreased with the decrease of RGD concentration. However, there was a particular phenomenon for bin “1”. Though bin “1” had the highest RGD concentration, there were fewer cells on bin “1” than bin “2”. This may be due to the not flat surface of bin 1, which can make it difficult for cells to adhere on the surface. Another interesting phenomenon was that there was little difference for cell adhesion density on bin “2”, “3” and “4”. This may be caused by the saturation of cell adhesion on bin “2”, “3” and “4”.

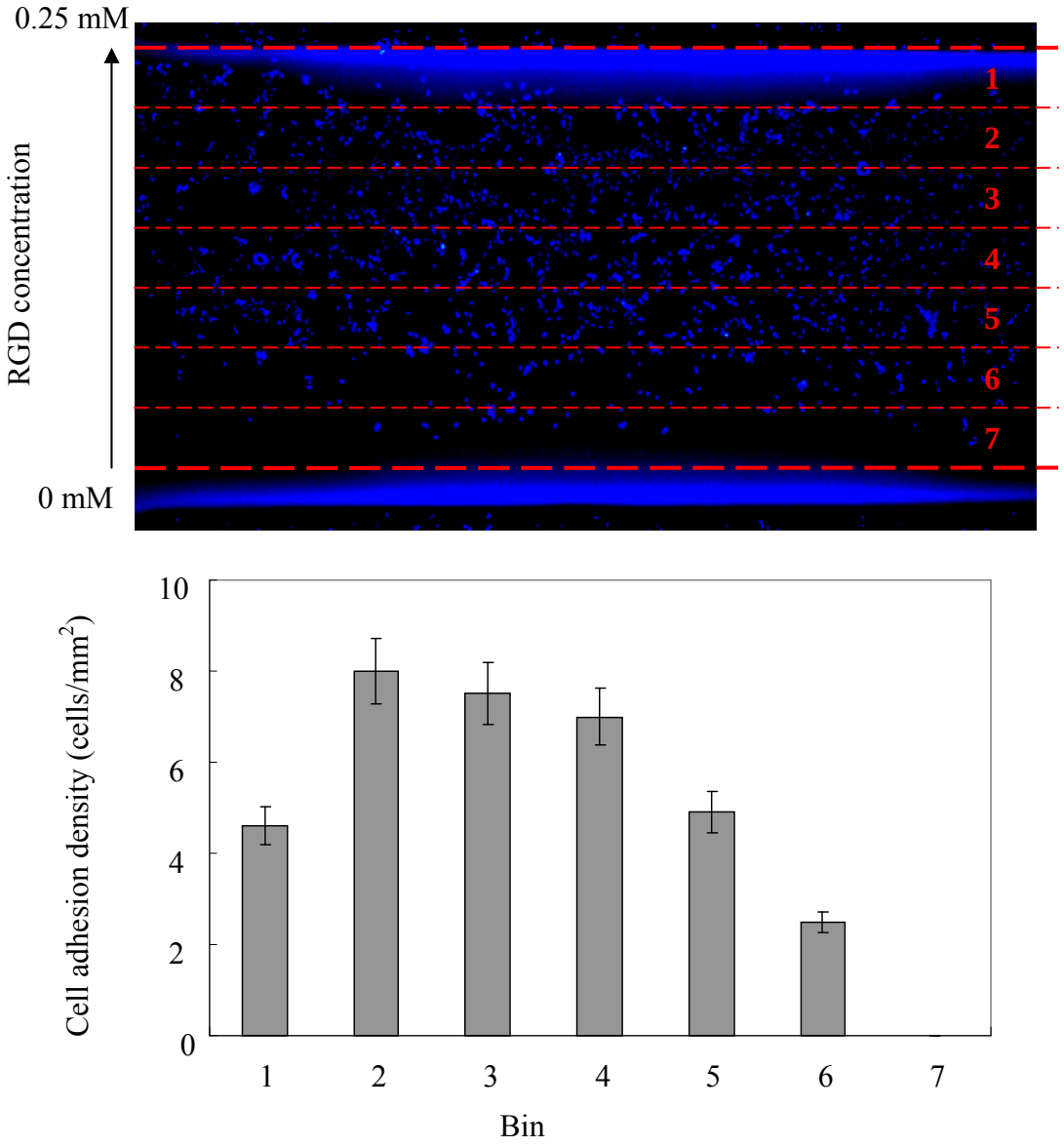

Figure 7.6 cell adhesion densities on 0-0.25 mM RGD gradient PEG hydrogel

Using the same method described above, the cell adhesion density on 0-0.5 mM, 0-1 mM and 0-2 mM RGD gradient was also calculated. The results were shown in Figure 7.7. For bin "7" of 0-0.25 mM and 0-0.5 mM RGD gradient, the cell adhesion density was zero. However, the cell adhesion density for bin "7" of 0-1 mM and 0-2 mM RGD gradient was not zero. This indicated that there were still some cell adhesion on the lowest concentration bin of 0-1 mM and 0-2 mM RGD gradient PEG

hydrogel. From bin "2" to bin "7", the RGD concentration decreased and the cell adhesion density also decreased for all the four RGD gradients. For bin "1" of the four gradient PEG hydrogel, the cell adhesion density decreased compared with bin "2". For bin "2", "3" and "4", the cell adhesion density had little difference for all the four gradients. However, the cell adhesion density for bin "5", "6" and "7" of the four gradients was very different.

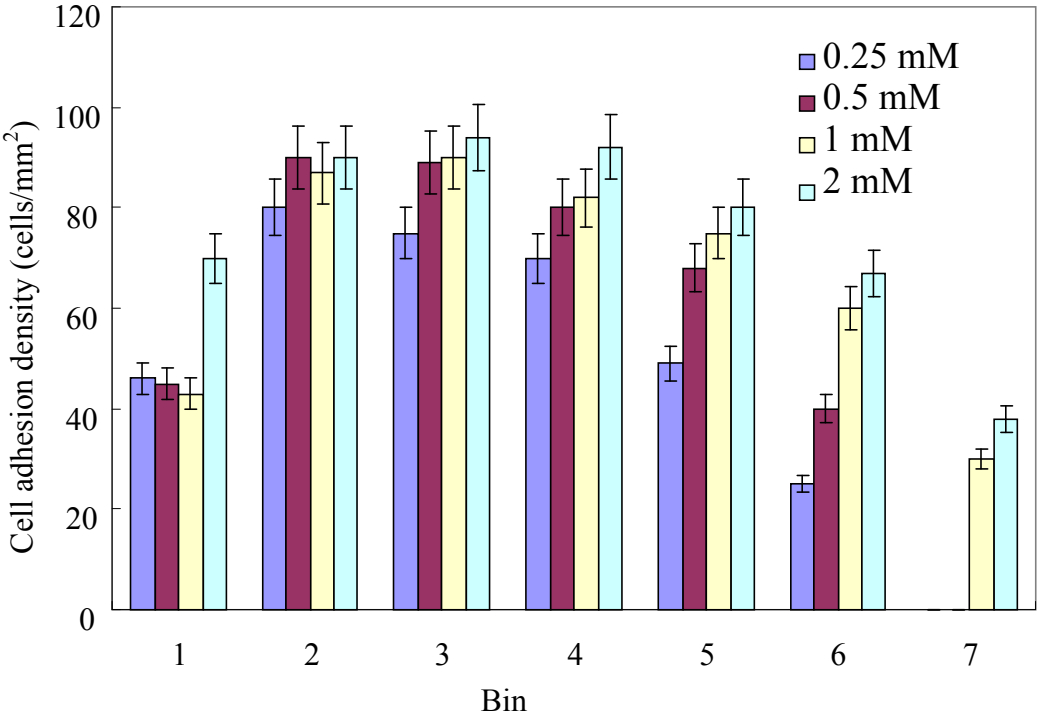

Figure 7.7 Cell adhesion densities on PEG hydrogel with RGD gradient 0.25 mM, 0.5 mM, 1 mM and 2 mM

The nucleus staining of cells can be used to calculate the cell adhesion density across the RGD gradient PEG hydrogel. The actin staining can be used for another application: calculating the cell adhesion area. The cell adhesion area indicates the cells morphology. If cells have spreading morphology, it will cover more adhesion area.

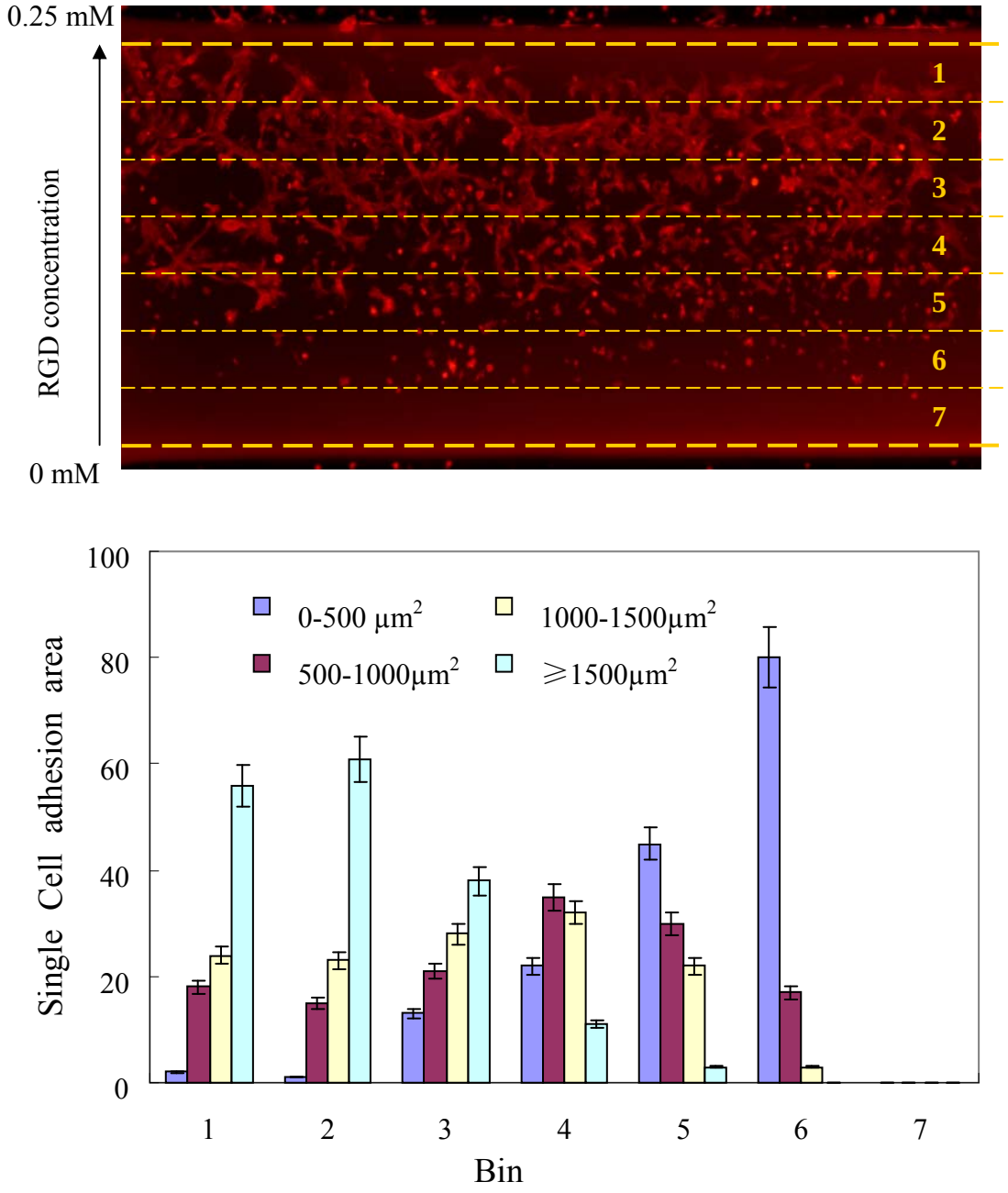

Figure 7.8 Single cell adhesion area on 0-0.25 mM RGD gradient PEG

Figure 7.8 shows the single cell adhesion area on 0-0.25 mM RGD gradient PEG hydrogel. The single cell adhesion area was calculated from actin staining images of MSCs on PEG hydrogel. The actin staining image was divided into 7 bins. The cell adhesion area was then divided into 4 categories: 0-500 μm^2, 500-1000μm^2, 1000-1500μm^2 and $\geq$1500μm^2. In each bin, the ratio of cell adhesion area for each category was calculated. From the diagram in Figure 7.8, it could be seen that the

cell adhesion area on bin "1", "2" and "3" were mostly more than 1500μm^2. On bin "4", the cell adhesion area was mainly between 500μm^2 to 1500μm^2. On bin "5" and "6", the cell adhesion area was mostly less than 500μm^2. As there were no cells on bin "7", the cell adhesion area was not calculated. The above analysis indicated that the cell adhesion area decreased with the decrease of RGD concentration.

The single cell adhesion area on PEG hydrogel with RGD gradient 0-0.5 mM, 0-1 mM and 0-2 mM was also calculated using the same method. The results are shown in Figure 7.9, 7.10 and 7.11. Figure 7.9 is for single cell adhesion area distribution on 0-0.5 mM RGD gradient. The cell adhesion area results in Figure 7.9 were similar to that in Figure 7.8. On bin "1", "2" and "3", the cell adhesion area was mostly more than 1500 μm^2. With the decrease of RGD concentration from bin "1" to "6", the cell adhesion area decreased. As there were also no cells on bin "7", the cell adhesion area was not calculated. Figure 7.10 and Figure 7.11 show the cell adhesion area distribution on 0-1 mM and 0-2 mM RGD gradient PEG hydrogel. Figure 7.8 and 7.9 showed that there was no cell adhesion on the bin "7" of 0-0.25 mM and 0-0.5 mM RGD gradient PEG hydrogel. However, MSCs could adhere on bin "7" of 0-1 mM and 0-2 mM RGD gradient PEG hydrogel and the adhesion area was mainly less than 500 μm^2. For bin from "1" to "6" on 0-1 mM and 0-2 mM RGD gradient PEG hydrogel, the single cell adhesion area was mostly more than 1500 μm^2. For the cell adhesion area of the four RGD gradients, there was a similar trend that the cell adhesion area decreased with the decrease of RGD concentration.

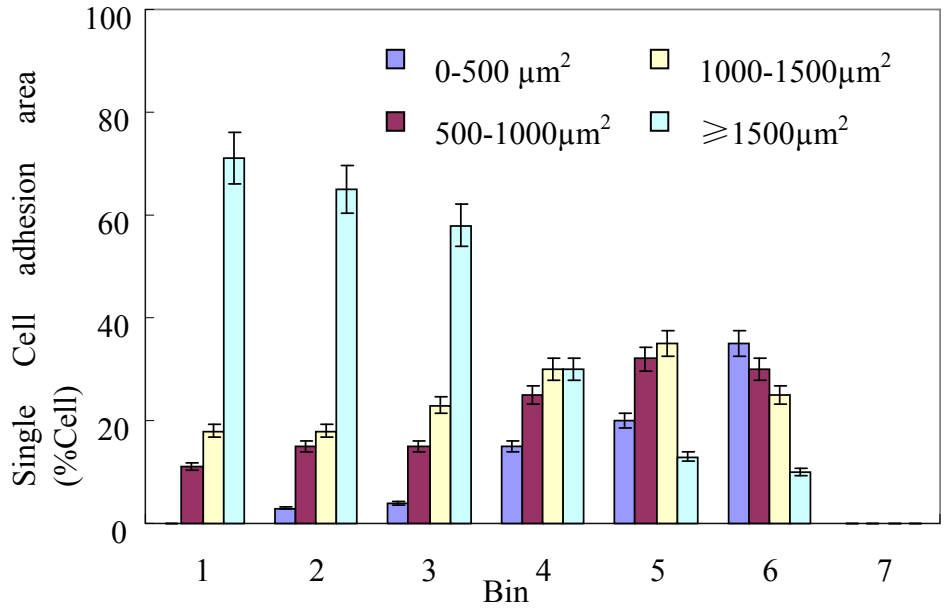

Figure 7.9 Single cell adhesion area on 0-0.5 mM RGD gradient PEG

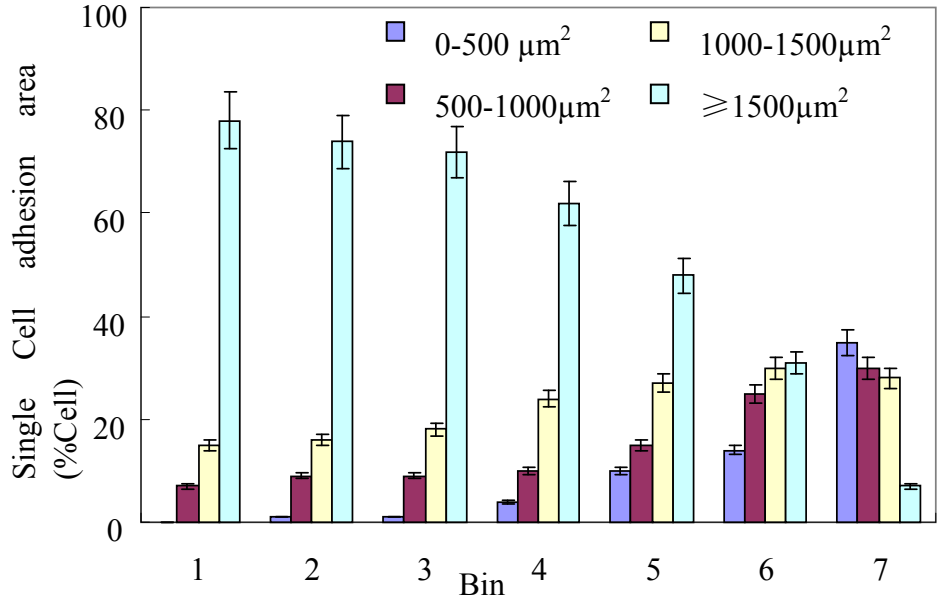

Figure 7.10 Single cell adhesion area on 0-1 mM RGD gradient PEG

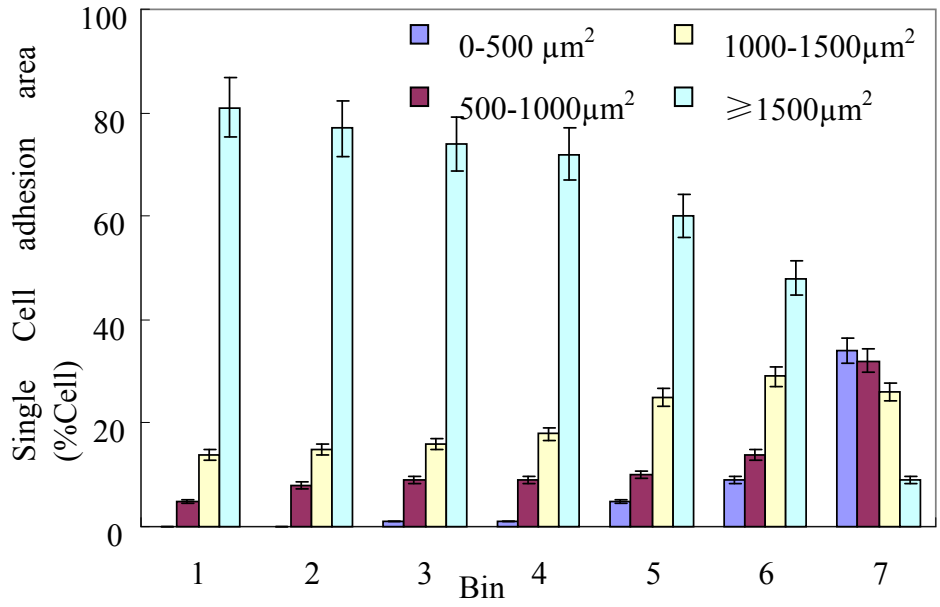

Figure 7.11 Single cell adhesion area on 0-2 mM RGD gradient PEG

7.4 Discussion

PEG hydrogel is a promising material for tissue engineering applications. Due to the hydrophilicity and bioinactivity of PEG, bioactive biomolecules can be immobilized to PEG hydrogel to control the bioactive factor presentation (Benoit DS et al., 2005; DeLong SA et al., 2005; Lee HJ et al., 2006). RGD peptide is the ligand for receptor mediated cell adhesion and has been incorporated to hydrogel to promote cell attachment (DeLong SA et al., 2005; Shu XZ et al., 2004). In chapter 5, RGD peptide was incorporated to PEG hydrogel and can promote MSCs adhesion and spreading. However, it was difficult to realize the continuous RGD concentration control, which was important *in vivo*. In this chapter, RGD gradient PEG hydrogel was fabricated in microfluidic device to achieve the gradient RGD concentration control.

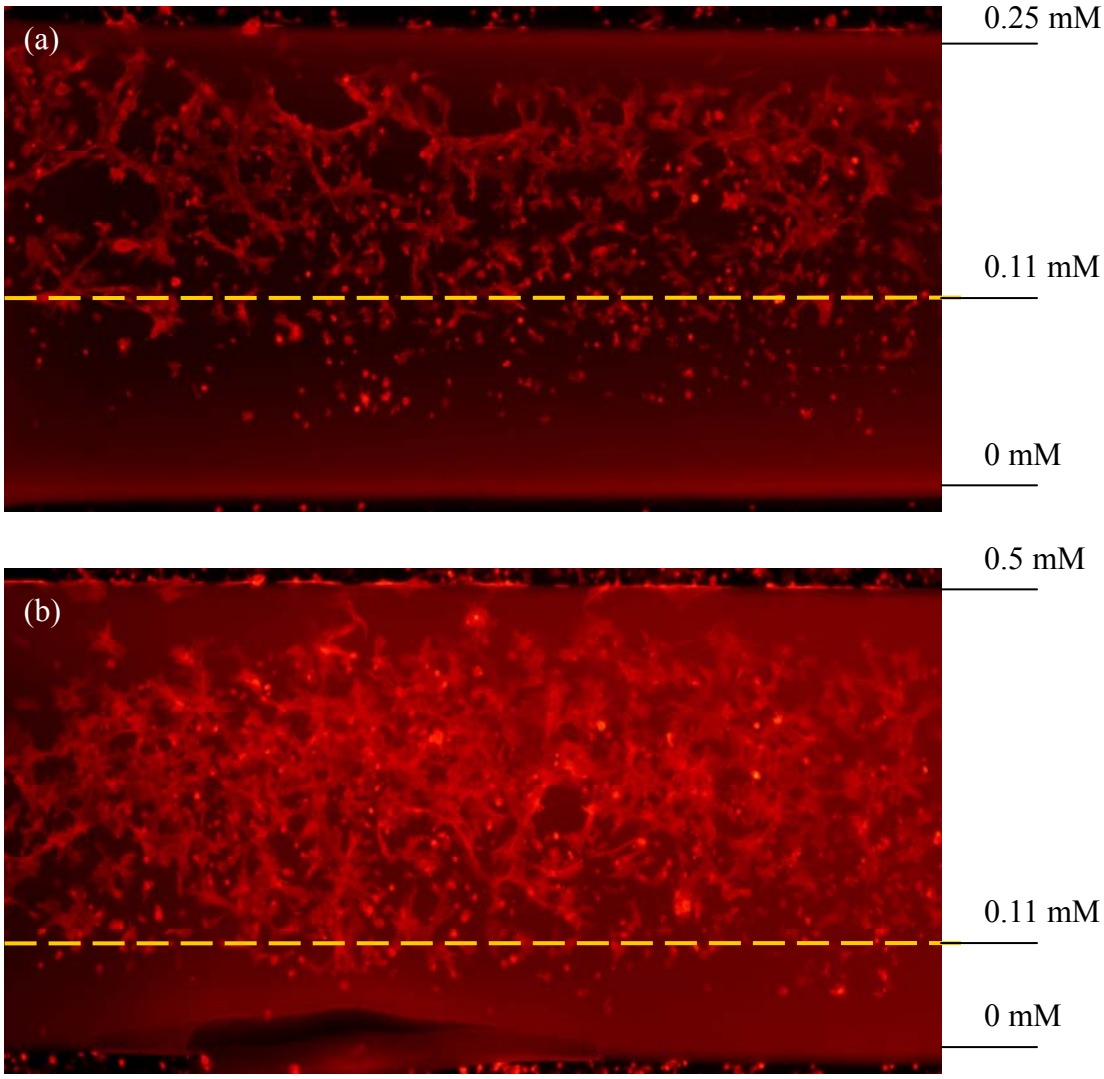

Figure 7.12 MSCs cultured on different RGD gradient PEG hydrogel for 1 day (4×). (a) 0-0.25 mM, actin staining, (b) 0-0.5 mM, actin staining,

In Chapter 6, the cell adhesion number had a largest jump in a RGD concentration range. However, it was difficult to know the concrete point for the jump. The results of MSCs adhesion on RGD gradient PEG hydrogel can give the answer. Figure 7.12 shows the MSCs adhesion on 0-0.25 mM and 0-0.5 mM RGD gradient PEG hydrogels. Yellow line was used to determine the jump point of RGD concentration for cell adhesion. Below the yellow line, there were few cells on the hydrogel surface and more than 80% cells covered a small adhesion area less than 800 μm^2. As it has been demonstrated that the gradient profile was linear across the hydrogel, the

concentration of the yellow line position can be calculated. Figure 7.12(a) and 7.12(b) show that the yellow lines had a RGD concentration about 0.11 mM. Thus, RGD concentration 0.11 mM was regarded as the critical concentration for cell adhesion on PEG hydrogel. MSCs can adhere on the PEG hydrogel surface through the interaction of integrins on cell membrane with RGD peptides (Chen CS et al., 2003). Below 0.11 mM, there may be not enough RGD sites interacting with cell integrins. Therefore, it was difficult for MSCs adhering on the PEG hydrogel with the RGD concentration less than 0.11 mM.

The RGD concentration of 0.11 mM was also in the threshold concentration range 0-0.5 mM, which was discussed in chapter 6. Therefore, the critical concentration obtained from the RGD gradient PEG hydrogel was consistent with the threshold concentration range obtained from the conventional method.

The critical RGD concentration for cell adhesion can be also regarded as the cell adhesion saturation concentration. On the RGD gradient PEG hydrogel with relatively low RGD concentration, the MSCs adhesion increased with the RGD concentration increase. Then on the RGD gradient PEG hydrogel with higher RGD concentration, the cell adhesion had little difference due to cell adhesion saturation which was shown in Figure 7.8 to Figure 7.11. The MSCs adhesion also had little difference on different RGD gradient PEG hydrogel with the same RGD concentration area. Therefore, MSCs adhesion was more sensitive to RGD concentration rather than the RGD gradient.

Chapter 8 Photoencapsulation of MSCs in PEG Hydrogel with RGD for Mesenchymal Stem Cells (MSC) Culture

Abstract

MSCs were encapsulated in PEG hydrogel with different RGD concentrations. The MSCs encapsulated hydrogel was then cultured in osteogenic medium. The cell viability was characterized by live/dead assay. The results showed that MSCs had better cell viability in 10% PEG hydrogel than in 30% PEG hydrogel. RGD can increase cells viability in 30% PEG hydrogel. Von kossa staining mineral deposits was used to characterize the osteogenisis of MSCs in PEG hydrogel.

8.1 Introduction

As mentioned in Chapter 6.1.2, photopolymerization is a method to covalently crosslink monomer or macromer solution to a three-dimensional network via chain polymerization mechanism. Photopolymerization can be used in fabrication of photosensitive biomaterials. Photopolymerization has been developed for fabricating hydrogel scaffolds. The reaction is the fast curing of polymer liquid into a crosslinked, water-swollen gel networks. Photosenstive hydrogel can be spatially and temporally controlled during the gelation process. During the photopolymerization, cells can be encapsulated into the hydrogels in situ. This process is called cellular photo-encapsulation.

A lot of research has been done to study cellular photoencapsulation in hydrogels. Anseth and colleagues have studied photopolymerizing PEG hydrogel for mesenchymal stem cells culture (Nuttelman CR et al., 2006; Salinas CN et al., 2008). Photoactive polyvinyl alcohol hydrogels (PVA) has also been investigated as tissue engineering scaffolds (Schmedlen RH et al., 2002).

In the cellular photoencapsulation reaction, there are two main parameters including photo light and photoinitiator, which can affect cells viability. For the photo light, the main function is to give energy to photoinitiator to start the reaction. Some research has been done to investigate the harmful effect of photo light on cells. It was found that cells can be still alive in the presence of low intensity initiating light (approximately 6 mW/cm^2 of 365 nm UV light and approximately 60 mw/cm^2 of

470-490 nm visible light) (Bryant SJ et al., 2000). For photoinitiator, it can be dissociated into high-energy radical state by light. This radical then induces the phtotopolymerization of a polymer solution. However, the high-energy radical in the system has the potential to induce oxidative damage to the encapsulated cells. Free radicals can cause damage to cells membrane, nucleic acids and proteins (Atsumi T et al., 1998; Moan J et al., 1989). In the research of Jennifer H. Elisseeff and colleagues, it was found that the photoinitiator 2-hydroxy-1-[4-(hydroxyethoxy)phenyl]-2-methyl-11propanone (Irgacure 2959) caused minimal toxicity (cell death) over a broad range of mammalian cell types and species. The cytotoxicity of photoinitiators has been thought to be due in part to the hydrophobicity since permeability through phospholipid bilayers of cellular membranes increases with the hydrophobicity of a compound. As Irgacure 2959 had less hydrophobicity, it did less harm to cells viability (Williams CG et al., 2005).

In Chapter 6, MSCs were cultured on PEG hydrogel with different RGD concentrations. In Chapter 7, MSCs were cultured on PEG hydrogel with RGD gradient. The cell culture in Chapter 6 and 7 was on 2-dimentional (2D) surface. However, cells *in vivo* are in a 3D environment. The cells in 3D environment often have different behaviors from that in 2D environment. Therefore, the culture of MSCs in 3D PEG hydrogel was done to study stem cells behaviors in this chapter. MSCs were encapsulated into PEG hydrogel in situ under UV light with low intensity. The cells viability was characterized for hydrogel with different PEG and RGD concentrations. The stem cells were also induced into osteogenic differentiation

to explore the different RGD concentration effects on MSCs differentiation.

8.2 Methodology

8.2.1 Fabrication of stem cells encapsulated PEG hydrogel for three dimentional (3D) cell culture

Poly(ethylene glycol) diacrylate (PEGDA, 3400 Da, Laysan Bio Inc., AL, USA) was used to for stem cell encapsulation of stem cells in PEG hydrogel. PEGDA and ACRL-PEG-RGD were mixed in sterilized PBS with penicillin (100 U/ml) and streptomycin (100 μg/ml) to make 10% and 30% (W/V) solution. Five different concentrations of RGD were tested: 0, 0.125, 0.25, 0.375 and 0.5 mM. Photoinitiator Irgacure 2959 was added to the PEG solution at a concentration of 0.05% (W/V). Passage 3 MSCs were then homogeneously suspended in PEG solution to make a concentration of 40 million cells/ml. The PEG solution containing stem cells was then injected into a PDMS chamber, the same to previously described in chapter 6.2.3. The PEG solution was then exposed to UV light (365nm, 70 mW/cm^2) for 1 min to get gelation. The PEG hydrogel on glass slide was put into a petri dish, which was filled with osteogenic culture medium.

8.2.2 In vitro cultivation

The PEG hydrogel samples were all incubated in 5% CO_2 in osteogenic culture medium (Lonza, Switzerland). Osteogenic medium consisted of high-glucose Dulbecco's modified Eagle medium (DMEM) supplemented with 10% fetal bovine serum, 100 nM dexamethasone, 50 μg/ml ascorbic acid 2-phosphate, 10 mM

β-glycerophosphate, 100 unit/ml penicillin and 100 μg/ml streptomycin. The cell culture petri dish was incubated in a humidified incubator at 37 ℃. Cell culture medium was changed every two or three days.

8.2.3 MSCs viability in PEG hydrogel

After 7 days culture, the MSCs viability in PEG hydrogel was characterized by live/dead assay. This assay is based on the fluorescence of two dyes, fluorescein diacetate (FDA) (Ilusa, USA) and propidium iodide (PI) (Invitrogen Corporation, USA). Living cells can actively convert the non-fluorescent FDA into the green fluorescent compound "fluorescin", which is a sign of viability. PI is an intercalating agent and a fluorescent molecule that can be used to stain DNA. PI is membrane impermeant and generally excluded from viable cells (Moore A et al., 1998). Therefore, FDA can be used to identify live cells while PI can be used to mark dead cells.

In the experiment, 2-3 μl FDA and 20 μl PI were mixed with 2 ml PBS solution to stain the cells. A few drops of mixed solution were added into the culture medium of PEG hydrogel samples for 15-20 minutes. Thereafter, the solution was removed from the samples, PBS solution was used to wash away the remaining liquid. Then the PEG hydrogel samples were placed under fluorescence microscope for further usual study.

8.2.4 Von kossa staining

The MSCs were induced to osteogenic differentiation in our study. The osteogenesis can result in the increase of osteopotin, alkaline phosphatase expression, mineralization and et al (Nuttelman CR et al., 2004; Yim EK et al., 2006). In our research, mineralization of PEG hydrogel was measured to characterize the osteogenisis of MSCs in PEG hydrogel after 7 days culture.

The PEG hydrogel samples were washed in PBS solution for several times. 4% paraformaldehyde was used to fix the PEG hydrogel. The PEG hydrogel was then incubated in 1% silver nitrate solution placed under UV light for 20 minutes. PBS solution was used to wash the PEG hydrogel samples. Then 5% sodium thiosulfate solution was used to remove un-reacted silver. After PBS washing, The PEG hdyrogel samples were counterstained with nuclear fast red for 5 minutes. Finally, PEG hydrogel was washed with PBS solution and observed under optical microscope. The black or brown-black color was the calcium salts. The red color was nuclei. The pink color was the cytoplasm.

8.3 Results

8.3.1 MSCs viability

The viability of MSCs encapsulated into PEG hydrogel was monitored for up to 7 days to assess the effects of PEG and RGD concentration on cell viability. Figure 8.1 shows cells viability in different PEG hydrogels. Red color represents dead cells. Cells with green color were alive. The left four images show the cell culture for 1

day while the right four images show the cell culture for 7 days. Figure 8.1(a) and 8.1(b) are about 10% PEG hydrogel without RGD. Figure 8.1(c) and 8.1(d) are about 10% PEG hydrogel with 0.5 mM RGD. Figure 8.1(e) and 8.1(f) show 30% PEG hydrogel without RGD. Figure 8.1(g) and 8.1(h) show 30% PEG hydrogel with 0.5mM RGD.

The effect of PEG concentration on cells viability was studied for 10% PEG hydrogel and 30% PEG hydrogel. Comparing Figure 8.1(a) and 8.1(b) with Figure 8.1(e) and 8.1(f), Figure 8.1(a) and 8.1(b) had more live cells. This result showed that hydrogel with lower PEG concentration can increase cells viability. Lower PEG concentration resulted in lower cross-linking degree of hydrogel networks. Lower cross-linking degree can further promote the transport of nutrients and other molecules from outside to inside. Therefore, cells in lower PEG concentration hydrogel had better viability. Burdick and Anseth had studied the photoencapsulation of osteoblasts in PEG hydrogel and got the similar results with our present study (Burdick JA et al., 2002).

Then, the effect of RGD concentration on cells viability was also explored. Comparing Figure 8.1(a) and 8.1(b) with Figure 8.1(c) and 8.1(d), most cells were alive and there was no obvious difference of cells viability. So RGD concentration had no effect on MSCs viability in lower PEG concentration hydrogel of 10%. However, there was significantly different effect of RGD concentration on MSCs viability in hydrogel with higher PEG concentration of 30%. In Figure 8.1(g) and

8.1(h), cells had better viability than cells in Figure 8.1(e) and 8.1(f). As mentioned above, nutrients and other molecules were difficult to transport between inside and outside in hydrogel with higher PEG concentration. The existence of RGD in hydrogel may affect the cells viability function so that cells in PEG hydrogel with RGD had better cells viability.

Finally, the cell culture time also had effect on cells viability. In Figure 8.1(a), 8.1(b), 8.1(c) and 8.1(d), most cells were live due to the low PEG concentration. Therefore, the cells viability had no obvious difference between day 1 and day 7 for hydogel with low PEG concentration. However, the cells viability was different between day 1 and day 7 for hydrogel with high PEG concentration as shown in Figure 8.1(e), 8.1(f), 8.1(g) and 8.1(h). More cells were dead on day 7, indicating that the cells viability decreased with the increase of cell culture time.

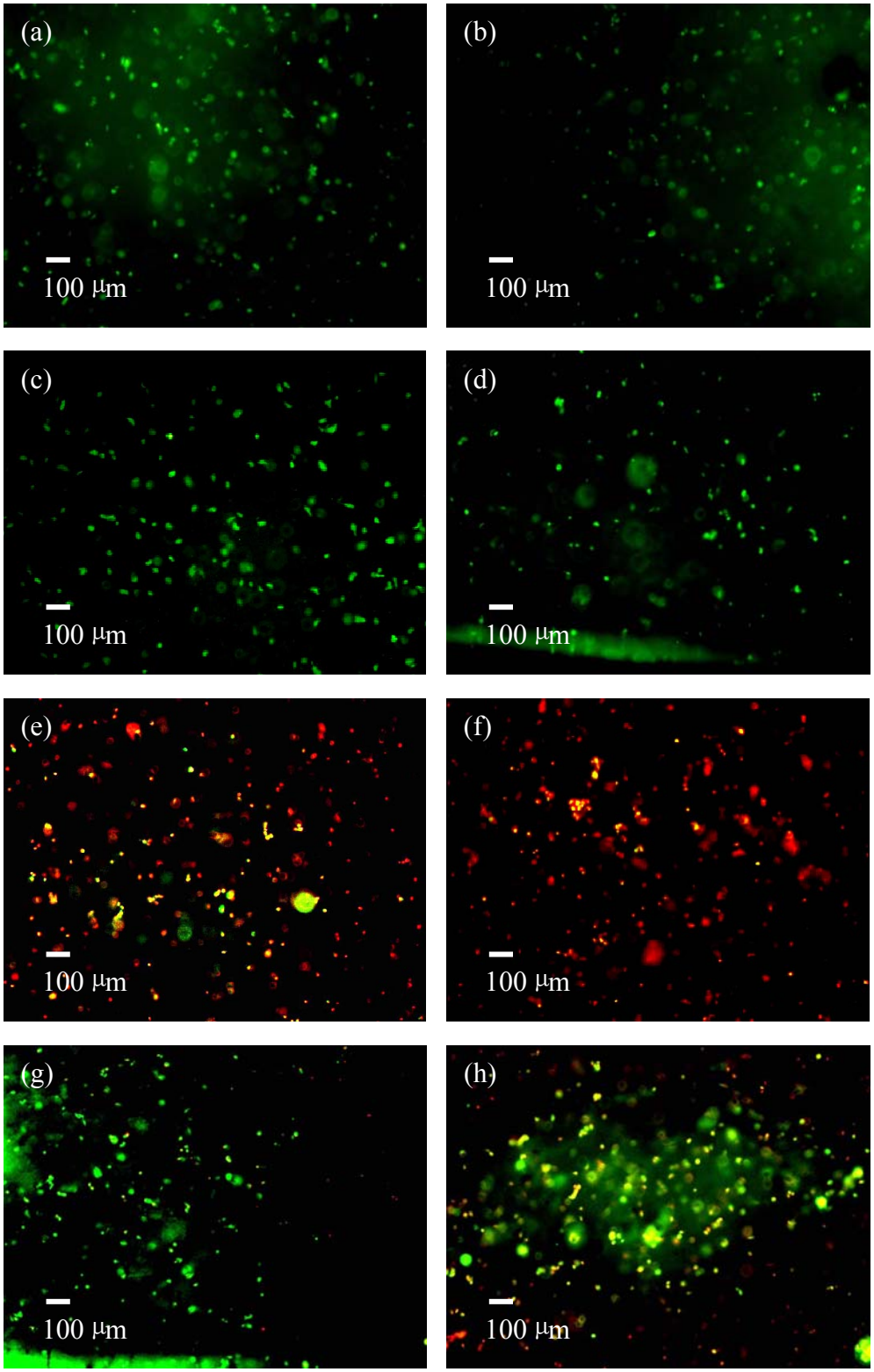

Figure 8.1 Viability of MSCs in PEG hydrogel. (a) 10% PEG hydrogel for 1 day, (b) 10% PEG hydrogel for 7 days, (c) 10% PEG hydrogel with 0.5 mM RGD for 1 day, (d) 10% PEG hydrogel with 0.5 mM RGD for 7 days, (e) 30% PEG hydrogel for 1 day, (f) 30% PEG hydrogel for 7 days, (g) 30% PEG hydrogel with 0.5 mM RGD for 1 day, (h) 30% PEG hydrogel with 0.5 mM RGD for 7 days

Figure 8.2 shows the statistics of MSCs viability for different PEG hydrogels. The cells viability was calculated from the ratio of live cells to the whole cells. For 10% PEG hydrogel with RGD or without RGD, the cells viability was nearly 100%. For 30% PEG hydrogel without RGD, MSCs had the least cells viability about 50%. After incorporation of 0.5 mM RGD into 30% PEG hydrogel, the cells viability increased to more than 80%.

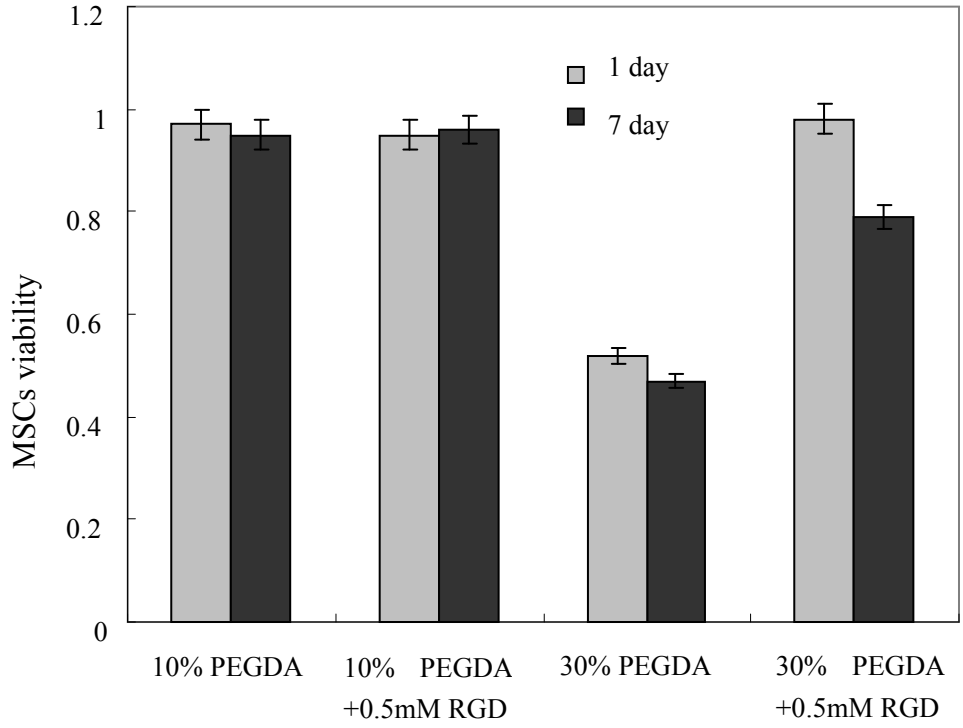

Figure 8.2 MSCs viability in hydrogel with different PEG and RGD concentrations

8.3.2 Von kossa staining

The MSCs encapsulated into PEG hydrogel were induced to osteogenic differentiation. Mineralization can be used to characterize the osteogenesis of MSCs. Von kossa staining was used to measure the mineral deposits in PEG hydrogel. Figure 8.3, 8.4, 8.5 and 8.6 show the mineralization of MSCs encapsulated in 10%

PEG hydrogel with different RGD concentrations by von kossa staining after culture for 1 day, 3 days, 7 days and 14 days. The black or brown-black color was the mineral deposits. Figure 8.5 had more mineral deposits than Figure 8.3 and 8.4. The mineral density in Figure 8.6 was further higher than that in Figure 8.5. Therefore, cell culture for longer time can increase the mineralization of MSCs in PEG hydrogel.

The RGD concentration also had important impact on MSCs mineralization. For 1 day cell culture shown in Figure 8.3, the mineral density was almost the same in PEG hydrogels with 0 mM, 0.5 mM and 1 mM RGD. For 3 days cell culture in Figure 8.4, there was also no significant difference between the four PEG hydrogels. For 7 days cell culture in Figure 8.5, the mineral density in PEG hydrogel with 1mM and 1.5 mM RGD concentration was much higher than that in PEG hydrogel with 0 mM and 0.5 mM RGD. For 14 days cell culture in Figure 8.6, the mineral density was significantly different and generally increased with the increase of RGD concentration. Therefore, the results indicated that RGD concentration almost had no effect on mineralization of MSCs in a short culture time such as less than 3 days. However, the RGD concentration can have important impact on mineralization of MSCs in long time culture such as more than 7 days. The enhanced mineralization suggested that RGD peptide can promote the mineralization of MSCs in PEG hydrogel. The research of Fan Yang and Jennifer Elisseeff had got the similar results that the osteogenesis of bone marrow stromal cells can be enhanced by incorporating RGD peptide (Yang F et al., 2005).

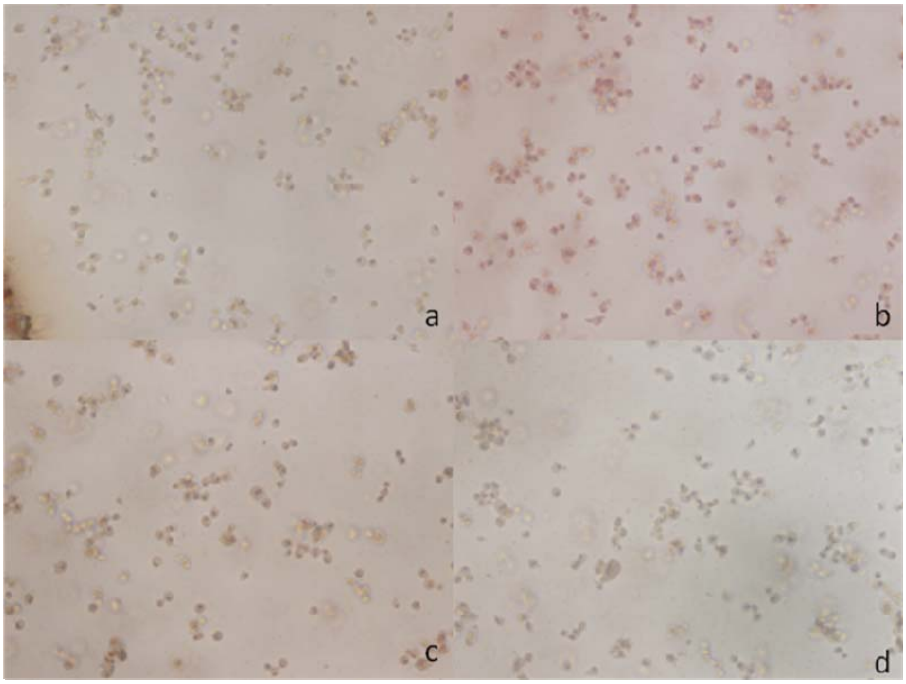

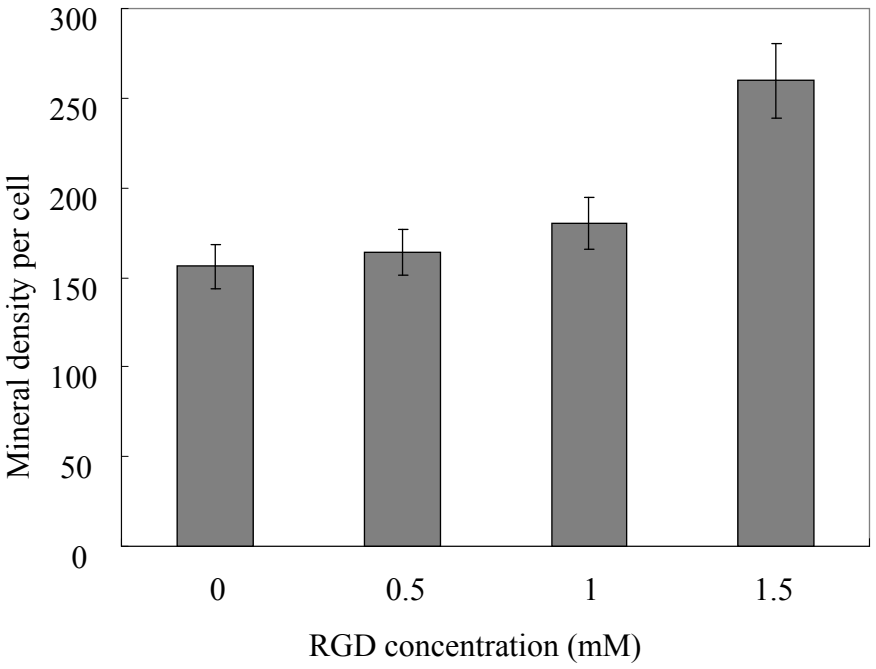

Figure 8.3 Mineralization of MSCs encapsulated in 10% PEG hdyrogel with different RGD concentrations for 1 day culture by von kossa staining. The stained mineral deposits were brown or black. a 0 mM RGD, b 0.5 mM RGD, c 1 mM RGD, d 1.5 mM

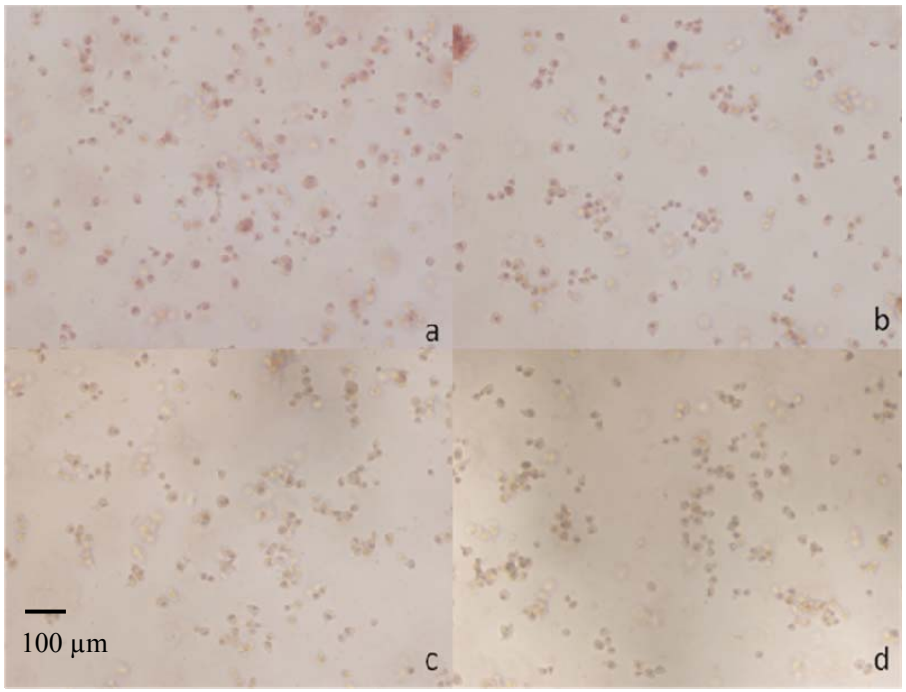

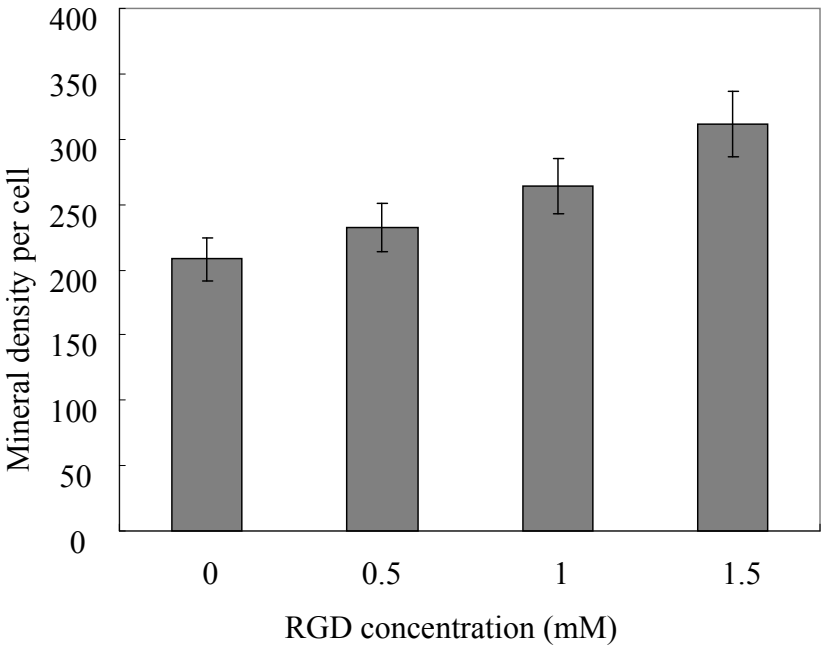

Figure 8.4 Mineralization of MSCs encapsulated in 10% PEG hdyrogel with different RGD concentrations for 3 days culture by von kossa staining. The stained mineral deposits were brown or black. a 0 mM RGD, b 0.5 mM RGD, c 1 mM RGD, d 1.5 mM

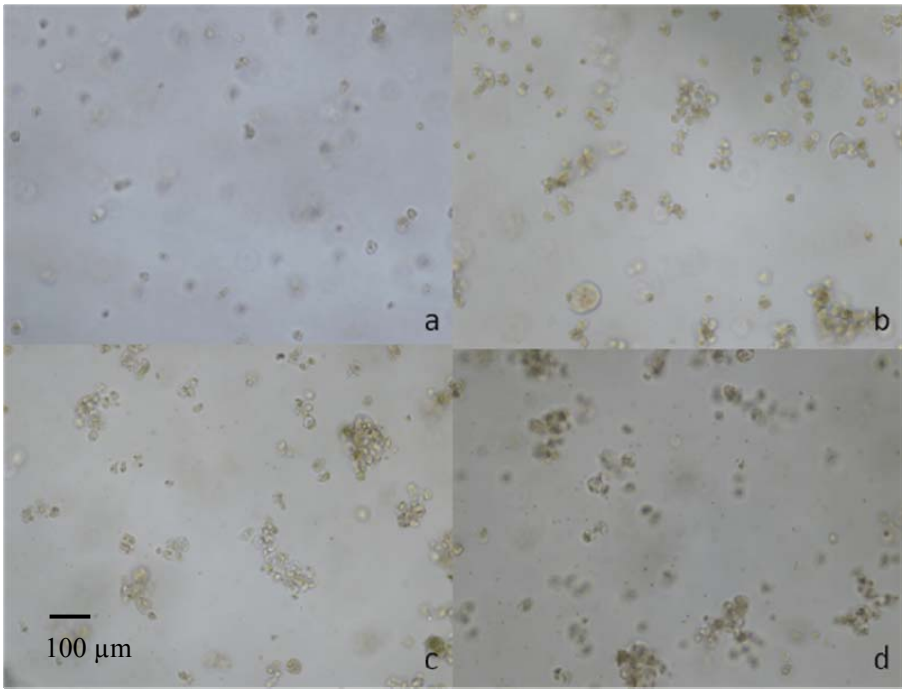

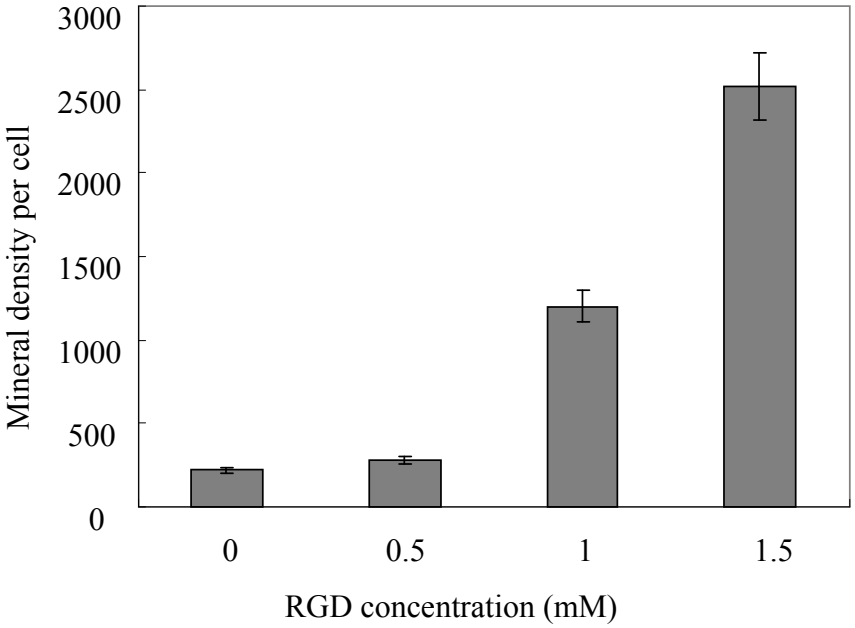

Figure 8.5 Mineralization of MSCs encapsulated in 10% PEG hdyrogel with different RGD concentrations for 7 days culture by von kossa staining. The stained mineral deposits were brown or black. a 0 mM RGD, b 0.5 mM RGD, c 1 mM RGD, d 1.5 mM

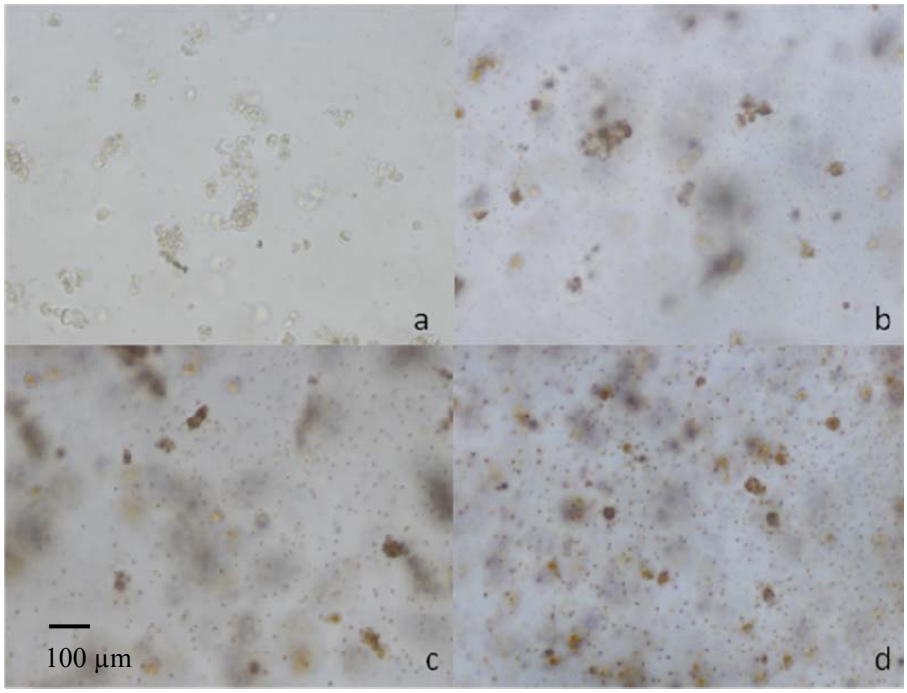

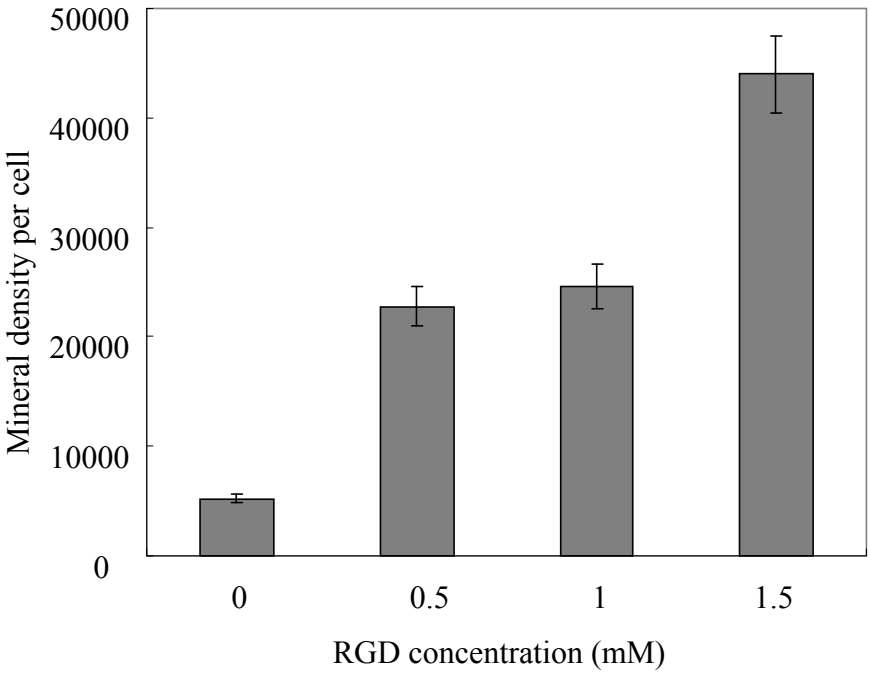

Figure 8.6 Mineralization of MSCs encapsulated in 10% PEG hdyrogel with different RGD concentrations for 14 days culture by von kossa staining. The stained mineral deposits were brown or black. a 0 mM RGD, b 0.5 mM RGD, c 1 mM RGD, d 1.5 mM

8.4 Discussion

The development of functionalized cell encapsulated biomaterials that can provide cells with survivability, adhesion, proliferation and differentiation is of interest in tissue engineering and regenerative medicine. An important area of present research is to provide cell signaling biomolecules such as proteins and growth factors to give cells support for signaling (Benoit DS et al., 2007). In this chapter, MSCs were encapsulated into RGD incorporated PEG hydrogel by UV cross-linking. The effect of RGD on stem cells behaviors was studied in 3D environment.

UV light was used to crosslink PEG hydogel to encapsulate cells. The initial viability of MSCs as shown in Figure 8.1 indicated that most cells were live and UV light did little harm to cells. The research of Xing-Zheng Wu and Satoshi Terada reported that UV light with wavelength less than 350 nm can decrease cells viability (Wu XZ et al., 2007). As the wavelength of UV light in our research was 365 nm which is longer than 350 nm and the dose was low, the UV light had little harm to cells. Photoinitiator and its concentration can also affect cells initial viability. The photoinitiator in PEG solution was 0.05% (W/V) Irgacure 2959, which was demonstrated biocompatible to cells (Williams CG et al., 2005).

Figure 8.1 also indicated that more cells were live in 10% PEG hydrogel compared with 30% PEG hydrogel. MSCs were in a 3D crosslinking network which can restrict cells mobility and transport of soluble factors between inside and outside. In

hydrogel with low PEG concentration, the soluble factors such as proteins can easily transport through hydrogel to cells. In hydrogel with high PEG concentration, it was difficult for the transport due to the more densified network. However, if RGD was incorporated into PEG hydrogel, the cells may have a spreading shape which made cells adsorb more nutrients and thus can increase cells viability.

RGD is a receptor-mediated cell adhesion peptide. Many researches have studied the effect of RGD peptide on cells adhesion and spreading. Recently, the effect of RGD on stem cells differentiation was examined. A lot of research showed that RGD peptide can promote the osteogenic differentiation of MSCs (Shin H et al., 2005; Yang F et al., 2005; Yang XB et al., 2001). In our research, the osteogenic differentiation of MSCs was done and characterized by von kossa staining of mineralization. The staining results showed that RGD peptide can promote the mineralization of MSCs in PEG hydrogel. As mentioned in above paragraph, RGD peptide may increase the cell adhesion and spreading in the 3D crosslinking network. Thus cells had a more spreading morphology with the increase of RGD concentration. The spreading morphology would further promote the interaction of MSCs with signaling biomolecules of osteogenesis. Von kossa staining of mineralization was just one characterization method of osteogenesis. A lot of work still needed to be done to characterize the differentiation with more methods.

Chapter 9 Photoencapsulation of MSCs in PEG Hydrogel with RGD Gradient for Mesenchymal Stem Cells (MSC) Culture

Abstract

MSCs were encapsulated in RGD gradient PEG hydrogel. The cells viability was tested by live/dead assay. MSCs were induced to osteogenic differentiation. Von kossa staining was used to characterize the mineralization of MSCs. The results showed that the cells viability increased with the increase of RGD concentration in the gradient PEG hydrogel. The mineralization experiment also revealed that RGD can promote the osteogenic differentiation of MSCs.

9.1 Introduction

As mentioned in chapter 6.1, cells *in vivo* are often in a gradient environment of certain molecule. Gradients play essential roles in many biological phenomena. In our research discussed in Chapter 6, RGD gradient PEG hydrogel was fabricated. MSCs were then cultured on the gradient PEG hydrogel. It was found that MSCs had different responses to different parts of the gradient PEG hydrogel. However, cells in vivo are in a 3D gradient environment, in which cells may have different behaviours from that in a 2D environment. Therefore, it is useful to fabricate cells encapsulated gradient PEG hydrogel to study MSCs behaviour in a 3D environment with biomolecules gradient.

In Chapter 7, photopolymerization was used to fabricate MSCs encapsulated PEG hydrogel. The results showed that the photopolymerization did little harm to cells viability and most cells in PEG hydrogel were live. Therefore, photopolymerization was a reliable method to encapsulate cells. In this chapter, photopolymerization was used to fabricate MSCs encapsulated PEG hydrogel with RGD gradient in situ. After cell culture, the effect of RGD gradient on cells viability was characterized. The MSCs were also induced to osteogenic differentiation. And mineralization of MSCs in PEG hydrogel was measured to characterize the osteogenesis of MSCs.

9.2 Methodology

9.2.1 Fabrication of stem cells encapsulated RGD gradient PEG hydrogel

The microfluidic gradient generator discussed in previous chapters was used for the

fabrication of MSCs encapsulated RGD gradient PEG hydrogel. The two inlets of the microfluidic gradient generator were first filled with ethanol. A dropper was used to fill the microchannel with ethanol from the outlet until no air bubbles present. After that, phosphate buffer solution (PBS) was used to replace the ethanol by using the same method. This method can prevent air bubbles in the microfluidic device. If PBS solution was directly injected into the device, air bubbles would form due to the hydrophobicity of PDMS. The microfluidic device injected with PBS solution was then sterilized under UV light in hood for 4 hours for later use.

Poly(ethylene glycol) diacrylate (PEGDA, 3400 Da, Laysan Bio Inc., AL, USA) was used to fabricate stem cells encapsulated PEG hydrogel. PEGDA and ACRL-PEG-RGD were mixed in sterilized PBS with penicillin (100 U/ml) and streptomycin (100 μg/ml) to make 10% and 30% (W/V) PEG solution. Photoinitiator Irgacure 2959 was added to the PEG solution at a concentration of 0.05% (W/V). Passage 3 MSCs were then homogeneously suspended in PEG solution to make a concentration of 40 million cells/ml.

Sterilized polyethylene tubing with steel needles was inserted into the inlet holes of the microfluidic device to make the fluidic connections. The piece of tubing was then connected to a syringe pump. Prepared MSCs encapsulated PEG solution without RGD was filled in one syringe while the other was filled with PEG solution with 0.5 mM RGD. The needles of the syringes were inserted into the inlets separately. The flow rate was firstly adjusted to 0.8 ml/hr. Several minutes later, the PEG solution

with RGD and without RGD were mixed, split and mixed along the channel again. Ultimately, a RGD gradient PEG solution with MSCs was generated in the microfluidic channel.

The RGD gradient PEG solution with stem cells was then exposed to UV light (365nm, 70 mW/cm^2) for 1 min to get gelation. The PEG hydrogel on glass slide was put into a petri dish, which was filled with osteogenic culture medium.

9.2.2 In vitro cultivation

The PEG hydrogel samples were all incubated in 5% CO_2 in osteogenic culture medium (Lonza, Switzerland). Osteogenic medium consisted of high-glucose Dulbecco's modified Eagle medium (DMEM) supplemented with 10% fetal bovine serum, 100 nM dexamethasone, 50 μg/ml ascorbic acid 2-phosphate, 10 mM β-glycerophosphate, 100 unit/ml penicillin and 100 μg/ml streptomycin. The cell culture petri dish was incubated in a humidified incubator at 37 ℃. Cell culture medium was changed every two or three days.

9.2.3 MSCs viability in PEG hydrogel

After 7 days culture, the MSCs viability in 30% PEG hydrogel was characterized by live/dead assay. The protocol of live/dead assay was the same to that described in chapter 7.2.3.

9.2.4 Von kossa staining

After 7 days culture, von kossa staining of MSCs encapsulated 10% PEG hydrogel was done to characterize mineralization of MSCs. The method of von kossa staining was the same to that described in 7.2.4.

9.3 Results

9.3.1 MSCs viability

In Chapter 7, it has been found that RGD can promote cells viability in 30% PEG hydrogel. Therefore, 30% PEG hydrogel was used to encapsulate MSCs and RGD gradient. The viability of MSCs encapsulated RGD gradient PEG hydrogel was monitored for up to 7 days to assess the effects of RGD concentration on cell viability. Figure 9.1 shows cell viability in RGD gradient 30% PEG hydrogel. Cells with red color were dead while cells with green color were alive. From left to right in the hydrogel, the RGD concentration increased from 0 to 0.5 mM. Most cells in the area of low RGD concentration were dead. Oppositely most cells in the area of high RGD concentration were live. Therefore, the cells viability increased with the increase of RGD concentration in the gradient PEG hydrogel.

Figure 9.2 shows the MSCs viability across the 3D gradient PEG hydrogel. The cells viability increased from 0% to about 70%. The results suggested that RGD can promote cells viability in 30% PEG hydrogel. The results of cells viability in RGD gradient PEG hydrogel was consistent with that in PEG hydrogel with different RGD concentrations which was shown in chapter 7.

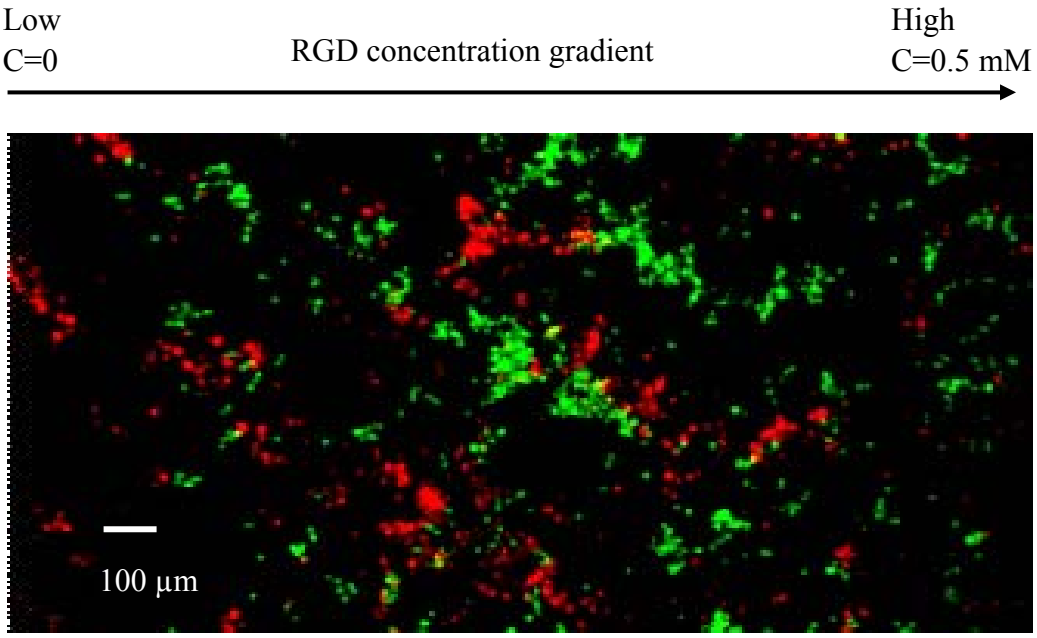

Figure 9.1 MSCs viability in 30% PEG hydrogel with 0-0.5 mM RGD gradient. Cells in PEG hydrogel were cultured for 7 days. Cells with red color were dead while cells with green color were live

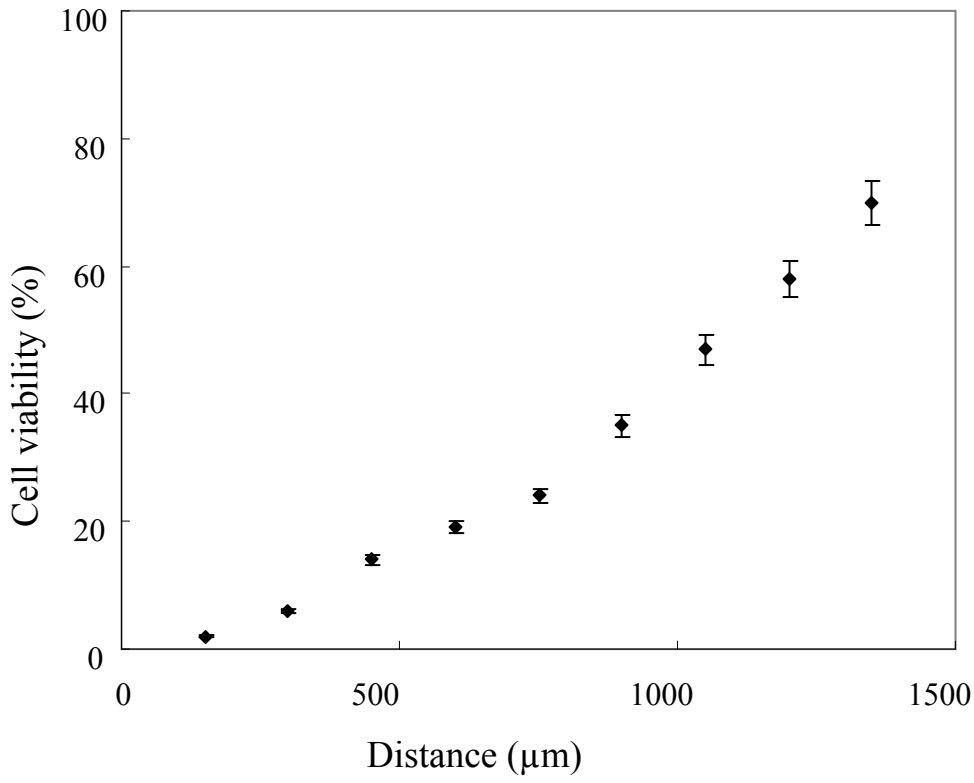

Figure 9.2 MSCs viability across the RGD gradient PEG hydrogel

9.3.2 Von kossa staining

MSCs encapsulated in RGD gradient PEG hydrogel were induced to osteogenic differentiation in our experiment. Osteogenic differentiation can increase the minerlization of MSCs in PEG hydrogel. Von kossa staining was used to measure the mineral deposits in gradient PEG hydrogel. In Chapter 7, it has been found that cells in 10% PEG hydrogel can remain alive as nutrients and other molecules can transport easily between inside and outside of the hydrogel. Therefore, 10% PEG hydrogel was used to encapsulate MSCs and study the differentiation of MSCs.

Figure 9.3 is the von kossa staining of mineral deposits in 0-0.5 mM RGD gradient PEG hydrogel. The black or brown-black color was the mineral deposits. With the increase of RGD concentration from 0 to 0.5 mM, the black color increased. The increase of black color suggested that RGD peptide can promote the mineralization of MSCs in PEG hydrogel.

As shown in Figure 9.3, the von kossa staining picture of gradient PEG hydrogel was then divided into 28 bins across the hydrogel. In each bin, the mineral density per cell was calculated and shown in Figure 9.4. The mineral density in bin 1 was about 40 while the mineral density in bin 28 was about 90. The results indicated that RGD peptide can promote the mineralization of MSCs in PEG hydrogel. The results of mineralization in RGD gradient PEG hydrogel were consistent with that in PEG hydrogel with different RGD concentrations which was discussed in Chapter 8.

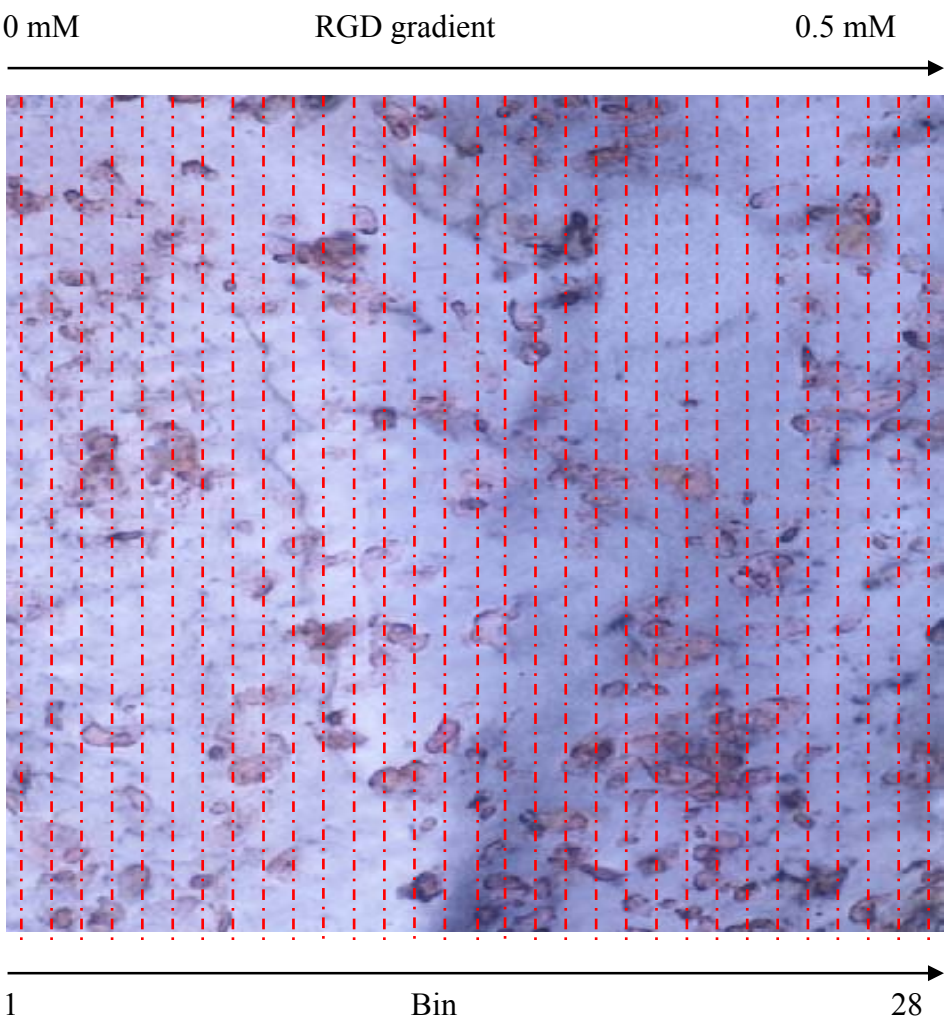

Figure 9.3 Von kossa staining of mineral deposits in MSCs encapsulated RGD gradient PEG hydrogel. RGD concentration was 10%. MSCs were cultured for 7 days in PEG hydrogel

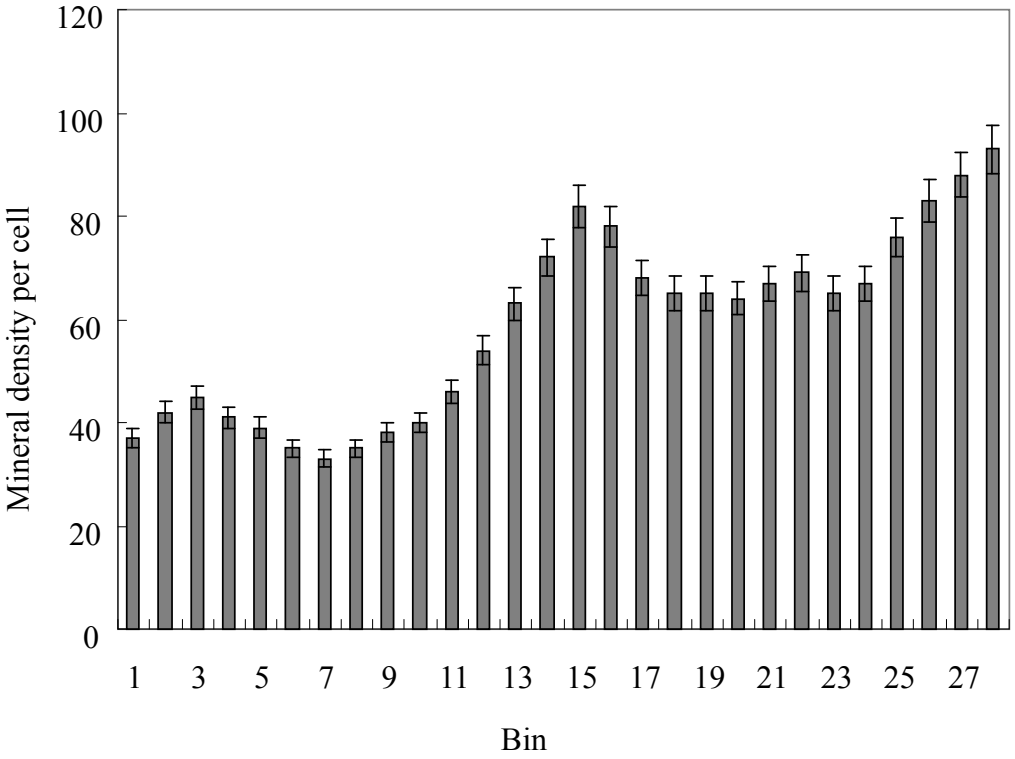

Figure 9.4 Mineral density of MSCs encapsulated in 10% PEG hydrogel with 0-0.5 mM RGD gradient

9.4 Discussion

In our research, photopolymerization was used to fabricate MSCs encapsulated PEG hydrogel. In this process, free radicals were first produced from photoinitiator Irgacure 2959 by UV light. The free radicals then reacted with the vinyl groups of PEG to start the polymerization. Some chemicals such as oxygen can inhibit the photopolymerization. Oxygen can react with the free radicals and then stop the polymerization (Biswal D et al., 2009; Dendukuri D et al., 2008).

In our study, PDMS microfluidic device was used to fabricate RGD gradient PEG hydrogel. As it is known, PDMS has permeable to oxygen and other gases (Charati SG et al., 1998). Oxygen can readily diffuse from outside through PDMS to the microchannels. Oxygen can then react with the radicals generated in the

polymerization of PEG solution in the microchannels. If the radicals were consumed by the oxygen, the PEG solution cannot polymerize into hydrogel. Therefore, there was always a layer of water solution named oxygen inhibition layer between PDMS and PEG hydrogel as shown in Figure 9.5. As it was difficult for oxygen to further diffuse in the PEG solution, the oxygen inhibition layer was thin with a thickness between 30 and 50 μm. In order to decrease the effect of oxygen inhibition layer, a higher PDMS channel with 150-200 μm was fabricated. As the height of the PDMS channel 150-200 μm was much larger than that of the oxygen inhibiton layer 30-50μm, the effect of oxygen inhibition layer on fabrication of PEG hydrogel can be neglected.

In the experiment, UV light and photoinitiator were used to initialize the photopolymerization. The photoinitiator and UV light can do harm to cells viability by destroying the nucleus acid and membrane of cells. There existed an optimal amount of photoinitiator and UV energy to polymerize the PEG solution into hydrogel without harming the cells. The UV light energy 70 mW/cm^2 for 1 min at 365 nm was used to fabricate cells encapsulated PEG hydrogel. It was found that this UV energy did little harm to cells viability and cells can survive the photopolymerization.

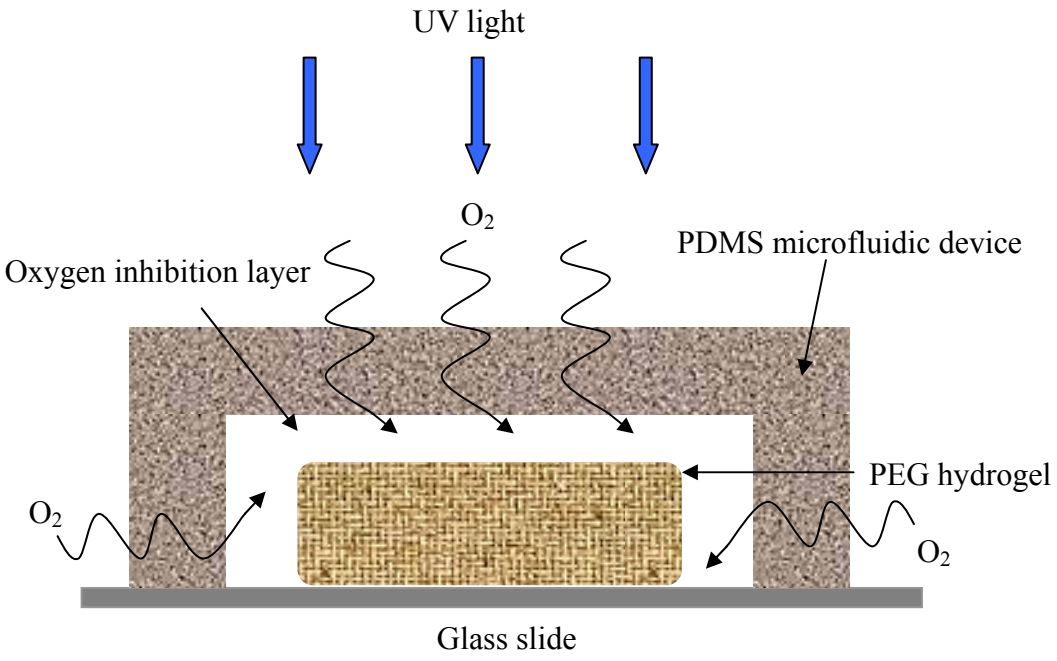

Figure 9.5 Cross-section of PEG hydrogel in microfluidic device

In Chapter 8, MSCs were encapsulated in PEG hydrogel with different RGD concentrations. The results indicated that RGD can promote cells viability and osteogenic differentiation in osteogenisis medium. Therefore, RGD peptide and its concentration had important impact on MSCs behavior in PEG hydrogel. In this chapter, the concentration control of RGD was integrated to a gradient PEG hydrogel fabricated in a microfluidic device. The results also showed that RGD can promote cells viability and osteogenesis which was the same to cell culture in PEG hydrogel with different RGD concentrations. However, the concentration control of RGD in a gradient PEG hydrogel was a more simple and effective method, which was also discussed in chapter 6.

In this chapter, von kossa staining of mineral deposits was used to characterize the osteogenisis of MSCs in RGD gradient PEG hydrogel. Von kossa staining was just one characterization method of osteogenesis. A lot of work still needed to be done to characterize the differentiation with more methods.

Chapter 10 Conclusion and Future Studies

10.1 Conclusions

A microfluidic gradient generator for generation of PEG-RGD continuous gradient is designed. Computational fluid dynamics simulations is explored to test the generation of RGD gradient in PEG solution and derive the optimal parameters for rapid generation of stable bio-molecule gradient. Simulation results show that the diffusion coefficient of fluid and pump driving velocity have important impacts on gradient profiles. Using the higher values of diffusion coefficient, a linear concentration profile across the ends of the microchannels was established, while the lowest value of diffusion coefficient did not allow complete mixing within the channels. For the effects of infusing velocity, higher velocity which is larger than 8×10^{-3} m/s could generate a step concentration profile at the end of the cell culture chamber, while a lower one could generate a linear profile.

Blue dye solution and fluorescence polymer microbeads were used to test the performance of the fabricated microfluidic gradient generator for color and beads gradient generation. Four flow rates 0.1, 0.5, 1 and 2 (ml/hr) were chosen to evaluate the effects of flow rate on the gradient generation. With the increase of the flow rate, the time for solution completing the channel decreased. The flow rates of 0.1 and 0.5 (ml/hr) showed better effect to form gradient, the concentration of which increased gradually and constantly. Flow rate about 1 ml/hr was a critical velocity for forming

the linear gradient. The velocity 1 ml/hr was conversed into the solution velocity of branched channel, which was about 5.3×10^{-3} m/s. This velocity value was close to the theoretical simulated critical value 8×10^{-3} m/s. Therefore, the practical result was consistent with the theoretical simulated result.

RGD, a ligand for integrin-mediated cell adhesion, was chemically incorporated to PEG molecule. Different concentration RGD peptide was polymerized with PEG diacrylate to form RGD incorporated PEG hydrogel. MSCs were then cultured on the 2D PEG hydrogel surface incorporated with RGD concentration of 0, 0.25mM, 0.5mM and 0.75mM. As RGD was chemically incorporated to PEG hdyrogel, it would not be released from PEG hydrogel during cell culture. With the increase of RGD concentration, more RGD sites were ready on the PEG hydrogel surface, which resulted in more cell adhesion sites on PEG hydrogel surface. Therefore, more cells could be adhered on the PEG hydrogel surface with higher RGD concentration. For cell culture half day on PEG (500 Da) hydrogel, the cell adhesion density had a large jump from 0 mM to 0.75 mM. This jump suggests that this concentration range from 0 mM to 0.75 mM is a critical window for cell adhesion of half day. For cell culture one day on the PEG (500 Da) hydrogel, the cell adhesion density had a jump from 0 mM to 0.5 mM. This jump also suggests that the concentration range from 0 mM to 0.5 mM is a critical window for cell culture of one day. The cells can occupy all the RGD sites on the PEG surface after one day. Therefore, there is no obvious difference of cell adhesion between one day and two days culture.

PEG hydrogel with RGD gradient was fabricated using PDMS microfluidic gradient generator. Four RGD gradients were fabricated 0-0.25 mM, 0-0.5 mM, 0-1 mM and 0-2 mM. On PEG hydrogel with low RGD concentration, fewer cells attached on the surface and the cell shape was round. On PEG hydrogel with high RGD concentration, more cells attached on the surface and the cells had a spreading shape. MSCs on 0-0.25 mM RGD gradient had largest distribution difference of cell adhesion. Therefore, MSCs were mostly sensitive to 0-0.25 mM RGD gradient profile.

In the study of MSCs culture on PEG hydrogel with different RGD concentrations, the cell adhesion number had a largest jump in a RGD concentration range. However, it was difficult to know the concrete point for the jump. The results of MSCs adhesion on RGD gradient PEG hydrogel gave the answer. MSCs adhesion on 0-0.25 mM and 0-0.5 mM RGD gradient PEG hydrogels had a same RGD concentration 0.11 mM, above which more cells can adhere on the hydrogel surface. Thus, RGD concentration 0.11 mM was regarded as the jump concentration for cell adhesion on PEG hydrogel. The RGD concentration 0.11 mM was also in the jump concentration range 0-0.5 mM. Therefore, the jump concentration got from the RGD gradient PEG hydrogel was consistent with the jump concentration range got from conventional method.

MSCs were encapsulated in PEG hydrogel with different PEG and RGD concentrations. The MSCs viability was characterized. For the effect of PEG

concentration, more cells were live in 10% PEG hydrogel compared with 30% PEG hydrogel. MSCs were in a 3D crosslinking network which can restrict cells mobility and transport of soluble factors between inside and outside. In hydrogel with low PEG concentration, the soluble factors such as proteins can easily transport through hydrogel to cells. In hydrogel with high PEG concentration, it was difficult for the transport due to the more densified network. Therefore, lower PEG concentration can increase cells viability. For RGD concentration, it had no effect on MSCs viability in lower PEG concentration hydrogel of 10%. However, there was significantly positive effect of RGD concentration on MSCs viability in hydrogel with higher PEG concentration of 30%. The existence of RGD in hydrogel may affect the cells viability function so that cells in PEG hydrogel with RGD had better cells viability.

The MSCs encapsulated into PEG hydrogel were induced to osteogenic differentiation. Mineralization was tested to characterize the osteogenesis of MSCs. Cell culture for longer time can increase the mineralization of MSCs in PEG hydrogel. The RGD concentration also had important impact on MSCs mineralization. The results indicated the RGD concentration almost had no effect on mineralization of MSCs in a short culture time such as less than 3 days. However, the RGD concentration can have important impact on mineralization of MSCs in long time culture such as more than 7 days. The enhanced mineralization suggested that RGD peptide can promote the mineralization of MSCs in PEG hydrogel.

MSCs were also encapsulated in 0-0.5mM RGD gradient PEG hydrogel. The cell

viability across the 3D gradient PEG hydrogel increased from 0% to about 70%. So RGD can promote cells viability in 30% PEG hydrogel. The results of cells viability in RGD gradient PEG hydrogel were consistent with that in PEG hydrogel with different RGD concentrations. MSCs in 0-0.5mM RGD gradient PEG hydrogel was induced to osteogenic differentiation. The mineralization increased with the increase of RGD concentration in PEG hydrogel.

10.2 Limitation

There were some limitations for the present research. The main limitation was the characterization of osteogenisis of MSCs in PEG hydrogel. In the research, mineralization stained by von kossa staining was used to characterize the osteogenisis. More methods such as biochemical analysis of alkaline phosphatise and osteocalcin, and RT-PCR of early osteogenesis marker should be employed for the characterization of osteogenisis. However, these methods can not be used due to the RGD concentration variation only in one PEG hydrogel. It was difficult to apply these analyses at one concrete concentration in the gradient PEG hydrogel. Therefore, more research should be done to explore the methods for the characterization of osteogenisis of MSCs.

10.3 Future studies

10.3.1 Characterization of osteogenic differention

As mentioned in 9.2, there were some limitations about the characterization of osteogenic differentiation. More methods should be used to characterize the

osteogenisis. Alkaline phosphatise (ALP) and Osteopontin (OPN) are produced in osteogenic differentiation of MSCs. A lot of research has stained the ALP and OPN for characterization of osteogenic differentiation (Benoit DS et al., 2008; Friedman MS et al., 2006). Therefore, the staining of ALP and OPN MSCs in PEG hydrogel can be done for characterization of osteogenic differentiation in the future study.

10.3.2 Chondrogenic and adipogenic differentiation of MSCs in PEG hydrogel

In the present research, MSCs were only induced to osteogenic differentiation in PEG hydrogel. However, MSCs also have the ability of chondrogenic and adipogenic differentiation. With the microfluidic platform in the present research, RGD gradient PEG hydrogel can be also fabricated for the study of choncrogenic and adipogenic differentiation.

10.3.4 The effect of other biological and chemical molecules on MSCs differentiation

The microfluidic gradient generator can achieve the identity and concentration control of molecules. For the identity control, the only effect of RGD gradient on MSCs behaviours was studied in my research. However, different biological and chemical molecules can have different effects on the differentiation of MSCs. Biological molecule heparin was found to promote the osteogenic differentiation of MSCs (Benoit DS et al., 2005; Benoit DS et al., 2007). Small functional groups were also found to control the differentiation of MSCs. For example, small molecules with hydrophobic groups had the potential to induce adiogenic differentiation while small molecules with acid groups had the ability to induce chondrogenic differentiation

without adding differentiation medium (Benoit DS et al., 2008). Therefore, more biological or chemical molecules can be used to fabricate gradient PEG hydrogel for the study of mesenchymal stem cells differentiation.

References

Allen LT, Fox EJ, Blute I, Kelly ZD, Rochev Y, Keenan AK, Dawson KA, Gallagher WM, 2003. Interaction of soft condensed materials with living cells: phenotype/transcriptome correlations for the hydrophobic effect. Proc Natl Acad Sci. 100:6331–6336.

Atsumi T, Murata J, Kamiyanagi I, Fujisawa S, Ueha T, 1998. Cytotoxicity of photosensitizers camphorquinone and 9-fluorenone with visible light irradiation on a human submandibularduct cell line in vitro. Arch Oral Biol. 43:73-81.

Babensee JE, McIntire LV, Mikos AG, 2000. Growth factor delivery for tissue engineering. Pharm Res. 17:497-504.

Barkefors I, Le Jan S, Jakobsson L, Hejll E, Carlson G, Johansson H, Jarvius J, Park JW, Li Jeon N, Kreuger J, 2008. J Biol Chem. 283:13905-13912.

Benoit DS, Anseth KS, 2005. Heparin functionalized PEG gels that modulate protein adsorption for hMSC adhesion and differentiation. Acta Biomaterials. 1:461-470.

Benoit DS, Durney AR, Anseth KS, 2007. The effect of heparin-functionalized PEG hydrogels on three-dimensional human mesenchymal stem cell osteogenic differentiation. Biomaterials. 28:66-77.

Benoit DS, Schwartz MP, Durney AR, Anseth KS, 2008. Small functional groups for controlled differentiation of hydrogel-encapsulated human mesenchymal stem cells. Nat Mater. 7:816-823.

Biswal D, Hilt JZ, 2009, Analysis of oxygen inhibition in photopolymerzations of hydrogel micropatterns using FTIR imaging. Macromolecules. 42:973-979.

Bryant SJ, Nuttelman CR, Anseth KS, 2000. Cytocompatibility of UV and visible light photoinitiating systems on cultured NIH/3T3 fibroblasts in vitro. J Biomater Sci Polym Ed. 11: 439-457.

Bryant SJ, Anseth KS, 2005. Photopolymerization of hydrogel scaffolds. Scaffolding in tissue engineering Taylor & Francis.

Brittberg M, Lindahl A, Nillson A, Ohlsson C, Isaksson O, Peterson L, 1994. Treatment of deep cartilage defects in the knee with autologous chondrocyte transplantation. N Engl J. 331:889-895.

Bruder SP, Kurth AA, Shea M, Hayes WC, Jaiswal N, Kadiyal S, 1998. Bone regeneration by implantation of purified, culture-expanded human mesenchymal stem cells. J Orthop Res. 16:155-162.

Burdick JA, Anseth KS, 2002. Photoencapsulation of osteoblasts in injectable RGD-modified PEG hydrogels for bone tissue engineering. Biomaterials. 23:4315–4323.

Burdick JA, Khademhosseini A, Langer R, 2004. Fabrication of gradient hydrogels using a microfluidics/photopolymerization process. Langmuir. 20:5153-5156.

Calplan AI, 1989. Cell delivery and tissue regeneration. J Control Release. 157-165.

Caplan AI, 1991. Mesenchymal stem cells. J Orthop Res. 9:641-650.

Calplan AI, 2005. Review: Mesenchymal stem cells: Cell-based reconstructive therapy in orthopedics. Tissue Eng. 11:1198–1211.

Cascone MG, Barbani N, Cristallini C, Giusti P, Ciardelli G, Lazzeri L, 2001. Bioartificial polymeric materials based on polysaccharides. J Biomater Sci: Polym Ed. 12:267-281.

Chang JC, Hsu SH, Chen DC, 2009. The promotion of chondrogenesis in adipose-derived adult stem cells by an RGD-chimeric protein in 3D alginate culture. Biomaterials. 30:6265-6275.

Charati SG, Stern SA, 1998, Diffusion of gases in silicone polymer: molecular

dynamics simulations. Macromolecules. 31:5529-5535.

Chen CS, Alonso JL, Ostuni E, Whitesides GM, Ingber DE, 2003. Cell shape provides global control of focal adhesion assembly. Biochem Bioph Res Commun. 307:355–61.

Chung BG, Flanagan LA, Rhee SW, Schwartz PH, Lee AP, Monuki ES, Jeon NL, 2005. Lab Chip. 5:401-406.

Costin CD, Olund RK, Staggmeier BA, Torgerson AK, Synovec RE, 2003. Difussion coefficient measurement in microfluidic analyzer using dual-beam microscale-refractive index gradient detection application to on-chip molecular size determination. J Chromatogr A. 1013: 77-91.

Curran JM, Chen R, Hunt JA, 2006. The guidance of human mesenchymal stem cell differentiation in vitro by controlled modifications to the cell substrate. Biomaterials. 27:4783-4793.

Cutler SM, Garcia AJ, 2003. Engineering cell adhesive surfaces that direct integrin a5b1 binding using a recombinant fragment of fibronectin. Biomaterials. 24:1759–70.

Dazzi F, Ramasamy R, Glennie S, Jones SP, Roberts I, 2006. The role of

mesenchymal stem cells in haemopoiesis. Blood Rev. 20:161-171.

DeLong SA, Moon JJ, West JA, 2005. Covalently immobilized gradients of bFGF on hydrogel scaffolds for directed cell migration. Biomaterials. 26:3227-3234.

DeMali KA, Wennerberg K, Burridge K, 2003. Integrin signaling to the actin cytoskeleton. Curr Opin Cell Biol. 15:572–582.

Dendukuri D, Panda P, Haghgooie R, Kim JM, Hatton TA, Doyle PS, 2008. Modeling of oxygen-inhibited free radical photopolymerization in a PDMS microfluidic device. Macromolecules. 41:8547-8556.

Dertinger SKW, Chiu DT, Jeon NL, Whitesides GM, 2001. Generation of gradients having complex shapes using microfluidic networks. Anal Chem. 73: 1240-1246.

Fittkau MH, Zilla P, Bezuidenhout D, Lutolf MP, Human P, Hubbell JA, Davies N, 2005. The selective modulation of endothelial cell mobility on RGD peptide containing surfaces by YIGSR peptides. Biomaterials. 26:167–174.

Freed LE, Marquis JC, Nohria A, Emmanual J, Mikos AG, Langer R, 1993. Neocartilage formation *in vitro* and *in vivo* using cells cultured on synthetic biodegradable polymers. J Biomed Mater Res. 27:11-23.

Friedman MS, Long MW, Hankenson KD, 2006. Osteogenic differentiation of human mesenchymal stem cells is regulated by bone morphogenetic protein-6. J Cell Biochem. 98:538-554.

Gaarcia AJ, 2005. Get a grip: integrins in cell-biomaterial interactions. Biomaterials. 26:7525-7529.

Goodman SL, Sims PA, Albrecht RM, 1996. Three-dimensional extracellular matrix textured biomaterials. Biomaterials. 17:2087–2095.

Grabarek Z, Gergely J, 1990. Zero-length crosslinking procedure with the use of active esters. Anal Biochem. 185:131-135.

Guarnieri D, Borzacchiello A, Capua AD, Ruvo M, Netti PA, 2008. Engineering of covalently immobilized gradients of RGD peptides on hydrogel scaffolds: effect on cell behaviour. Macromolecular Symposia. 266:36-40.

Gunawan RC, Silvestre J, Gaskins HR, Kenis PJ, Leckband DE, 2006. Cell migration and polarity on microfabricated gradients of extracellular matrix proteins. 22:4250-4258.

Hersel U, Dahmen C, Kessler H, 2003. RGD modified polymers: biomaterials for stimulated cell adhesion and beyond. Biomaterials. 24:4385-4415.

Hoemann CD, EI-Gabalawy, McKee MD, 2009. In vitro osteogenesis assays: Influence of the primary cell source on alkaline phosphatase activity and mineralization. Pathol Biol. 57:318-323.

Hubbell JA, Massia SP, Desai NP, Drumheller PD, 1991. Endothelial cell-selective materials for tissue engineering in the vascular graft via a new receptor. Biotechnology. 9:568-572.

Humphries MJ, Akiyama SK, Komoriya A, Olden K, Yamada KM, 1986. Identification of an alternatively spliced site in human plasma fibronectin that mediates cell type specific adhesion. J Cell Biol. 103:2637-2647.

Hwang NS, Varghese S, Zhang Z, Elisseeff J, 2006. Chondrogenic differentiation of human embryonic stem cell-derived cells in Arginine-Glycine-Aspartate modified hydrogels. Tissue Eng. 12:2695-2706.

Hwang NS, Zhang C, Hwang YS, 2009. Mesenchymal stem cell differentiation and roles in regenerative medicine. WIREs Systems Biology and Medicine. 1:97-106.

Hynes R, 2002. Integrins: bidirectional, allosteric signaling machines. Cell. 110: 673–687.

Jackson L, Jones DR, Scotting P, Sottile V. Adult mesenchymal stem cells: differentiation potential and therapeutic applications, 2007. J Postgrad Med. 53:121-127.

Jain RA, 2000. The manufacturing techniques of various drug loaded biodegradable poly(lactide-co-glycolide) (PLGA) devices. Biomaterials. 21:2475-2490.

Jeanie LD, David JM, 2003. Hydrogels for tissue engineering: scaffold design variables and applications. Biomaterials. 24:4337-4351.

Jeon NL, Dertinger SKW, Chiu DT, Choi IS, Stroock AD, Whitesides GM, 2000. Generation of solution and surface gradients using microfluidic systems. Langmuir. 16:8311-8316.

Jones SW, 2000. Photolithography.

Jung HJ, Park K, Kim JJ, Lee JH, Han KO, Han DK, 2008. Effect of RGD-immobilized dual-pore poly(L-Lactic acid) scaffolds on chondrocyte proliferation and extracellular matrix production. Artif Organs, 32:981-989.

Keenan TM, Folch A, 2008. Biomolecular gradients in cell culture systems. Lab Chip. 8:34-57.

Kirincic S, Klofutar C, 1999. Viscosity of aqueous solutions of poly(ethylene glycol)s at 298.15 K. Fluid Phase Equilibr. 155: 311-325.

Kokubu E, Yoshinari M, Matsuzaka K, Inoue T, 2009. Behavior of rat periodontal ligament cells on fibroblast growth factor-2-immobilized titanium surfaces treated by plasma modification. J Biomed Mater Res A. 91:69-75.

Krampera M, Pizzolo G, Aprili G, Franchini M, 2006. Mesenchymal stem cells for bone, cartilage, tendon and skeletal muscle repair. Bone. 39:678-683.

Lee HJ, Lee JS, Chansakui T, Yu C, Elisseeff JH, Yu SM, 2006. Collagen mimetic peptide-conjugated photopolymerizable PEG hdyrogel. Biomaterials. 27:5268-5276.

Li X, Yao J, Yang X, Tian W, Liu L, 2008. Surface modification with fibronectin or collagen to improve the cell adhesion. Appl Surf Sci. 255:459-461.

Lin F, Nguyen CM, Wang SJ, Saadi W, Gross SP, Jeon NL, 2005. Neutrophil migration in opposing chemoattractant gradient using microfluidic chemotaxis devices. Ann Biomed Eng. 33:475-482.

Lin YC, Brayfield CA, Gerlach JC, Rubin JP, Marra KG, 2009. Peptide modification of polyethersulfone surfaces to improve adipose-drived stem cell adhesion. Acta Biomater. 5:1416-1424.

Liu L, Ratner BD, Sage EH, Jiang S, 2007. Endothelial cell migration on surface-density gradients of fibronectin, VEGF, or both proteins. Langmuir. 23:11168-11173.

Liu Z; Deng X; Wang M; Chen J; Zhang A; Gu Z; Zhao C, 2009. BSA-modified polyethersulfone membrane: preparation, characterization and biocompatibility. J Biomater Sci Polym Ed. 20:377-397.

Luhmann T, Hall H, 2009. Cell guidance by 3D-gradients in hydrogel matrices: importance for biomedical applications. Materials. 2:1058-1083.

Mann BK, Tsai AT, Scott-Burden T, West JL, 1999. Modification of surfaces with cell adhesion peptides alters extracellular matrix deposition. Biomaterials. 20:2281–2286.

Mann BK, Schmedlen RH, West JL, 2001. Tethered-TGF-β increases extracellular matrix production of vascular smooth muscle cells. 22:439-444.

Ma PX, Choi JW, 2001. Biodegradable polymer scaffolds with well-defined interconnected spherical pore network. Tissue Eng. 7:23-33.

Massia SP, Stark J, 2001. Immobilized RGD peptides on surface-grafted dextran

promote biospecific cell attachment. J Biomed Mater Res. 56:390–399.

McDonald JC, Duffy D, Anderson JR, Chiu DT, Wu H, Schueller OJA, Whitesides GM, 1999. Fabrication of microfluidic systems in poly(dimethylsiloxane). Electrophoresis. 21:27-40.

Mcmillan R, Meeks B, Bensebaa F, Deslandes Y, Sheardown H, 2001. Cell adhesion peptide modification of gold-coated polyuthanes for vascular endothelial cell adhesion. J Biomed Mater Res. 54:272-283.

Min JY, Sullivan MF, Yang Y, Zhang JP, Converso KL, Morgan JP, 2002. Significant improvement of heart function by cotransplantation of human mesenchymal stem cells and fetal cardiomyocytes in postinfarcted pigs. Ann Thorac Surg. 74:1568-1575.

Miralles G, Baudoin R, Dumas D, Baptiste D, Hubert P, Stoltz JF, Dellacherie E, Mainard D, Netter P, Payan E, 2001. Sodium alginate sponges with or without sodium hyaluronate: in vitro engineering of cartilage. J Biomed Mater Res. 57: 278-278.

Moan J, Berg K, Kvam E, Western A, Malik Z, Ruck A, Schneckenburger H, 1989. Intracellular localization of photosensitizers. Ciba Found Symp. 146:95-107.

Moore A, Donahue CJ, Bauer KD, Mather JP, 1998. Simultaneous measurement of cell cycle and apoptotic cell death. Methods Cell Biol. 57:265-278.

Morpurgo M, Bayer EA, Wilchek M, 1999. N-hydroxysuccinimide carbonates and carbamates are useful reactive reagents for coupling ligands to lysines on proteins. J Biochem Biophys Methods. 38:17–28.

Murphy JM, Kavalkovitch KW, Fink D, Barry FP, 2000. Regeneration of meniscal tissue and protection of articular cartilage by injection of mesenchymal stem cells. Osteoarthritis Cartilage. 8(Suppl B):S25.

Nair LS, Laurencin CT, 2007. Biodegradable polymers as biomaterials. Prog Polym Sci. 32:762-798.

Nguyen KT, West JL, 2002. Photopolymerizable hydrogels for tissue engineering applications. Biomaterials. 23:4307-4314.

Niu X, Wang Y, Luo Y, Xin J, Li Y, 2005. Arg-Gly-Asp (RGD) modified biomimetic polymeric materials. J Mater Sci Technol. 21:571-576.

Nuttelman CR, Tripodi MC, Anseth KS, 2004. In vitro osteogenic differentiation of human mesenchymal stem cells photoencapsulation in PEG hydrogel. J Biomed Mater Res PtA. 68A:773-782.

Nuttelman CR, Tripodi MC, Anseth KS, 2005. Synthetic hydrogel niches that promote hMSC viability. Matrix Biology. 24:208-218.

Nuttelman CR, Benoit DSW, Tripodi MC, Anseth KS, 2006. The effect of ethylene glycol methacrylate phosphate in PEG hydrogels on mineralization and viability of encapsulated hMSCs. Biomaterials. 27:1377-1386.

Oerther S, Le Gall H, Payan E, Lapicque F, Presle N, Hubert P, Dexheimer J, Netter P, Lapicque F, 1999. Hyaluronate-alginate gel as a novel biomaterial: mechanical properties and formation mechanism. Biotech Bioeng. 63:206-215.

Patrick CW, Mikos AG, McIntire LV, 1998. Frontiers in Tissue engineering. Pergamon: Oxford.

Peppas NA, Huang Y, Torres-Lugo M, Ward JH, Zhang J, 2000. Physicochemical foundations and structural design of hydrogels in medicine and biology. Annu Rev Biomed Eng. 2: 9-29.

Pfaff M, 1997. Recognition sites of RGD-dependent integrins. Integrin-Ligand Interaction. Heidelberg: Springer-Verlag. 101–121.

Pittenger MF, Martin BJ, 2004. Mesenchymal stem cells and their potential as

cardiac therapeutics. Circ Res. 95:9-20.

Pierschbacher MD, Ruoslahti E, 1984. Variants of the cell recognition site of fibronectin that retain attachmentpromoting activity. Proc Natl Acad Sci. 81, 5985–5988.

Qin D, Xia Y, Rogers JA, Jackman RJ, Zhao X, Whitesides GM, 1998. Microfabrication, Microstructures and Microsystems. Topics in Current Chemistry. 1-20.

Rosso F, Giordano A, Barbarisi M, Barbarsi A, 2004. From Cell-ECM interactions to Tissue engineering. J Cell Physiol. 199:174-180.

Rowley JA, Mooney DJ, 2002. Alginate type and RGD density control myoblast phenotype. J Biomed Mater Res. 60: 217–223.

Ruoslahti E, Pierschbacher MD, 1987. New perspectives in cell adhesion: RGD and integrins. Science. 238:491-497.

Sakaguchi Y, Sekiya I, Yagishita K, Muneta T, 2005. Comparison of human stem cells derived from various mesenchymal tissues: superiority of synvovium as a cell source. Arthritis Rheum. 52:2521-2529.

Salinas CN, Anseth KS, 2008. The enchancement of chondrogenic differentiation of human mesenchymal stem cells by enzymatically regulated RGD functionalities. Biomaterials. 29:2370-2377.

Sargeant TD, Rao MS, Koh CY, Stupp SI, 2008. Covalent functionalization of NiTi surfaces with bioactive peptide amphiphile nanofibers. Biomaterials. 29:1085-1098.

Sasai Y, Matsuzaki N, Kondo S, Kuzuya M, 2008. Introduction of carboxyl group onto polystyrene surface using plasma techniques. Surf Coat Tech. 202:5724-5727.

Schmedlen RH, Masters KS, West JL, 2002. Photopcrosslinkable polyvinyl alcohol hydrogels that can be modified with cell adhesion peptides for use in tissue engineering. Biomaterials. 23:4325-4332.

Shin H, Jo S, Mikos AG, 2002. Modulation of marrow stromal osteoblast adhesion on biomimetic oligo[poly(ethylene glycol) fumarate] hydrogels modified with Arg–Gly–Asp peptides and a poly(ethylene glycol) spacer. J Biomed Mater Res. 61:169–179.

Shin H, Temenoff JS, Bowden GC, Zygourakis K, Farach-Carson MC, Yaszemski MJ, Mikos AG, 2005. Osteogenic differentiation of rat bone marrow stromal cells cultured on Arg-Gly-Asp modified hydrogels without dexamethasone and β-glycerol phosphate. Biomaterials. 26:3645-3654.

Shin H, Temenoff JS, Bowden GC, Zygourakis K, Farach-Carson MC, Yaszemski MJ, Mikos AG, 2005. Osteogenic differentiation of rat bone marrow stromal cells cultured on Arg-Gly-Asp modified hydrogels without dexamethasone and beta-glycerol phosphate. Biomaterials. 26:3645-3654.

Shin H, 2007. Fabrication methods of an engineered microenvironment for analysis of cell-biomaterial interactions. Biomaterials. 28:126-133.

Shu XZ, Ghosh K, Liu Y, Palumbo FS, Luo Y, Clark RA, Prestwich GD, 2004. Attchment and spreading of fibroblasts on an RGD peptide-modified injectable hyaluronan hydrogel. J Biomed Mater Res A. 68:365-375.

Steele JG, Dalton BA, Johnson G, Underwood PA, 1995. Adsorption of fibronectin and vitronectin onto promaiaTM and tissue culture polystyrene and relationship to the mechanism of initial attachment of human vein endothelial cells and BHK-21 fibroblasts. Biomaterials. 16:1057-1067.

Steffens GCM, Northdurft L, Buse G, Thissen H, Hocker H, Klee D, 2002. High density binding of proteins and peptides to poly(D,L-lactide) grafted with polyacrylic acid. Biomaterials. 23:3523-3531.

Takagi J, 2004. Structural basis for ligand recognition by RGD

(Arg-Gly-Asp)-dependent integrins. Biochem Soc T. 32:403-406.

Tessmar JK, Gopferich AM, 2007. Customized PEG-derived copolymers for tissue-engineering applications. Macromol Biosci. 7:23-29.

Tirella A, Marano M, Vozzi F, Ahluwalia A, 2008. A microfluidic gradient maker for toxicit testing of bupivacaine and lidocaine. Toxicol In Vitro. 22: 1957-1964.

Van Der Flier A, Sonnenberg A, 2001. Function and interactions of integrins. Cell Tissue Res. 305:285-98.

Varqhese S, Hwang NS, Canver AC, Theprunqsirikul P, Lin DW, Elisseeff J, 2008. Chondroitin sulphate based niches for chondrogenic differentiation of mesenchymal stem cells. Matrix Biol. 27:12-21.

Weibel DB, Diluzio WR, Whitesides GM, 2007. Microfabrication meets microbiology. Nat Rev Microbiol. 5:209-218.

Whitaker MJ, Quirk RA, Howdle SM, Shakesheff KM, 2001. Growth factor release from tissue engineering scaffolds. J Pharm Pharmacol. 53:1427-1437.

Whitsides GM, 2006. The origins and the future of microfluidics. Nature. 442:368-373.

Williams CG, Malik AN, T Kim TK, Manson PN, Elisseeff JH, 2005. Vairable cytocompatibility of six cell lines with photoinitiators used for polymerizing hydrogels and cell encapsulation. Biomaterials. 26:1211-1218.

Wu XZ, Kato T, Tsuji Y, Terada S, 2007. Hazard identification on a single cell level using a laser beam. Anal Chem Insights. 2:119-124.

Xia Y, 1998. Soft lithography. Annu Rev Mater Sci. 28:153-184.

Yang F, Williams CG, Wang DA, Lee H, Manson PN, Elisseeeff J, 2005. The effect of incorporating RGD adhesive peptide in polyethylene glycol diacrylate hydrogel on osteogenesis of bone marrow stromal cells. Biomaterials. 26:5991-5998.

Yang XB, Roach HI, Clarke NM, Howdle SM, Quirk R, Shakesheff KM, Oreffo RO, 2001. Human osteoprogenitor growth and differentiation on synthetic biodegradable structures after surface modification Bone. 29:523-531.

Yamada Y, Kleinman HK, 1992. Functional domains of cell adhesion molecules. Curr Opin Cell Biol. 4:819-823.

Yim EK, Wan AC, Visage CL, Liao IC, Leong KW, 2006. Proliferation and differentiation of human mesenchymal stem cell encapsulated in polyelectrolyte

complexation fibrous scaffold. Biomaterials. 27: 6111-6122.

Yliperttula M, Chung BG, Navaladi A, Manbachi A, Urtti A, 2008. High-throughput screening of cell responsed to biomaterials. Eur J Pharm Sci. 25:151-160.

Zaari N, Rajagopalan P, Kim SK, Engler AJ, Wong JY, 2004. Photopolymerization in microfluidic gradient generators: microscale control of substrate compliance to manipulate cell response. Adv Mater. 16:2133-2137.

Zhang H, Lin C, Hollister SJ, 2009. The interaction between bone marrow stromal cells and RGD-modified three-dimensional porous polycaprolactone scaffolds. Biomaterials. 30:4063-4069.

Zreiqat H, Ahu Akin F, Howlett CR, Markovic B, Haynes D, Lateef S, Hanley L, 2002. Differentiaton of human bone-derived cells grown on GRGDSP-peptide bound titanium surfaces. J Biomed Mater Res. 64A: 105-113.

.